

Climate Change Impacts on the Safety of Concrete Arch Dams in South Africa

Report to the Water Research Commission

by

Prof Pilate Moyo

Mr Bukhosi Nyoni

University of Cape Town

WRC Report No. 2749/1/20

ISBN 978-0-6392-0199-3



November 2020

Obtainable from

Water Research Commission

Private Bag X03

GEZINA, 0031

orders@wrc.org.za or download from www.wrc.org.za

DISCLAIMER

This report has been reviewed by the Water Research Commission (WRC) and approved for publication. Approval does not signify that the contents necessarily reflect the views and policies of the WRC nor does mention of trade names or commercial products constitute endorsement or recommendation for use.

Summary

The reality of climate change can no longer be ignored as evidenced by the observed temperature increases. In South Africa the temperature increase is projected to reach more than 3°C, by year 2050. Existing concrete arch dams were not designed anticipating climate change. Therefore the temperature rise coupled with possible dry or wet weather will progressively lead to the deterioration of the structural integrity of concrete dams. This study has shown that concrete arch dams are likely to be overstressed in future leading to cracking and this may compromise their structural integrity. Concrete arch dams impound 39% of South Africa's total volume of water in storage reservoirs. Therefore a 'no regrets' approach is recommended to ensure their safety in the long term. Dam surveillance programs need to incorporate climate change impacts, to ensure that the onset of possible dam failure is detected and resolved before it becomes catastrophic.

Abstract

Climate change is now a reality facing our planet. South Africa is expected to be generally warmer than the period 1961-2000 by up to 3°C or higher by 2050 (Engelbrecht et al., 2015; Dosio and Panitz, 2016; Dosio, 2017). Owing to the large variability of climatic conditions in South Africa, four future climate scenarios have been identified namely, 1) warmer and drier (temperature rise up to 3°C, with low annual rainfall), 2) warmer and wetter (temperature rise up to 3°C, with high annual rainfall), 3) hotter and drier (temperature rise greater 3°C, with low annual rainfall), 4) hotter and wetter (temperature rise greater than 3°C with high annual rainfall). This temperature rise coupled with extreme precipitation conditions will compromise the structural integrity of dams, thereby threatening water supply in South Africa which is already a water stressed country. Concrete arch dams are particularly susceptible to temperature variations and this is a key structural design parameter for these structures. Long term changes in temperature will result in the re-distribution of stresses within the dam walls which has the potential to induce damage and even structural failure. It is therefore essential to consider climate change in the safety evaluation of existing arch dams. In accounting for climate change in the dam safety evaluation process, the uncertainties associated with climate change predictions should be well considered. These uncertainties can be reduced if sufficient data is available on the past climate and the structural behaviour of the dams. In this project long-term dam surveillance data and ambient vibration testing were used to develop finite element models of two concrete arch dams to mimic their current behaviour as closely as possible. The finite element models were then used to estimate the projected future structural behaviour of the dams under various climate change scenarios. The two dams used in this study are Roode Elsberg Dam located on the Sanddrift River in the Western Cape Province, South Africa, and Kouga Dam located on Kouga River in the Eastern Cape Province, South Africa.

The structural performance assessment of the dams show that climate change will cause the concrete arch dams to displace permanently in the upstream direction. This will increase tensile stresses on the dam wall which will structurally lead to cracking. Under high hydrostatic loads, the thrust forces at foundation level will also increase, thereby increasing the risk of structural failure at foundation level. In addition to increasing the magnitudes of stresses on the dam wall, increased temperature will accelerate swelling of dams due to chemical reactions, such as observed for Kouga Dam, further increasing both tensile and compressive stresses in the dam wall.

The results of this research demonstrate that there are potential adverse effects induced by climate change on the structural integrity of dams. With concrete arch dams accounting for 39% of the total impounded volume of water in South Africa, it is imperative to apply the results of this work in the safety evaluation of other concrete arch dams. The critical aspect of reliable dam safety

evaluation is availability of relevant, good quality data. It is therefore recommended that the monitoring systems on concrete arch dams be maintained and kept operational to ensure robust early detection of unusual structural behaviour. Weather stations should be installed at all dam sites as part of monitoring and surveillance systems. This will provide on-site weather data for climate change tracking. This study should be extended to investigate the effects of extreme events such as flooding and heat waves on the structural integrity of concrete dams.

This page was intentionally left blank

Executive summary

1 Introduction

It is now widely accepted that the earth's surface temperature is increasing due to anthropogenic greenhouse gas emissions. One impact of this climate change is an increased likelihood of extreme weather and climate events such as droughts, floods, wildfires, extreme temperatures, thunderstorms and rise in sea levels. The effects of climate change are thus potentially devastating to human beings, the environment, physical infrastructure and the economy. Thus, adaptation and mitigation measures are essential to minimise the negative effects of climate change.

South Africa is a water-scarce country and largely relies on water impounded by dams for its agricultural, domestic and industrial needs. There are more than 5 500 dams with a safety risk in the Department of Water and Sanitation's register and 132 of them are concrete arch dams. While the number of concrete arch dams is relative small, they account for 39% of the total capacity of all dams with a safety risk. In addition, 67% of the concrete arch dams have been categorised as having high consequences of failure (their failure would result in significant loss of life, high economic loss and inadequate water supplies). It is therefore paramount to ensure their safety.

Existing dams were not designed for changing climatic parameters and their associated effects. With dams generally designed to operate safely for at least 100 years, these structures will be exposed to climate change and its impacts. Compared to other types of dams, concrete arch dams are subject to significant thermal stresses induced by seasonal temperature variations. Not only is the magnitude of these stresses strongly dependent on the prevailing temperature conditions at the time of construction but also on the seasonal temperature range. A significant increase of temperature above temperature conditions during construction or an increase in the seasonal temperature range leads to an increase in thermal stresses which could compromise the structural integrity of the arch wall.

Swelling due to chemical reaction of the concrete (due to the reactions between aggregates and cement paste also known as alkali aggregate reaction (AAR) or alkali silica reaction (ASR)) represents another major load condition that, if present, will adversely affect the stress situation and integrity of a concrete arch wall. As the extent of the swelling is directly related to the temperature of the concrete, any increase in temperature due to climate change will also lead to an acceleration in swelling of the concrete. This in turn will lead to changes in the stress condition as well as an increase in the deterioration of the concrete structure. It is Important to note that swelling due to chemical reaction is irreversible and will ultimately lead to the loss of structural integrity in a concrete structure and subsequent failure.

With future temperatures expected to be higher than current temperatures, it is therefore important to investigate the implications of the increased temperature on the safety of concrete arch dams. This project focuses on the effects of 1) increased temperatures, 2) hydrostatic loads, and 3) swelling due to chemical reaction of the concrete on the safety of concrete arch dams.

2 Objectives

The implications of climate change on the structural performance and safety of concrete arch dams has not been quantified in South Africa. The main objective of this project is to quantify and evaluate the structural behaviour of concrete arch dams under various climate change scenarios. The specific objectives of the project are to:

- i) Identify South African climate change scenarios that would impact dam safety.
- ii) Identify potential failure modes of concrete arch dams.
- iii) Develop, calibrate and validate finite element models of concrete arch dams selected for the study.
- iv) Predict the structural behaviour of the dams subjected to current and future climates.
- v) Evaluate the effect of climate change on structural performance.

3 Methodology

3.1 Review of climate change scenarios for South Africa

The future climatic change scenarios were obtained from various in-depth studies carried out on climate projections for South Africa.

3.2 Identification of potential failure modes of concrete arch dams

The typical potential failure modes of concrete arch dams were identified from international best practice publications, including those of The International Commission on Large Dams, (ICOLD).

3.3 Evaluation of the behaviour of arch dams especially the effect of climate change

Two concrete arch dams namely, Roode Elsberg Dam located in the Western Cape and Kouga Dam located in the Eastern Cape, have been selected as case studies for this research. Both dams are double curvature concrete arch dams owned by the Department of Water and Sanitation and both have some monitoring records (both static as well as dynamic monitoring records) which were used in this project. In addition, Kouga Dam is subjected to swelling due to chemical reaction

since construction while Roode Elsberg Dam has not shown any signs of the reaction since completion.

Due to the complicated structural response of concrete arch dams, finite element models (FEM) are generally used to evaluate the current structural response as well as the future response of these structures. The proper calibration of these numerical methods is however of extreme importance as an incorrectly calibrated model will provide incorrect predictions of the structural behaviour. It is also important to note that effect of swelling due to chemical reaction were also included as a separate modelling component. The calibration of a finite element model is normally done in three distinct steps: 1) calibration of the dynamic properties, 2) thermal calibration, and 3) deformation calibration. Where swelling due to chemical reactions also plays a role an additional calibration step is added.

In this project the calibration of the dynamic properties was performed using the results of ambient vibration testing. The deformation calibration in turn used the results of the static monitoring (deformation monitoring). In the case of Kouga Dam the effect of the swelling due to chemical reaction was included. Due to unavailability of concrete temperature monitoring results for both dams, the thermal calibration was done using available ambient temperature results and careful tracking of the sun's path around the dam walls. The thermal modelling also requires appropriate climate information and heat conduction parameters for the concrete and the water body. Projections were made of the expected temperature and rainfall up to year 2050 based on information obtained from literature. Difficulties were experienced sourcing local climate information resulting in significant amounts of uncertainty in the predictions. These were mitigated by considering a range of temperature increases.

Once calibrated, the FEM models were used to determine the future behaviour of each of these dams for different climate change scenarios. It is important to note that for the purposes of this project only the change in temperature was considered. The impacts of flooding, sedimentation and heat waves were not evaluated.

The following climate change load scenarios were considered:

- i) Summer (high temperature) with the water level low – Scenario A;
- ii) Winter (low temperature) with high water level – Scenario B; and
- iii) Summer (high temperature) with high water level – Scenario C.

4 Results and observations

4.1 Future climate change scenarios for South Africa

Based on literature and the and the narrative methodology adopted by The Third National Communication (DEA, 2018), the following plausible climate change scenarios are expected in South Africa by 2050:

- i) Warmer (<3°C above 1961-2000) and wetter, with greater frequency of extreme rainfall events.
- ii) Warmer (<3°C above 1961-2000) and drier, with an increase in the frequency of drought events and somewhat greater frequency of extreme rainfall events.
- iii) Hotter (>3°C above 1961-2000) and wetter, with substantially greater frequency of extreme rainfall events.
- iv) Hotter (>3°C above 1961-2000) and drier, with a substantial increase in the frequency of drought events and greater frequency of extreme rainfall events.

4.2 Potential failure modes of concrete arch dams

Failure modes of concrete arch dams are generally associated with loss of strength and or water tightness of the foundation or the dam wall. At the foundation level, failure can be triggered by cracking and sliding, caused by stresses, hydraulic gradients, differential movement between foundation and wall, internal erosion, clogging of drains and degradation of grouting. Failure of the dam wall can be triggered by cracking, sliding and shearing caused by seasonal water level and temperature variations, swelling due to chemical reactions, shrinkage and creep and degradation of joints. The most prevalent failure modes of concrete arch dams are:

- i) Shear failure of the foundation
- ii) Shear failure of the concrete wall
- iii) Shear at the wall-foundation interface.
- iv) Buckling failure of the concrete wall
- v) Excessive cracking of concrete wall

4.3 Evaluation of the behaviour of arch dams under climate change

Finite element models of the two dams were successfully calibrated and validated using the combination of ambient vibration testing and deformation measurements. Computed dynamic properties and structural deformations were within 5% of the observed measurements.

From the analysis considering future effects of climate change the following was evident:

i) General

- a. Increases in temperature will result in the overall upstream displacement of the arch structure. Swelling due to chemical reaction will also have a similar effect.

ii) Kouga Dam

- a. Based on geodetic measurements taken on the dam wall since 1973, the dam wall has displaced upstream with largest displacement occurring on the right flank. This is largely attributed to increased compression forces induced by swelling due to chemical reactions. With increasing temperature due to climate change, this upstream displacement will continue to increase not only due swelling due to chemical reactions, but also due to temperature increases.
- b. For Scenario A the downstream tensile stresses due to the combined effect of temperature increase and swelling due to chemical reaction, will increase by about 25%. Therefore, under this loading scenario the cracking is expected to increase on the downstream face of the dam. AAR increases the compressive stress at the wall-foundation interface, thereby minimising the possibility of cracking at the wall-foundation interface.
- c. For Scenario B the tensile stress on the upstream side is reduced by about 25%. This is especially significant for the upstream side of the wall-foundation interface which is generally susceptible to cracking due to high tensile stresses. While there is a decrease in upstream tensile stresses, there is an equivalent increase in the thrust forces at the abutments resulting in increased shear stress which can lead to overstressing of the foundation that could trigger to shear failure.
- d. For Scenario C the effects of temperature increase and swelling due to ASR relive tensile stresses for both upstream and downstream faces of the dam wall. However, this scenario results in the highest thrust forces at the abutments, which could trigger shear failure.

iii) Roode Elsberg Dam:

- a. For Scenario A the downstream tensile stresses increase by about 16% for a 3°C temperature increase. Tensile stresses at on the dam wall will exceed 3MPa in future, which will lead to cracking and possible block separation.
- b. For Scenario B the tensile stresses on the upstream side of the dam are reduced by about 16%.
- c. For Scenario C the effect of temperature increase will relive both upstream and downstream stresses on the dam wall. The thrust forces at abutments will increase leading to concerns of shear failure at foundation level.

5 Conclusions

Based on the results of this study the following conclusions are drawn:

- i) Gradual temperature increase will lead to:
 - a. Increased thermal tensile stresses on the downstream side of the foundation-wall interface which could lead to cracking. However for dams subjected to AAR, this increase is negated by increased compression at this level.
 - b. Increased tensile stresses on the abutments, central part the wall and the crest level of the wall which could lead to cracking.
 - c. Increased thrust forces at foundation level and this can lead to foundation failure where the bedrock is heavily jointed.
 - d. Permanent displacements in the upstream direction causing increases in tensile stresses on the dam wall, downstream side of foundation-wall interface abutments and crest of level of the dam wall. This is exacerbated by the effect of swelling due to chemical reaction.
- ii) Global warming will lead to gradual deterioration of the structural integrity of concrete arch dams.
- iii) The evaluation of the effects of global warming on the structural integrity of concrete dams should consider the most prevalent failure modes which include: 1) shear failure of the foundation-wall interface, 2) shear failure of the wall, 3) sliding failure along abutments, 4) structural failure of wall.
- iv) Proper monitoring of concrete arch dams is essential for the behavioural analysis of the structure without which no opinion of the safety of the structure is possible.
- v) The availability of local climate data is essential for reliable climate change projections. Such data was lacking for this project.

6 Recommendations

It is recommended that a 'no regrets'-approach is adopted to mitigate against the impacts of climate change on dam safety of concrete arch dams as well as other types of concrete dams. To this end the following recommendations are made:

- i) Extend the study to investigate the effects of extreme events (flooding, heat waves, siltation) on the safety arch dams.
- ii) Extend the study to investigate other dam types.
- iii) Consideration should be given to include the effects of climate change in the safety evaluation of concrete arch dams.
- iv) Improve dam surveillance and monitoring program. Continuous monitoring of dams provides the necessary information to detect the onset of possible failure early. In addition to enabling early detection of adverse events, such information provide the basis for tracking the effects of climate change on dam safety. It is thus critical to ensure that data collection is done diligently and that all instrumentation is in working order all the time.
- v) Install weather stations and instrumentation to measure climate related data at each major dam site in South Africa. This is essential to provide site specific data for prediction of future climate, which was a major limitation for this project.

Acknowledgements

The authors gratefully acknowledge the Water Research Commission for funding the project and the Department of Water and Sanitation for supporting this project. We are especially grateful to Mr Wandile Nomqophu for managing the project efficiently and competently. The authors are indebted to members of the reference group for their critical input. There reference group members for this project were:

Mr Louis Hatting

Dr Sifiso Nhleko

Prof Mark Alexander

Prof Jan Wium

Dr Chris Lenard

Table of Contents

Summary.....ii

Abstract.....iv

Executive summary.....vii

Acknowledgementsxiv

1 Introduction1

1.1 Objectives of the study.....2

1.2 Research methodology.....2

 1.2.1 Review of climate change scenarios for South Africa.....2

 1.2.2 Identification of potential failure modes of concrete arch dams.....2

 1.2.3 Evaluation of the behaviour of arch dams.....3

2 Climate change scenarios for South Africa5

2.1 South African Climatic Regions5

2.2 Current South African climate6

2.3 Future South African climate.....7

 2.3.1 Climate change models.....7

 2.3.2 Climate change scenarios.....8

 2.3.3 Adaptation scenarios.....10

2.4 Impact of climate change on physical infrastructure.....11

2.5 Adaptation needs and research gaps for infrastructure13

2.6 Climatic conditions at sites of case studies.....13

2.7 Summary of climate change scenarios18

3 Failure modes of concrete arch dams19

3.1 Introduction.....19

3.2 Potential failure modes of concrete arch dams21

3.2.1	<i>Foundation failure</i>	22
3.2.2	<i>Loss of stability</i>	23
3.2.3	<i>Structural failure</i>	24
4	Case studies	25
4.1	Roode Elseberg Dam.....	25
4.1.1	<i>Instrumentation at Roode Elsberg Dam</i>	26
4.1.2	<i>Observations from dam monitoring systems at Roode Elsberg Dam</i>	29
4.2	Kouga Dam	34
4.2.1	<i>Dam monitoring</i>	35
4.2.2	<i>Observations from dam monitoring systems at Kouga Dam</i>	40
5	Finite element modelling, validation and validation	50
5.1	Roode Elsberg Dam model calibration and validation	50
5.1.1	<i>Model Geometry</i>	50
5.1.2	<i>Thermal load modelling</i>	51
5.1.3	<i>Hydrostatic load modelling</i>	52
5.1.4	<i>Calibration of the dynamic properties</i>	52
5.1.5	<i>Deformation calibration</i>	54
5.2	Kouga Dam model calibration and validation	56
5.2.1	<i>Model Geometry</i>	56
5.2.2	<i>Thermal load modelling</i>	57
5.2.3	<i>Hydrostatic load modelling</i>	58
5.2.4	<i>Aggregate Alkali Reaction</i>	58
5.2.5	<i>AAR Calibration</i>	61
5.2.6	<i>Calibration of the dynamic properties</i>	62
5.2.7	<i>Deformation calibration</i>	65
6	Structural performance under future climate	66
6.1	Future climate scenarios.....	66

6.2	Roode Elsberg dam.....	66
6.2.1	<i>Deformations</i>	66
6.2.2	<i>Stress distribution</i>	68
6.3	Kouga dam.....	73
6.3.1	<i>Deformation behaviour</i>	74
6.3.2	<i>Stress distribution</i>	75
7	Conclusions	81
8	Recommendations	82
9	References	83

List figures

Figure 2.1: South Africa’s climate regions. Source SANS 204-2.....	5
Figure 2.2: Köppen-Geiger climate classification (Conradie, 2012).....	6
Figure 2.3: Mean annual temperature over South Africa for the period 1961-1991. Source: DST (2010)	7
Figure 2.4: Mean annual rainfall over South Africa for the period 1961-1991. Source: DST (2010)	7
Figure 2.5: Plausible climate change scenarios (DEA, 2016d)	10
Figure 2.6: Flood risk on dams in South Africa. Source: DEA (2016a).....	13
Figure 2.7: Patensie Weather Station: Temperature 1993-2015.....	15
Figure 2.8: Worcester Weather Station: Temperature 1990-2015.....	16
Figure 2.9: Patensie rainfall: 1954-2017	17
Figure 2.10: Worcester rainfall: 1954-2017.....	17
Figure 3.1: Risk analysis process (Hartford & Baecher, 2004).....	20
Figure 3.2: Risk assessment framework (Hartford & Baecher, 2004)	21
Figure 3.3: Foundation discontinuities	22
Figure 3.4: Foundation failure.....	23
Figure 3.5: Sliding along abutment.....	23
Figure 3.6: Downstream erosion at spillway (FERC 1999)	24
Figure 3.7: Joint opening in arch dam	24
Figure 4.1: Roode Elsberg Dam located in Worcester Western Cape, South Africa	25
Figure 4.2: Roode Elsberg Dam plan	26
Figure 4.3: Geodetic measurement points viewed from downstream direction	26
Figure 4.4: Roode Elsberg dam: Positions of crack width gauges viewed from downstream direction	27
Figure 4.5: Weather station installed on the dam crest near the spillway.....	28
Figure 4.6: GPS network on Roode Elsberg dam.....	29
Figure 4.7: Accelerometers on the dam crest and data acquisition system in the upper dam gallery	29
Figure 4.8: Roode Elsberg Water level fluctuations since 1971	30
Figure 4.9: Roode Elsberg daily average ambient temperature	30
Figure 4.10: Roode Elsberg Water temperature and dam wall surface temperature.....	31
Figure 4.11:Roode Elsberg geodetic measurements at points 204 and 205	32
Figure 4.12: Roode Elsberg geodeitic measurements at points 202 and 207	32

Figure 4.13: Roode Elsberg displacement in the radial tangential direction plane near crest level	33
Figure 4.14: Roode Elsberg Air temperature and deformation variation with time.....	33
Figure 4.15: Roode Elsberg variation of 1 st natural frequency and water level with time	34
Figure 4.16: Roode Elsberg Water 1 st natural frequency vs water level.....	34
Figure 4.17: Roode Elsberg radial displacement at point 203 vs water level	34
Figure 4.18: Kouga Dam	35
Figure 4.19: Locations of thermometers on upstream face.....	36
Figure 4.20: Downstream general elevation of monitoring points	37
Figure 4.21: Kouga Dam GNSS/GPS Network (Pretorius et al., 2013).....	37
Figure 4.22: Kouga dam: Positions of crack width gauges viewed from downstream direction (DWS, 2019)	38
Figure 4.23: Trivec system components (Naude, 2002)	38
Figure 4.24: Locations of Trivec systems	39
Figure 4.25: AVM system.....	40
Figure 4.26: Trajectory of the Sun across the dam wall.....	41
Figure 4.27: Kouga Water level	41
Figure 4.28: Kouga flood condition	42
Figure 4.29: Lowest water level.....	42
Figure 4.30: Geodetic measurements	44
Figure 4.31: Schematic of permanent x-y displacement of dam wall	44
Figure 4.32: Displacement data for left flank (KG12)	45
Figure 4.33: Displacement data for right flank (KG13).....	45
Figure 4.34: Displacement and WL data for left flank	46
Figure 4.35: Displacement and WL data for right flank	46
Figure 4.36: Displacement vs Water Level	47
Figure 4.37: Displacement and Temperature data for left flank	47
Figure 4.38: Displacement and Temperature data for right flank	48
Figure 4.39: Displacement VS Temperature.....	48
Figure 5.1: Roode Elsberg FEM geometry	50
Figure 5.2: Roode Elsberg foundation partitioning.....	51
Figure 5.3: Sun's trajectory at Roode Elsberg Dam.....	52
Figure 5.4: Roode Elsberg Dam theoretical mode shapes.....	54
Figure 5.5: Roode Elsberg displacement.....	55

Figure 5.6: Roode Elsberg displacement in the radial tangential direction plane near crest level	56
Figure 5.7: Kouga Dam Finite element model geometry	57
Figure 5.8: Sun's trajectory at Kouga Dam	58
Figure 5.9: Normalised Expansion curve (Saouma, 2014)	59
Figure 5.10: Degradation of E and f_t' (Saouma & Perotti, 2006)	60
Figure 5.11: Calibrated expansion curve	61
Figure 5.12: AAR Calibration	62
Figure 5.13: Comparison of the first four modes extracted from the model and ambient vibrations tests	64
Figure 6.1: Roode Elsberg: Displacements of centre block for 1.5°C and 3°C temperature increases	67
Figure 6.2: Roode Elsberg: Radial displacements near crest level for 1.5°C and 3°C temperature increases	68
Figure 6.3: Roode Elsberg: Scenario A (summer with dam full) , current climate stresses	70
Figure 6.4: Roode Elsberg: Scenario B (winter with dam full) , current climate stresses	71
Figure 6.5: Roode Elsberg: possible crack locations	73
Figure 6.6: Kouga dam: Thermal displacements	74
Figure 6.7: Winter stress distributions	75
Figure 6.8: Thermal stress distributions	76
Figure 6.9: AAR and hydrostatic stress distribution	77
Figure 6.10: Kouga Dam possible crack locations	80

List of Tables

Table 2.1: Projected Provincial projections of rainfall and temperature by 2050: Baseline 1971-2003 (DEA 2016d)	10
Table 2.2: Weather stations.....	14
Table 3.1: Category classification of dams with a safety risk (SA Gov 2012).....	19
Table 3.2: Size classification (SA Gov 2012).....	19
Table 3.3: Hazard potential classification SA Gov 2012)	19
Table 4.1: Levels and height of Trivec systems	39
Table 5.1: Elastic material properties of Roode Eslberg Dam wall and foundation	51
Table 5.2: Thermal material properties used for the concrete wall.....	52
Table 5.3: Comparison of theoretical and measured natural frequencies for Roode-Elsberg Dam	53
Table 5.4: Linear elastic material properties of dam wall and foundation part.....	57
Table 5.5: Thermal material properties used for the concrete wall.....	58
Table 5.6: Kouga Dam AVT and FEM Natural Frequencies when Dam is full.....	63
Table 5.7: Kouga Dam measured and theoretical natural frequencies (Dam full)	63
Table 5.8: Seasonal radial displacement values.....	65
Table 6.1: Dominant tensile stresses.....	72
Table 6.2: Dominant compression stresses.....	72
Table 6.3: Foundation tensile stresses	72
Table 6.4: Wall tensile stresses.....	72
Table 6.5: Abutment tensile stresses.....	72
Table 6.6: Tensile stress at critical locations	78
Table 6.7: Compressive stress at critical locations	78
Table 6.8: Foundation tensile stresses	79
Table 6.9: Wall tensile stresses.....	79
Table 6.10: Abutment tensile stresses.....	80

This page was intentionally left blank

1 Introduction

The phenomenon of climate change and its negative effects on the earth is now widely accepted as a reality. Climate change is the ongoing change of the earth's weather conditions due to a gradual rise in the earth's surface temperature. The rise in the earth's surface temperature, also referred to as global warming is due to the formation and intensification of an insulating layer of gases in the atmosphere which reduces the amount of radiation of the sun's heat back to the atmosphere. This temperature rise destabilises weather patterns and leads to extreme events such as long periods of drought, wildfires, heat waves, storms, melting of ice in the polar regions, rise in sea levels and floods. These events inevitably lead to damage to physical infrastructure, compromised food and water security, increased waterborne diseases, adding to socio-economic challenges facing many countries. In order to minimise the impact of global warming, mitigation and adaptation measures are necessary across all sectors including physical infrastructure, water, biodiversity, agriculture and mining. DEA (2011) recommends three levels of climate change adaptation strategies namely, early warning and forecasting systems, medium-term climate forecasting and long-term climate projections. This requires ongoing updating of climate conditions informed by evidence-based scientific research.

In South Africa the largest cost increase incurred by the Government as a result of climate change effects will be due damage to infrastructure (DEA, 2011, DEA, 2016). It is expected that damage to infrastructure will account for approximately 0.6% of GDP representing the largest cost increase in all sectors including agriculture, forestry, biodiversity and ecosystems and wildlife. Therefore, it is important to develop measures to increase infrastructure resilience to the effects of climate change. This project seeks to develop an understanding of the impact of climate change on the safety of concrete arch dams in South Africa. Concrete arch dams impound 39% of the total volume of water in all dams in South Africa. With more than 65% of South Africa's water supply needs provided through dams, failure of any of these dams would severely compromise water availability in addition to possible loss of lives, environment damage and economic loss accompanying dam failure. Concrete arch dams are designed to resist the same loads as other types of dams except for temperature load which has a significant effect during the operation of arch dams. The temperature load results from the difference between the closure temperature of the dam (grouting temperature) and the prevailing temperatures during the operation of the dam. If this temperature difference is large, significant thermal stresses can be induced on the dam leading to cracking of the concrete wall. The design of concrete arch dams is detailed in U.S. Bureau of Reclamation (1977), U.S. Army Corps of Engineers (1994) and Pedro (1999).

With global warming due to climate change set to increase temperatures significantly, by 2050 (DEA, 2011), the safety of concrete arch dams maybe compromised. Thus the evaluation of the

safety of these dams under future climates, exhibiting higher temperatures is essential to inform future decisions and planning for any possible adverse effects.

1.1 Objectives of the study

The goal of this research is to evaluate the effect of the changing load models on concrete arch dams. Loading on concrete arch dams include, hydrostatic load from impounded water and silt, temperature effects and in some cases swelling due aggregate alkali reactions (AAR). These parameters are usually measured using monitoring systems installed on dams. A key element of the research is thus, to use available data from instrumentation installed on dams in conjunction with finite element models to evaluate the effect of the changing loading on the structural behaviour of concrete arch dams. The research will focus on the effects of temperature, water level and AAR on the long-term structural performance of concrete dams. The research will rely on climate change predictions available in technical literature. Specifically, the research aims to:

- i) Identify South African climate change scenarios that would impact dam safety.
- ii) Identify potential failure modes of concrete arch dams.
- iii) Develop, calibrate and validate finite element models of concrete arch dams selected for the study.
- iv) Predict the structural behaviour of the dams subjected to current and future climates.
- v) Evaluate the effect of climate change on structural performance.

1.2 Research methodology

In order to adequately assess the effect of climate change on the structural performance of concrete arch dams it was essential to establish the commonly agreed climate change scenarios for South Africa and use existing dams, with some information on their as built structural behaviour. Therefore, this project consisted of three main tasks described in the sections that follow.

1.2.1 Review of climate change scenarios for South Africa

The future climatic change scenarios were obtained from various in-depth studies carried out on climate projections for South Africa. The majority of these studies were carried out jointly by the Department of Environmental Affairs with various Research Councils and Universities.

1.2.2 Identification of potential failure modes of concrete arch dams

The typical potential failure modes of concrete arch dams were identified from international best practice publications, including those of The International Commission on Large Dams (ICOLD).

1.2.3 Evaluation of the behaviour of arch dams

Two concrete arch dams namely, Roode Elsberg Dam located in the Western Cape and Kouga Dam located in the Eastern Cape, have been selected as case studies for this research. Both dams are double curvature concrete arch dams owned by the Department of Water and Sanitation and both have some monitoring records (both static as well as dynamic monitoring records) which were used in this project. In addition, Kouga Dam is subjected to swelling due to chemical reaction since construction while Roode Elsberg Dam has not shown any signs of the reaction since completion.

Due to the complicated structural response of concrete arch dams, finite element models (FEM) are generally used to evaluate the current structural response as well as the future response of these structures. The proper calibration of these numerical methods is however of extreme importance as an incorrectly calibrated model will provide incorrect predictions of the structural behaviour. It is also important to note that effect of swelling due to chemical reaction were also included as a separate modelling component. The calibration of a finite element model is normally done in three distinct steps: 1) calibration of the dynamic properties, 2) thermal calibration and 3) deformation calibration. Where swelling due to chemical reactions also plays a role an additional calibration step is added.

In this project the calibration of the dynamic properties was conducted using the results of ambient vibration testing. The deformation calibration in turn used the results of the static monitoring (deformation monitoring). In the case of Kouga Dam the effect of the swelling due to chemical reaction was included. Due to unavailability of no concrete temperature monitoring results for both dams, the thermal calibration was done using available ambient temperature results and careful tracking of the sun's path around the dam walls. The thermal modelling also requires appropriate climate information and heat conduction parameters for the concrete and the water body. Projections were made of the expected temperature and rainfall up to year 2050 based on information obtained from literature. Difficulties were experienced sourcing localised climate information resulting in significant amounts of uncertainty in the predictions. These were mitigated by considering a range of temperature increases.

Once calibrated, the FEM models were used to determine the future behaviour of each of these dams for different climate change scenarios. It is important to note that for the purposes of the project only the change in temperature was considered in and not any of the other potential climate change impacts for example flooding and increase sediment loads.

The following climate change load scenarios were considered:

- i) Summer (high temperature) with the water level low – Scenario A;
- ii) Winter (low temperature) with high water level – Scenario B; and
- iii) Summer (high temperature) with high water level – Scenario C.

2 Climate change scenarios for South Africa

2.1 South African Climatic Regions

South Africa is broadly divided into six climatic regions with a temperate coastal climate in the south and west coast, sub-tropical climate in the east coast and interior climates ranging from cold climate along the central plateau to arid climate in the western region as shown in Figure 2.1 (SANS 204-2, 2008). This variation in the climate reflects the complex topology of the country and the region and the variety of currents that control weather patterns in Southern Africa. Conradie (2012) provide a more detailed so called Köppen-Geiger climate classification (Figure 2.2). This detailed classification is helpful in providing local climatic variations. For example, according to the SANS classification, the two case studies used in this research fall within the same climatic region, but the Köppen-Geiger classification clearly shows that one area receives winter rains while the other receives summer rains and their climates are not identical.

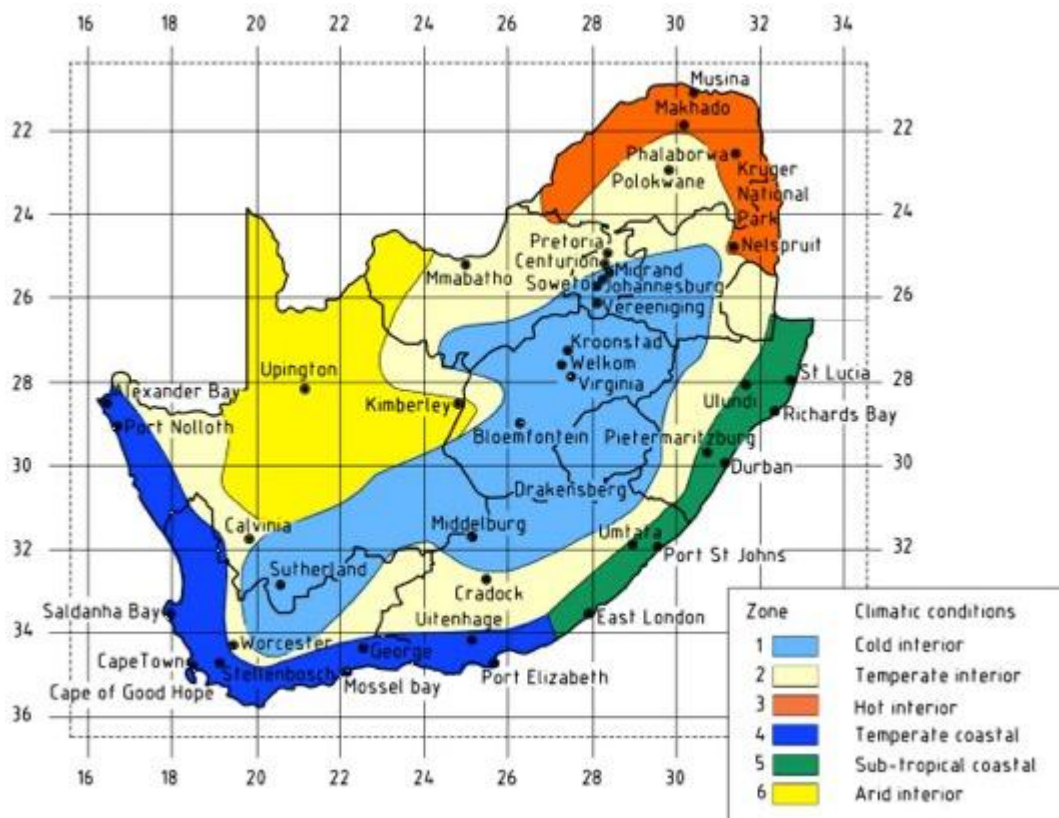


Figure 2.1: South Africa's climate regions. Source SANS 204-2

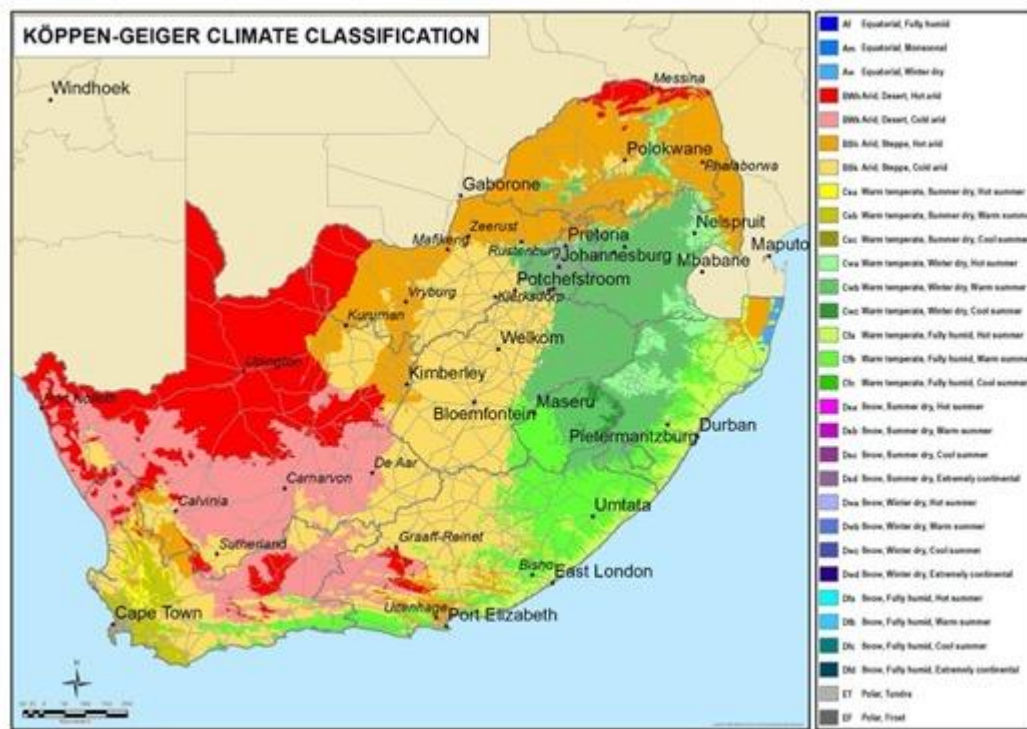


Figure 2.2: Köppen-Geiger climate classification (Conradie, 2012)

2.2 Current South African climate

The commonly used meteorological parameters for describing climatic conditions are temperature and rainfall. In this project the current South African climate is as described in DST (2010), in which the long-term weather conditions for the period 1961-1990 were used. South Africa has a predominantly subtropical climate characterised by high variability of weather and regional climates. This high variability of weather and climate, combined with complex local topology variations makes weather predictions and forecasting over South Africa particularly challenging (DST, 2010).

Figure 2.3 shows the distribution of South Africa's annual average temperature (DST, 2010) for the period 1961-1990. Most of the country exhibits a warm climate, above 17°C, with cooler weather on the southern and eastern escarpments and warmest weather in the Lowveld (KwaZulu-Natal, Mpumalanga and Limpopo), east coast, and the interior of the Northern Cape. Temperatures in coastal regions are largely moderated by the oceans, with warmer east coast dominated by the warm Agulhas current and cooler west coast significantly influenced by the cold Benguela current.

Figure 2.4 shows the average rainfall received in South Africa in the period 1961-1990 (DST, 2010). The map shows high variability in rainfall ranging from as low as 28 mm per year in the west coast to 1300 mm per year in the east coast. The west coast and western interior of the country are arid to semi-arid receiving less than 400 mm of rainfall per year. The eastern escarpment and pockets of the Southern Cape receive the highest rainfall.

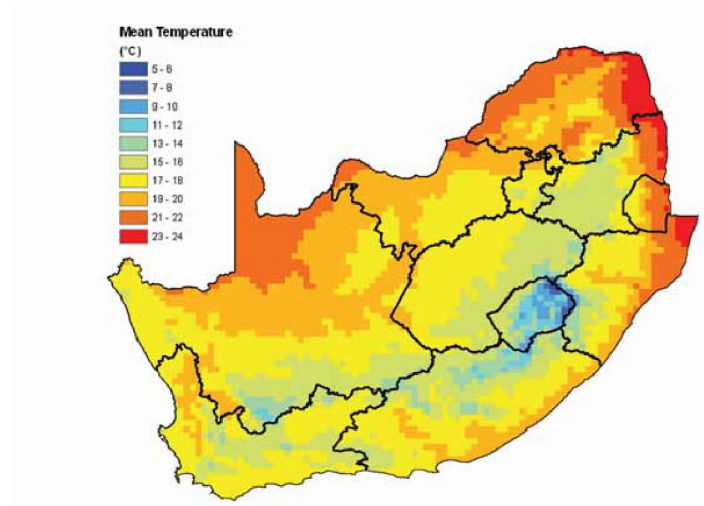


Figure 2.3: Mean annual temperature over South Africa for the period 1961-1991. Source: DST (2010)

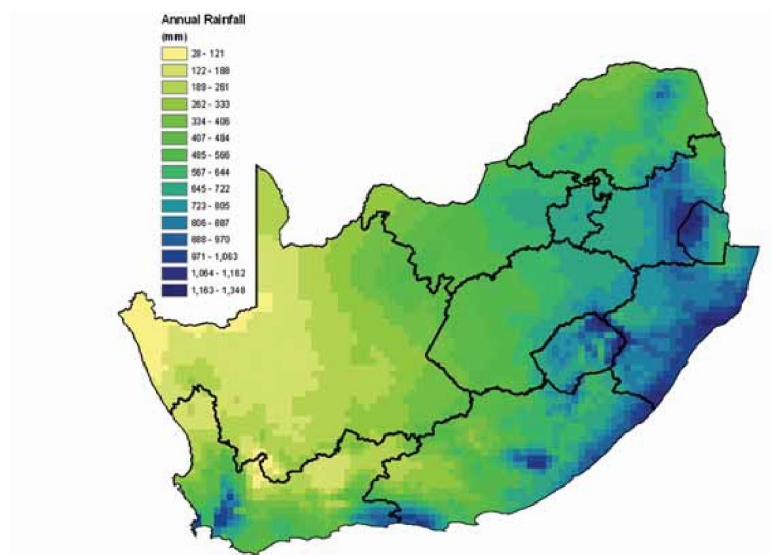


Figure 2.4: Mean annual rainfall over South Africa for the period 1961-1991. Source: DST (2010)

2.3 Future South African climate

2.3.1 Climate change models

Based on temperature observations, since records began in 1880, there has been a long-term increase on the earth's surface temperature (Seidel et al., 2008). It is widely accepted that this trend is driven by human activities, largely burning of fossil fuels and deforestation, which produce greenhouse gases, mainly carbon dioxide (CO₂) and water vapour. Global warming leads to climate change and accompanying severe weather patterns. The frequency of the extreme weather events such as storms, flooding, heat waves, etc. continues to increase globally, disrupting settlements, economic activities and threatening livelihoods. With continued industrial and population growth, the emission of greenhouse gases is unavoidable. However, mitigation measures are necessary to reduce greenhouse gas emissions to globally acceptable levels. This

requires sufficiently robust assessment of future climate and weather patterns. Global Climate Models (GCMs) are used for climate change projections. These models are based on atmospheric flow dynamics and laws of physics. While these mathematical models are complex and account for many variables, inherent uncertainties such as our limited understanding of flow dynamics and physics of the atmosphere and limitations in numerical modelling means that the outputs from these models contain uncertainties. Thus, interpretation of any climate change projections must be in the context of associated uncertainty levels. Common practice to minimise uncertainties inherent in GCMs is to combine a number outputs from different GCMs through ensemble averaging.

The projection of these parameters is based on agreed greenhouse gas concentration trajectories viewed as the most realistic scenarios (IPCC, 2013). There are four agreed representative concentration pathways (RCPs) for greenhouse gases namely, 1) RCP2.6 representing low concentration, 2) RCP4.5 – medium to low concentration, 3) RCP6.0 medium concentration and 4) RCP8.5 – high concentration (WRC and SAWS, 2017). Scenario RCP4.5 assumes active efforts to reduce greenhouse gas emissions to a ceiling by 2100 while RCP8.5 assumes no action is taken to mitigate against increasing greenhouse gas concentrations. The climate change projections for South Africa presented in this report are based on DST (2010) and WRC and SAWS (2017).

2.3.2 Climate change scenarios

2.3.2.1 DST (2010): Projection period 2070-2100: Base 1975-2005

The DST (2010) projections is based on the medium to high scenario of greenhouse gas concentrations for the period 2070 to 2100 compared to the period 1975-2005. 25th percentile, medium and 75th percentile was calculated for each period. The following mean temperature and mean rainfall projections were obtained for the period 2070-2100 using greenhouse gas concentration scenario RCP4.5:

- i) Temperature increase of more than 3°C over the central and northern interior regions (Appendix A: Map 1).
- ii) Temperature increase of about 2°C over the coastal regions (Appendix A: Map 1). Areas that receive summer rainfall will generally experience drier spring and autumn seasons and wetter summer (Appendix A: Map 2).
- iii) Increase in spring and winter rainfall over the eastern regions but a decrease over the north-eastern region (Appendix A: Map 2)
- iv) Decrease in winter rainfall over the south-eastern Cape region (Appendix A: Map 2).

2.3.2.2 WRC & SAWS (2017): Projection periods 2036-2095 & 2065-2095: Base 1976-2005

The latest climate change atlas of South Africa (WRC and SAWS, 2017) is based on RCP4.5 and RCP8.5 for periods 2036-2065 & 2066-2095 with models benchmarked using 1976-2005 data. In each case, 10th percentiles, 90th percentiles and median are reported. The following projections are expected by 2095:

For the RCP4.5 scenario (Maps 2, 3 & 4, Appendix B):

- i) The highest annual average (median) temperature increase of about 2.5-3°C is expected over the central and northern interior regions.
- ii) An annual average temperature increase of about 1.5-2°C is expected over the coastal regions.

Annual average rainfall is expected to decrease in most parts of the country except for the east coast and central interior, where annual average rainfall is expected to increase by up to 30-50 mm.

For the RCP8.5 scenario (Maps 5, 6 & 7: Appendix B):

The highest annual average (median) temperature increase of about 4.5-5°C is expected over the central and northern interior regions.

- i) An annual average temperature increase of about 3-3.5°C is expected over the coastal regions.
- ii) Annual average rainfall is expected to decrease in most parts of the country with some areas receiving 70-100 mm less than annual average. Pockets of areas in the east coast and central interior are expected to receive higher than annual average rainfall by up to 30-50 mm.

Both scenarios (RCP4.5 & RCP8.5) predict that: 1) the highest temperature increase will occur in spring (September, October, November) and autumn (March, April, May) respectively; 2) the highest rainfall increase will occur in summer (December, January, February) in the central and northern interior as well as east coast; 3) the western and parts of the southern Cape, which receives winter rains will experience a decrease in rainfall in all seasons.

2.3.2.3 DEA (2016d): Summary of climate change scenarios: Projection period 2001:2050: Base 1961:2000

DEA (2016d) provide the following as a plausible summary of South Africa's climate change scenarios up to 2050:

- i) Warmer (<3°C above 1961-2000) and wetter, with greater frequency of extreme rainfall events.
- ii) Warmer (<3°C above 1961-2000) and drier, with an increase in the frequency of drought events and somewhat greater frequency of extreme rainfall events.

- iii) Hotter (>3°C above 1961-2000) and wetter, with substantially greater frequency of extreme rainfall events.
- iv) Hotter (>3°C above 1961-2000) and drier, with a substantial increase in the frequency of drought events and greater frequency of extreme rainfall events.

These four scenarios are shown in Figure 2.5.

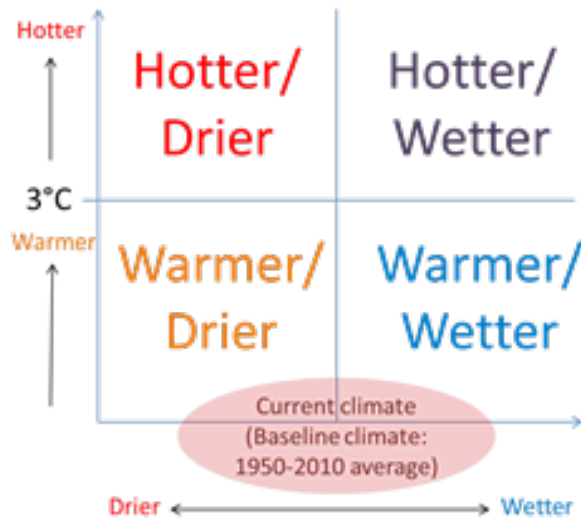


Figure 2.5: Plausible climate change scenarios (DEA, 2016d)

Table 2.1 shows projected provincial changes in rainfall and temperature by 2050 compared to the period 1971-2003.

Table 2.1: Projected Provincial projections of rainfall and temperature by 2050: Baseline 1971-2003 (DEA 2016d)

Province	Projected changes in rainfall (%)			Projected changes in temperature (°C)		
	10th	median	90th	10th	median	90th
Western Cape	-8.2	-1.5	2.0	2.9	2.6	1.3
Eastern Cape	-7.1	1.4	6.5	2.3	2.1	1.1
Northern Cape	-14.8	0.2	9.3	2.5	2.3	1.1
Free State	-9.0	1.9	9.1	2.8	2.7	1.5
Kwazulu Natal	-6.2	1.3	6.5	2.3	2.1	1.3
Northwest	-10.4	0.4	7.2	3.2	2.9	1.8
Gauteng	-7.9	0.6	5.8	2.9	2.5	1.6
Limpopo	-9.7	-0.6	5.2	2.9	2.5	1.6
Mpumalanga	-7.9	0.0	4.6	2.7	2.4	1.5

2.3.3 Adaptation scenarios

In order to respond effectively to the effects of climate change, adaptation strategies should be formulated on the basis of expected climate change situations and the country's development goals. Such strategies inform actions required to adapt to climate change as well as mitigate the

effects of climate change. While all the climate change projections agree broadly, their harmonisation to a common base is complex. DEA (2016d) proposes three adaptation scenarios.

- i) Adaptation Scenario 1: A warmer but drier climate in South Africa. Temperature increases of $< 3^{\circ}\text{C}$ and reduced rainfall. In this scenario, the frequency of droughts is expected to be high, resulting in water scarcity, and threats of wild fires.
- ii) Adaptation Scenario 2: A warmer but wetter climate in South Africa. Temperature increases of $< 3^{\circ}\text{C}$ and increased rainfall. This scenario is characterised by extreme rainfall events leading to flooding and damage to infrastructure.
- iii) Adaptation Scenario 3: A hotter climate in South Africa. Temperature increases of $> 3^{\circ}\text{C}$. In this scenario, intense heat accompanied by extreme weather conditions, and sea level rise is expected. Under this scenario, people, flora & fauna as well as infrastructure will struggle to cope.

2.4 Impact of climate change on physical infrastructure

Physical infrastructure such as dams, roads, bridges, buildings, water and waste water treatment plants, hospitals, schools support human livelihoods and economic activities. A compromise of the proper functioning of infrastructure always impacts human settlements and economic activities negatively. Global warming and climate change is shifting the climate and loading events to levels which were not considered at the time of their design and construction. For example, an increase in temperature would result in increased biological activities in water bodies leading to waterborne diseases if water treatment processes are not changed (DEA, 2011). These impacts can be viewed as long-term impacts and short-term impacts. Long-term impacts here refer to gradual changes in infrastructure performance due to long-term temperature and rainfall pattern changes. Examples would include long-term material deterioration, change in biological activity in water bodies, siltation of dams. Short-term impacts refer to damage to infrastructure caused by extreme events such as floods, storms and fires.

In South Africa the largest short-term impact on infrastructure is expected to be damage due to flooding (DEA, 2011; DEA, 2016b) as a result of increased occurrence of extreme events. In monetary terms, damage due to increased flooding events will cost an additional ZAR 3.5 billion per year compared to a projected amount of ZAR 670 million, in the absence of climate change (DEA, 2011). This is the largest cost increase in all sectors considered by DEA (2011) which include agriculture, forestry, biodiversity and ecosystems and wild life, accounting for approximately 0.6% of GDP. Thus well-defined adaptation strategies are necessary to minimise the negative impacts of climate change on physical infrastructure. DEA (2011) recommends three levels of climate change adaptation strategies namely, early warning and forecasting systems, medium-term climate forecasting and long-term climate projections. This requires ongoing

updating of climate conditions based on scientific research and supported by technological developments.

South Africa is already a water scarce country and largely relies on water impounded by dams for its agricultural, domestic and industrial needs. Climate change adaptation strategies are thus necessary to ensure that dams continue to provide water while remaining structural safe. This project is focused on developing strategies for minimising the impact of climate change on concrete dams, both in the short-term and long-term.

In the long term, the safety and performance of concrete dams is depended on the deterioration of concrete. Concrete deterioration is the progressive reduction in of concrete properties such as cross-section, young's modulus and density, which leads to failure in the service limit state such as excessive cracking, or failure in the ultimate limit state, dam collapse. The common deterioration mechanisms of concrete, relevant to South African environment are, alkali-aggregate reactions (AAR), sulphate attack, abrasion erosion and cavitation damage. Many dams in South Africa are subjected to AAR. This reaction occurs in the presence of water and is temperature dependent. A temperature rise will accelerate the reaction and longer periods of exposure of concrete to water ensures that the reaction continues. Concrete deterioration due to AAR leads to cracking of concrete and the reduction of young's modulus thereby compromising both serviceability and structural safety of dams. First observed in the 1940s this reaction was expected to slow down significantly 40-50 years after initiation. Current evidence (Sellier et al., 2017) shows that this is not the case for many dams, where the reaction continues after 60 years. In South Africa dams subjected to AAR in the central and northern interior as well as east coast regions would be of concern as these regions are likely to experience an increase in both temperature and rainfall. Thus owing to the uncertainties associated with the long-term effects AAR, this project will focus on developing a sound understanding of AAR using both numerical modelling and monitoring.

DEA (2016a) emphasises the importance of continuous monitoring of weather patterns to predict droughts and floods and thus enable communities to be disaster ready. Considering short-term climate change impacts, the reduction in the return period of extreme floods has been identified as posing the biggest risk to the structural integrity of dams (DEA, 2016a). It is projected that more than 900 dams will be exposed to high flood risk (DEA, 2016a) by 2050 (Figure 2.6). The consequences of failure of any of the dams would be devastating for communities and the economy. For key physical infrastructure, continuous monitoring should go beyond weather systems, to more dam specific structural monitoring systems. This will significantly improve the assessment of structural integrity and safety of dams prior and post extreme events as well as build a sound and realistic database for future projections of structural performance. A critical element of future projections of structural performance of dams under flood loading is the prediction of inflows into

the dams. While the impact of flood related inflows on the structural behaviour of dams can be captured using continuous monitoring systems installed on the dams, coupling the dams' response to predicted flood hydrographs would be ideal.

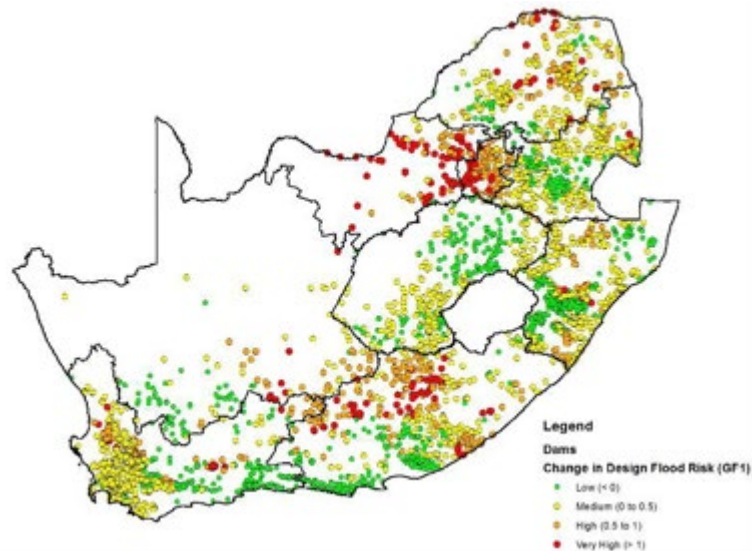


Figure 2.6: Flood risk on dams in South Africa. Source: DEA (2016a)

2.5 Adaptation needs and research gaps for infrastructure

DEA (2016d) recommends the following actions to mitigate climate change impacts on infrastructure:

- i) Improve existing early warning systems and disaster risk reduction approaches.
- ii) Mainstream climate resilience into urban, coastal and rural settlement design.
- iii) Build robust infrastructure with an understanding of long term versus short term costs & benefits

In addition to the recommendations for adaptation response DEA (2016d) identified research needs aimed at improving adaptation response.

- i) Drought and flood modelling
- ii) Identification of critical sections of infrastructure threatened by climate change
- iii) Review of design standards for infrastructure
- iv) Review of current dam operating rules in the context of increased probability of flooding

2.6 Climatic conditions at sites of case studies

According to the SANS map of South Africa's climatic regions, Figure 2.1, both dams are located within the temperate interior climate (Kouga dam (33.7333°S, 24.6000°E) and Roode Elsberg (33.4361°S, 19.5680°E). The Köppen-Geiger climate places Kouga Dam in a warm temperate

climate, fully humid and warm summer while Roode Elsberg has a warm temperate, dry and warm summer climate.

The two dams do not have weather stations located onsite. Typical weather was assumed to be similar to the nearest weather stations owned and managed by The South Africa Weather Services. Table 2.2 provides the details of the recording stations and recording period. Kouga dams has a catchment area of 3887 km² and Roode Elsberg has a medium sized catchment area of 139 km².

Table 2.2: Weather stations

Dam	Station	Location	Data Type	Period
Kouga Dam	Patensie	33.7653°S, 24.8233°E	Temperature	1990-2018
	Patensie-POL	33.7564°S, 24.4700°E	Rainfall	1954-2018
Roode Elsberg Dam	Worcester AWS	33.6200°S, 19.4700°E	Temperature	1990-2015
	Worcester AWS	33.6200°S, 19.4700°E	Rainfall	1954-2018

Figure 2.7 shows the maximum daily temperature, minimum daily temperature, average daily temperature and temperature range (maximum temperature minus minimum temperature) measured at Patensie Weather Station (about 25 km from Kouga Dam) in the period February 1991-December 2015. Temperature in Patensie reach a maximum value in February/March and a minimum value in August/September. The annual average temperature increased by about 0.4°C during the 22 year period. Both minimum and maximum daily temperatures increased over the period 1991-2015 and the temperature range (difference between daily maximum and daily minimum) remained unchanged.

Figure 2.8 shows the maximum daily temperature, minimum daily temperature, average daily temperature and temperature range (maximum temperature minus minimum temperature) at the Worcester Weather station for the period 1991-2015. During the period 1991-2015, maximum temperatures increased by about 0.4°C while minimum temperatures decreased by the same amount. An interesting observation from the temperature records from Worcester is the increase in the temperature range during this period from a maximum of about 24°C to a maximum of about 28°C. It is not clear whether this is related to instrumentation or real change in the temperature range

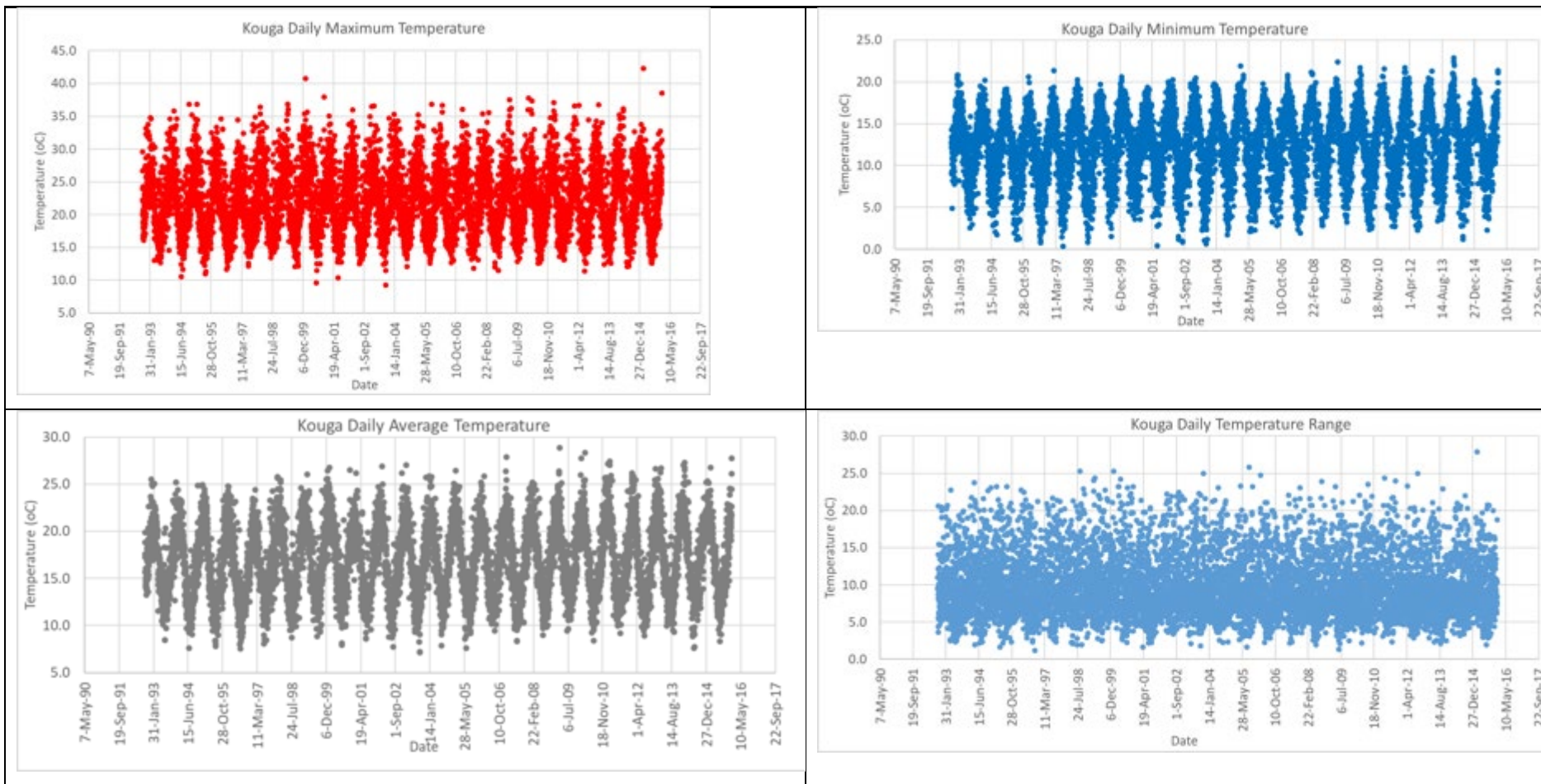


Figure 2.7: Patensie Weather Station: Temperature 1993-2015

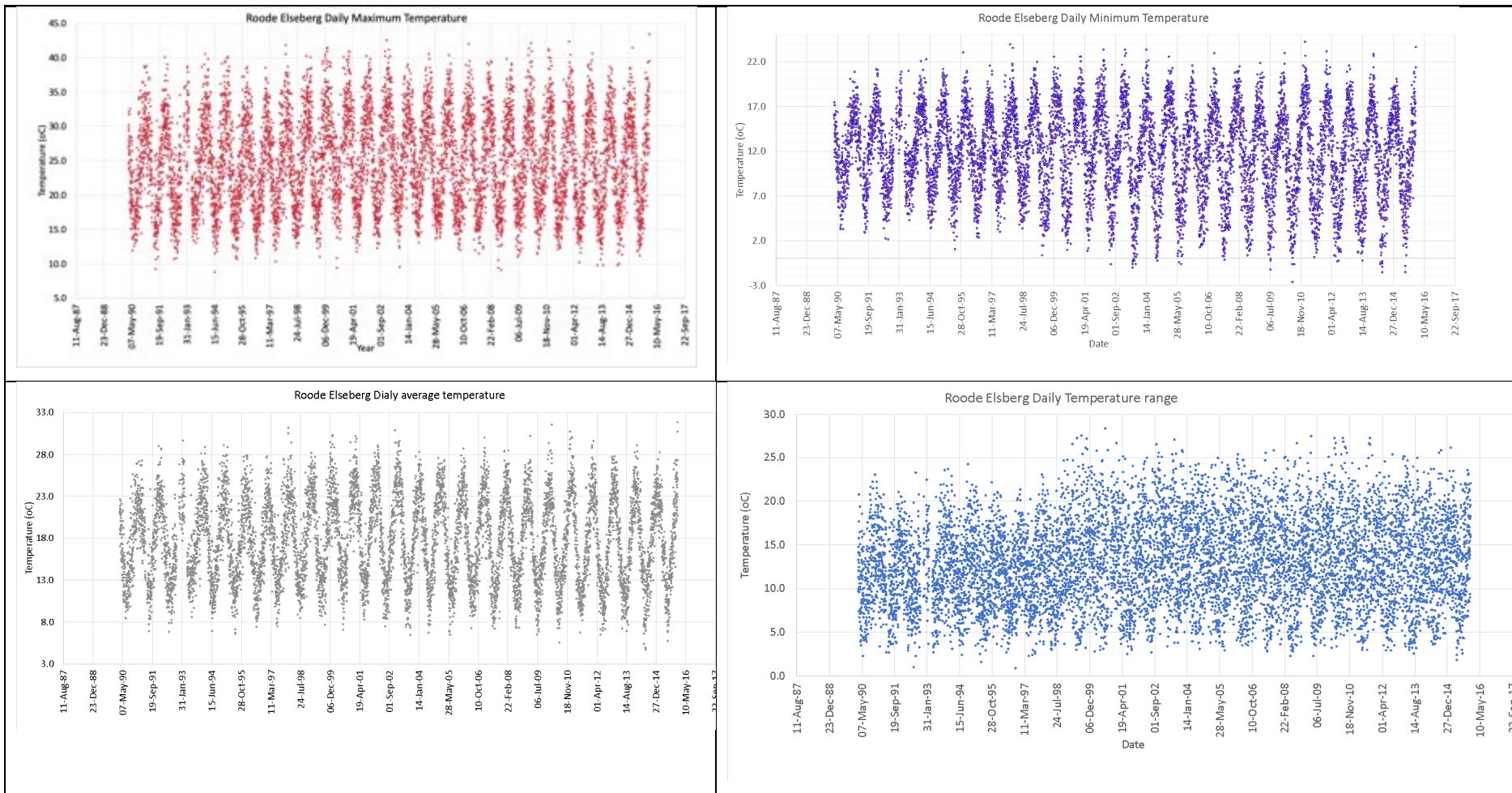


Figure 2.8: Worchester Weather Station: Temperature 1990-2015

Figure 2.9 shows the annual rainfall recorded at the Patensie Weather Station in the period 1954-2017. Rainfall pattern shows significant variability in the period 1955-1990 with spells of high rainfall and spells of very low rainfall (annual average of 365 mm per year). In the period 1991-2017, the annual rainfall is generally above 300 mm per year with dips in 2008 and 2017 (annual average 457 mm per year). The rainfall season for Patensie Valley is November to February.

Figure 2.10 shows the annual rainfall recorded at Worcester in the period 1954-2017. Three distinct periods can be observed from Figure 2.10, namely 1954-1976, 1977-1997 and 2001-2017. The average annual rainfall during these periods are 629 mm, 551 mm and 514 mm, which is a steady decrease in average annual rainfall from 1954 to 2017. Worcester receives most of its rains during the winter months (June, July August).

Rainfall patterns from both dams are consistent with climate change projections, that is, increase in rainfall in the Eastern Cape and reduction in rainfall amounts in the Western Cape.

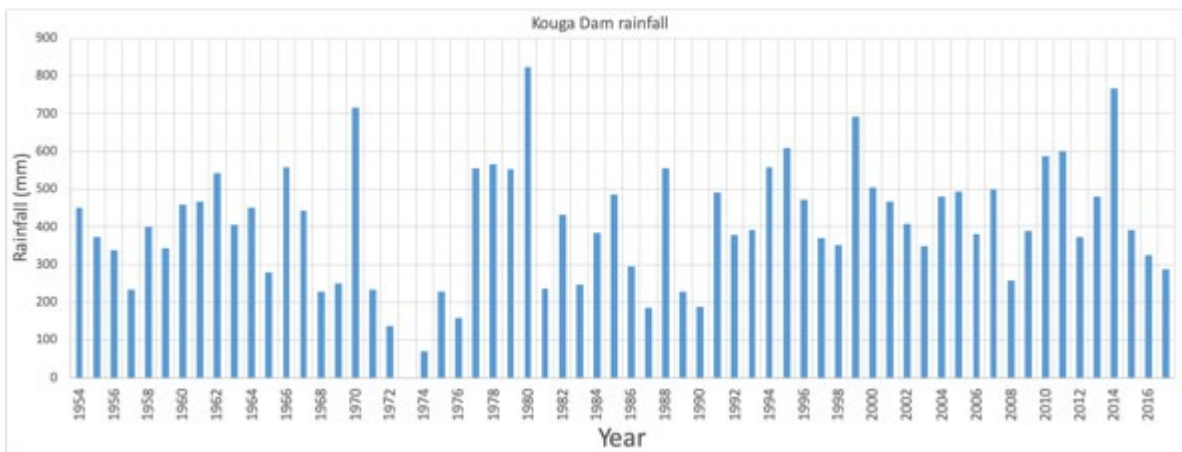


Figure 2.9: Patensie rainfall: 1954-2017

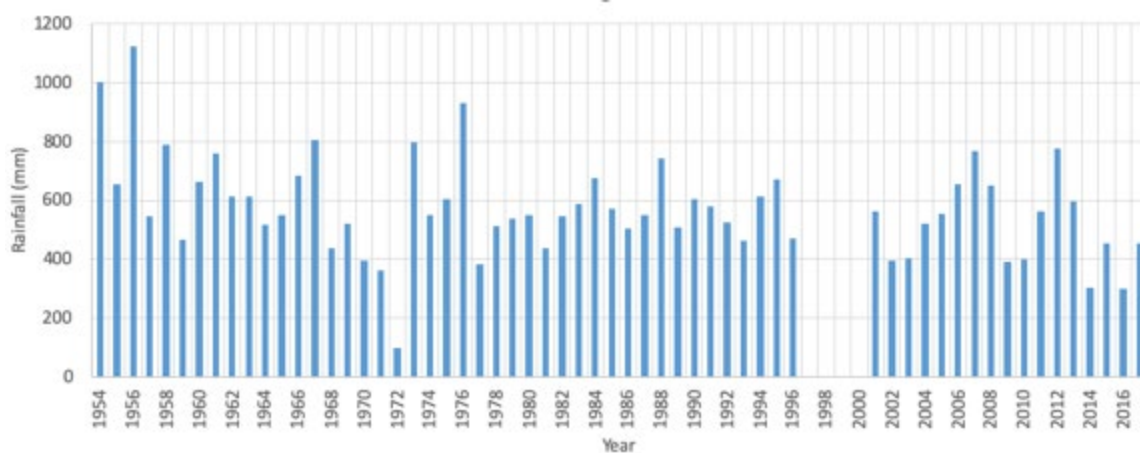


Figure 2.10: Worcester rainfall: 1954-2017

2.7 Summary of climate change scenarios

The South African climate is characterised by large variability, from temperature climate to semi-desert climates due to variability in topography and sea currents along coastal areas. Global warming is expected to lead to a temperature increase of up 3°C by 2050, compared to temperatures during the period 1961-2000.

Available temperature data for the selected dam sites is limited to a period of about 25 years. This is a short period to observe effective change in the climate. Therefore, while there are noticeable changes it cannot be concluded that they are due to climate change. On the other hand available rainfall data is for a period of about 60 years. Based on this data, Patensie Valley's average annual rainfall increased in the period 1990-2016, compared to earlier years, while Worcester's average annual rainfall has been declining since 1976.

3 Failure modes of concrete arch dams

3.1 Introduction

Dam failure is the major uncontrolled and unintended release of retained water, or an event whereby a dam is rendered unfit to safely retain water because of a total loss of structural integrity (UK Environment Agency, 2011). Dam failure would potentially lead to loss of life, economic activity and water scarcity. Given the severity of the consequences of dam failure, many countries have legislated dam safety management (ICOLD, 2017). In South Africa dam safety management is legislated under the Water Act (SA Gov 1998) and the associated regulations are given in SA Gov (2012). The regulations require dams to be classified according to the safety risk in terms of size and hazard potential, with three main consequences considered namely, potential loss of life, potential economic loss and potential adverse impact on resource quality. These classifications are summaries in Tables 3.1 to 3.3.

Table 3.1: Category classification of dams with a safety risk (SA Gov, 2012)

Size class	Hazard potential rating		
	Low	Significant	High
Small	Category I	Category II	Category II
Medium	Category II	Category II	Category III
Large	Category III	Category III	Category III

Table 3.2: Size classification (SA Gov, 2012)

Size class	Maximum wall height in (m)
Small	Less than 12 m
Medium	Equal to or more than 12 m but less than 30 m
Large	Equal to or more than 30 m

Table 3.3: Hazard potential classification SA Gov, 2012)

Hazard potential rating	Potential loss of life	Potential economic loss	Potential adverse impact on resource quality
Low	None	Minimal	Low
Significant	Not more than 10	Significant	Significant
High	More than 10	Great	Severe

The dam safety evaluation process specified in the South African Regulations require risk analysis and risk assessment including calculation of probabilities of failure. Figure 3.1 shows the typical

process followed in the risk analysis of dams. The first step is the identification of hazards. A hazard is a situation that may result in human injury, infrastructure damage and/or other undesirable effects, for example excessive deformations. Hazards can trigger dam failure through associated potential failure modes. For example, excessive deformations could result in loss of stability and structural failure of a dam. The second step in risk analysis is the identification of the potential failure modes associated with hazards. Once potential failure modes have been identified, the risk, i.e. the measure of the probability and severity of an adverse effect to life, health, property or the environment given by the product of probability of failure times cost (ICOLD, 2005) is estimated.

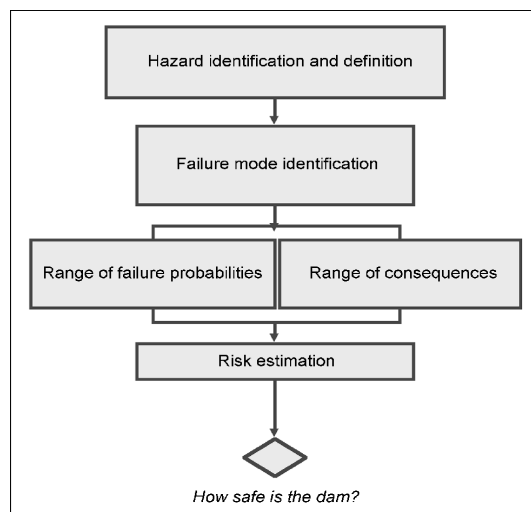


Figure 3.1: Risk analysis process (Hartford & Baecher, 2004)

The results of risk analysis provide a basis for making appropriate risk management decisions (Figure 3.2). More often, these decisions concern society as a whole and thus go beyond the need of the owners. Thus, it is essential to understand the different perceptions of societal groups and take into account the public’s concern. Tolerable risk is defined as risk within a range that society can live with so as to secure the benefits provided by the dam (US Bureau of Reclamation & US Army Corps of Engineers, 2015). Within the tolerable risk understanding, the “as low as reasonably practicable” (ALARP) principle has been developed and is used to qualify safety goals since absolute safety cannot be guaranteed as there will always be uncertainty. ALARP takes into consideration that risk reduction beyond a certain level may not be justifiable due to the cost of further risk reduction being disproportional to the benefits expected. In South Africa, the potential loss of more than 10 lives is classified in the dam safety regulations as high hazard potential.

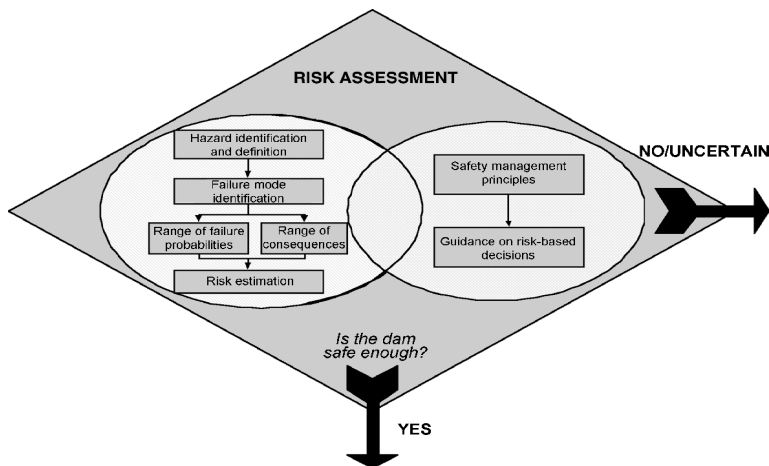


Figure 3.2: Risk assessment framework (Hartford & Baecher, 2004)

Risk analysis and risk assessment inform dam safety activities which include dam surveillance and non-engineering aspects. Dam surveillance activities include routine inspections, instrumented monitoring, structural analysis, special inspections and non-engineering aspects include the evaluation of the environmental, social, cultural, ethical, legal and political factors that may impact the safety of a dam. The end goal is to identify safety issues early before potential failure modes can initiate. In South Africa dam safety is an integral part of management of dams in operation.

3.2 Potential failure modes of concrete arch dams

A mode of failure is the mechanism by which a hazard leads to uncontrolled release of water retained in a dam. For example, high uplift pressures on foundation (hazard) can lead to sliding failure of a dam (failure mode). The correct identification and characterisation of potential modes of failure is perhaps the most critical exercise in risk analysis and dam safety assessment. Potential failure identification requires sound knowledge about site specific conditions of a given dam including the geology, flood risk, seismic activity, previous safety evaluations of the dam, dam operations, construction records for the dam, and instrumentation on the dam. Once a potential failure mode has been identified, the potential failure process must be fully traced and documented from initiation to eventual failure and the consequences of failure. The potential failure mode process has the ability to (FERC, 2017):

- i) Enhance the dam safety inspection process by helping to focus on the most critical areas of concern unique to the dam under consideration;
- ii) Identify operational related potential failure modes;
- iii) Identify structural related potential failure modes (e.g. piping) not covered by the commonly used analytical methods (e.g. slope stability, seismic analysis);
- iv) Enhance and focus the visual surveillance and/or instrumented monitoring program

- v) Identify shortcomings or oversights in data, information or analyses necessary to evaluate dam safety and each potential failure mode;
- vi) Help identify the most effective dam safety risk reduction measures; and
- vii) Document the results of the study for guidance on future dam safety inspections. By updating the documentation (as a living document), the benefit of increased understanding and insight lives on.

Failure modes of concrete arch dams are generally associated with loss of strength and or water tightness of the foundation or the dam wall. At the foundation level, failure can be triggered by cracking and sliding, caused by stresses, hydraulic gradients, differential movement between foundation and wall, internal erosion, clogging of drains and degradation of grouting. Failure of the dam wall can be triggered by cracking, sliding and shearing caused by seasonal water level and temperature variations, swelling due to chemical reactions, shrinkage and creep and degradation of joints. Lists of other threats and hazards that may trigger the failure concrete arch dams are given in Appendix C and Appendix D.

3.2.1 Foundation failure

Foundation failure of concrete arch dams is governed by discontinuities, faults and the strength rock shear strength (Figures 3.3). The presence of discontinuities and faults can result in loss of stability or local overstressing in the foundation. These weak zones in the foundation can lead to excessive differential displacement, seepage, increased uplift pressure and foundation failure (Figure 3.4). These hazards can be initiated by high flows, seismic events, and erosion at foundation level.

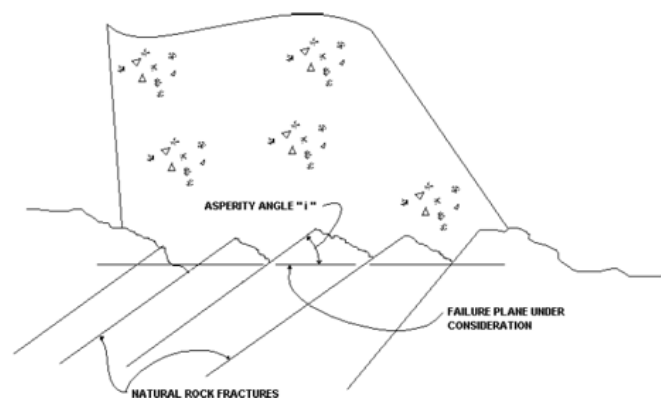


Figure 3.3: Foundation discontinuities



Figure 3.4: Foundation failure

3.2.2 Loss of stability

Loss of stability in concrete arch dams occurs when the design loads exceed the concrete, foundation or concrete-foundation interface strength leading to the dam sliding. Sliding occurs along planes of failure where the applied shear stress exceeds the resisting shear stress. The assessment of the potential for sliding should take into account all the external and internal forces acting on the dam, including dead loads. Internal forces include the hydrostatic uplift and, in some cases, forces due to internal chemical reactions. Uplift pressures exist between dam and its foundation, in contact planes within the foundation as well as cracks within the dam (Figure 3.5). In addition to the hydrostatic load, uplift pressures are affected by reservoir silt, seismic events and flooding.

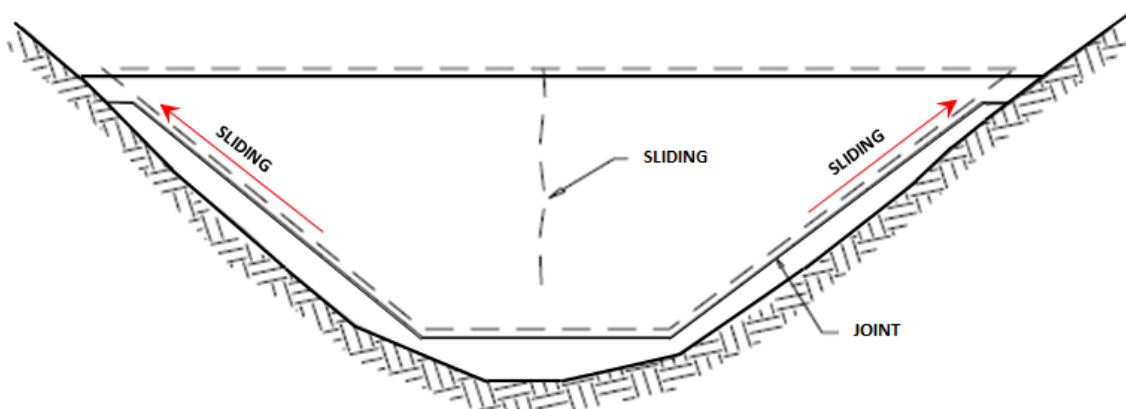


Figure 3.5: Sliding along abutment

While sliding failure is less likely in arch dams, inadequate shear strength at abutment thrust blocks, concrete deterioration due to alkali-aggregate reactions and downstream foundation erosion at spillways (Figure 3.6) should be carefully considered.

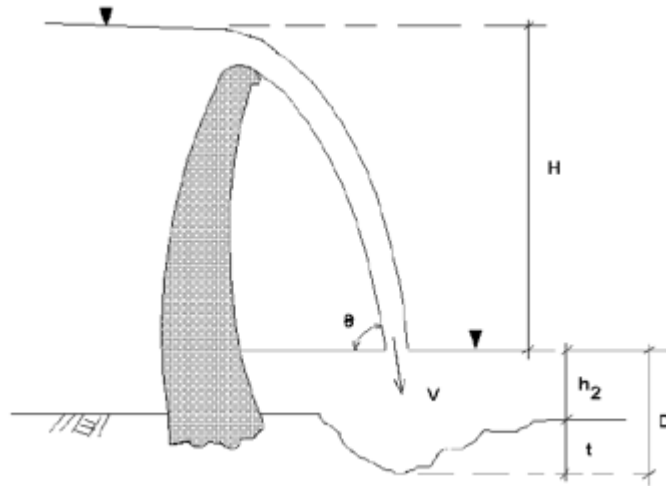


Figure 3.6: Downstream erosion at spillway (FERC 1999)

3.2.3 Structural failure

This mode of failure, also referred to as overstressing is mainly pertinent to concrete arch dams. The ultimate load carrying capacity of an arch dam is dependent on the compressive strength of concrete which is in turn influenced by tensile stress distribution. High tensile stresses lead to joint opening and extensive cracking (Figure 3.7) resulting in load redistribution. Such load redistribution may reduce the capacity of concrete to carry compression. Thus potential structural failure mode evaluation involves analysing the deformation (deflections and stresses) of concrete dams under static or dynamic loading which includes, dead loads, hydraulic loads, thermal loading, seismic loading and loading due to alkali-aggregate reactions.

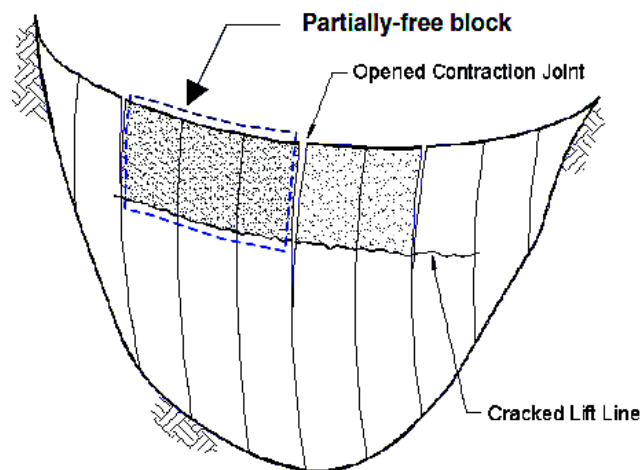


Figure 3.7: Joint opening in arch dam

4 Case studies

Two concrete arch dams namely, Roode Elsberg Dam located in the Western Cape and Kouga Dam located in the Eastern Cape were selected as case studies for this project. Both dams are double curvature concrete arch dams owned by the Department of Water and Sanitation and both have some monitoring records (both static as well as dynamic monitoring records) which were used in this project. In addition, Kouga Dam has been subjected to swelling due to chemical reaction since its completion in 1969 while Roode Elsberg Dam has not shown any signs of the reaction since completion in 1968.

4.1 Roode Elsberg Dam

Roode Elsberg Dam (Figure 4.1) lies in the Sanddrift River and is located at $33^{\circ}25'39''S$ latitude and $19^{\circ}34'01''E$ longitude which is 9 km west of the town of De Doorns and 30km north-west of the town of Worcester, in the Western Cape Province of South Africa. The dam is the lower of two storage dams built on the Sanddrift River to provide supplementary water for 2535 hectares of land under irrigation. A concrete lined tunnel, 1.98 m in diameter and 5.2 km long conveys the water from the dam to Hexriver Valley where distribution is by an enclosed pipe system (Department of Water Affairs, 1971).

The double curvature arch dam has a centrally located, uncontrolled spillway. The height of the dam from the lowest foundation level is 72 m and the reservoir capacity is 8.21 *million m³*. The dam was built with a pulvino pad which acts as cushion layer, assisting in distributing the load into the abutments and foundation. The dam was completed in 1968 (Department of Water Affairs, 1971)



Figure 4.1: Roode Elsberg Dam located in Worcester Western Cape, South Africa

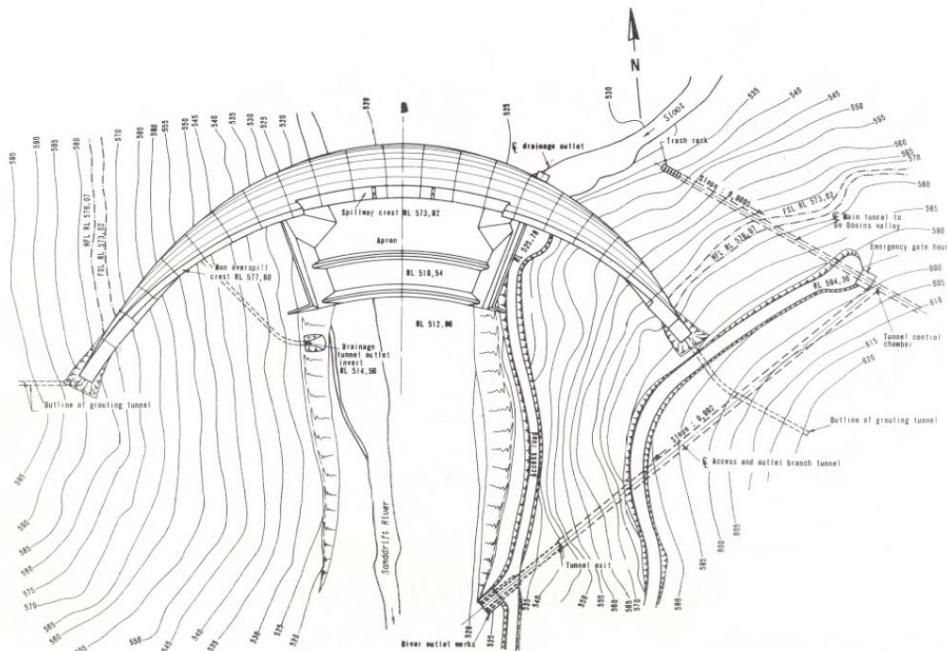


Figure 4.2: Roode Elsberg Dam plan

4.1.1 Instrumentation at Roode Elsberg Dam

A suite of static monitoring instrumentation has been in operation since 1984. They include, clinometers, geodetic survey targets, crack gauges as well as Trivecs. The latest additions in 2010 and 2013 respectively are: a continuously monitored GPS system and a continuous ambient vibration monitoring (AVM) system. In addition, there is a weather station to monitor the ambient conditions at the dam and also a set of temperature sensors to measure water temperatures.

4.1.1.1 Geodetic measurements

Displacements of Roode Elsberg have been monitored by Department of Water Affairs and Sanitation (DWA) using geodetic survey methods twice a year since 1984. Figure 4.3 shows the location of geodetic targets on the dam wall.

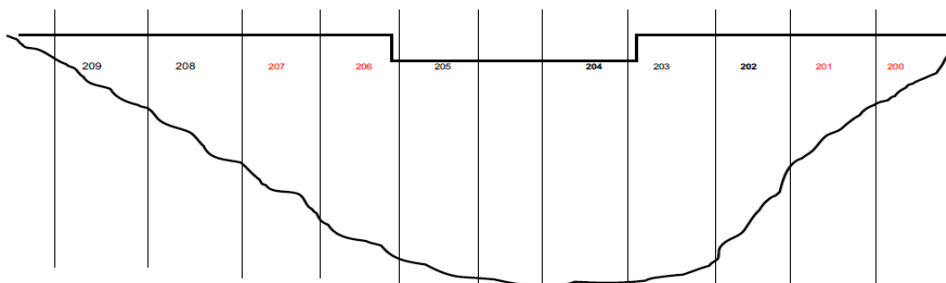


Figure 4.3: Geodetic measurement points viewed from downstream direction

4.1.1.2 Crack gauges

The Department of Water and Sanitation developed in-house crack width measuring devices in the 1990s, which were then implemented throughout the country (Oosthuizen et al., 2003). The three-dimensional crack width gauges are still used at Roode Elsberg Dam, and many other dams in South Africa, even though there has been an upgrade nationally to automatic crack width systems. The device allows the crack widths (translations) and relative rotations (tilt) to be measured across cracks or joints. The readings are manually recorded on a monthly basis with electronic digital indicator gauges. The accuracy of crack width gauges in the x (across the crack or tangential direction), y (vertical) and z (radial) directions is 0.02 mm. Figure 4.4 shows the location of crack gauges at Roode Elsberg Dam.

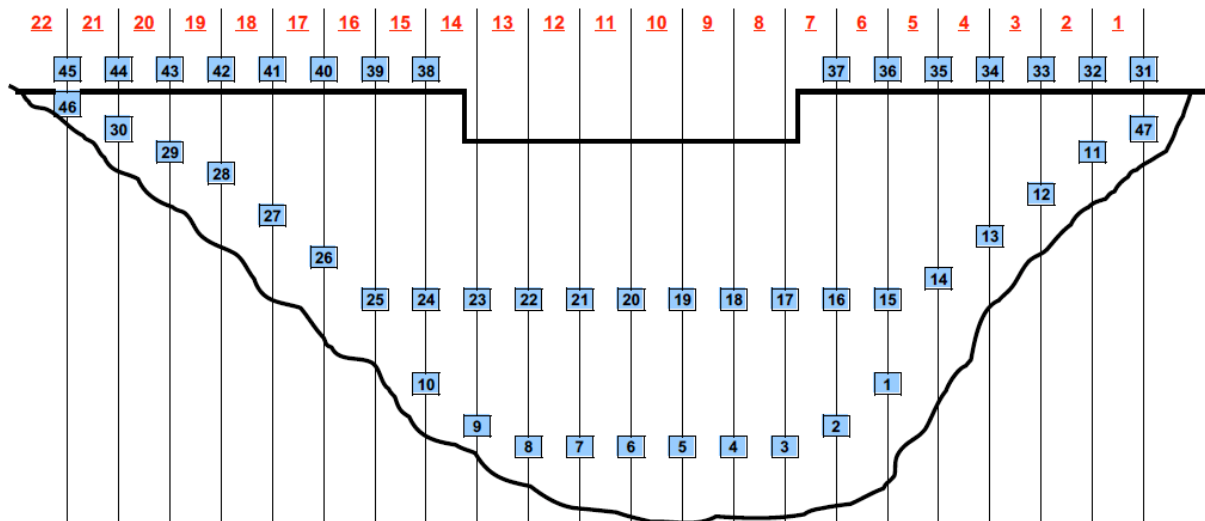


Figure 4.4: Roode Elsberg dam: Positions of crack width gauges viewed from downstream direction

4.1.1.3 Water levels

The fluctuation levels of the Roode Elsberg reservoir have been monitored on a daily basis since 1974.

4.1.1.4 Temperature monitoring

A weather station (Figure 4.5) was installed in November 2013, on the dam crest to measure ambient temperatures and there are thermometers that are embedded into the dam wall to measure reservoir water temperatures at different water levels.



Figure 4.5: Weather station installed on the dam crest near the spillway

4.1.1.5 GNSS

In 2010 the Department implemented an automatic deformation monitoring system on the dam using Global Navigation Satellite Systems (GNSS) as shown in Figure 4.6. The system comprises of the following:

Four GNSS receivers, each powered by solar energy and two 12 V batteries, two secondary sensors on the crest of the dam structure, one on each side of the spillway and two base station sensors up and downstream of the dam wall.

Poynting Wi-Fi network streaming all the receiver data to a server in a central control room.

The two secondary GNSS sensors on the crest of the dam wall (P203 on left flank and P206 on right flank) are used to calculate real-time kinematic positions of the points and to detect any sudden movement at the crest of the dam, as well as the base points. The two base GNSS sensors up and downstream of the dam wall are used as fixed stations. All the satellite data is accessible to DWS staff via a web interface.

Two base stations (Figure 4.6) were set up on the existing Geodetic Deformation network stations of the dam. These base stations are used as reference stations for the relative positioning in the post-processing mode. The base stations are occupied permanently in order to achieve high accuracy in the estimation baseline lengths between base stations.



Figure 4.6: GPS network on Roode Elsberg dam

4.1.1.6 Ambient vibration monitoring

The ambient vibration monitoring system consists of three force balance tri-axial accelerometers (Figure 4.7) with a dynamic range of more than 125 dB at ± 2 g full scale within a frequency range of 0.1 Hz to 200 Hz. The accelerometers are connected to a 24bit digitizer which communicates with the industrial computer. The data acquisition system (industrial computer and the digitizer) is placed on the dam wall inside the upper gallery of the dam to avoid any environmental effects (Figure 4.7). The data is sampled at 50 Hz and stored at hourly intervals.



Figure 4.7: Accelerometers on the dam crest and data acquisition system in the upper dam gallery

4.1.2 Observations from dam monitoring systems at Roode Elsberg Dam

Temperature data, water level, geodetic measurements and GPS measurements will be discussed for the purposes of this report.

4.1.2.1 Water level

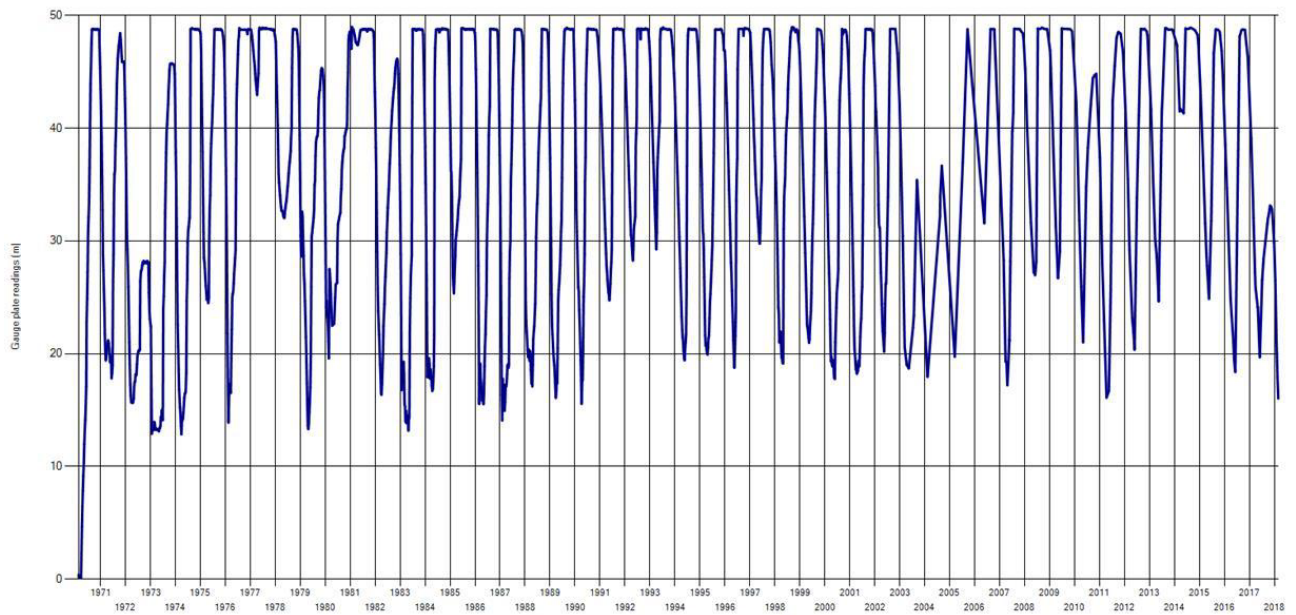


Figure 4.8: Roode Elsberg Water level fluctuations since 1971

Roode Elsberg dam's water level fluctuations (Figure 4.8) are characterised by high water levels in winter and low water levels in summer. The longest period of low water levels is between 2003 and 2005 where the water level was less than 35 m.

4.1.2.2 Temperature

The maximum average daily temperature recorded at the dam in the period January 2012 to August 2017 is 31.7°C (Figure 4.9) while the surface temperature of the dam wall reached 35°C during the same period (Figure 4.10). The maximum temperature of water recorded at Roode Elsberg is about 22°C. The water temperature is about 8°C cooler than the ambient temperature at Roode Elsberg dam.

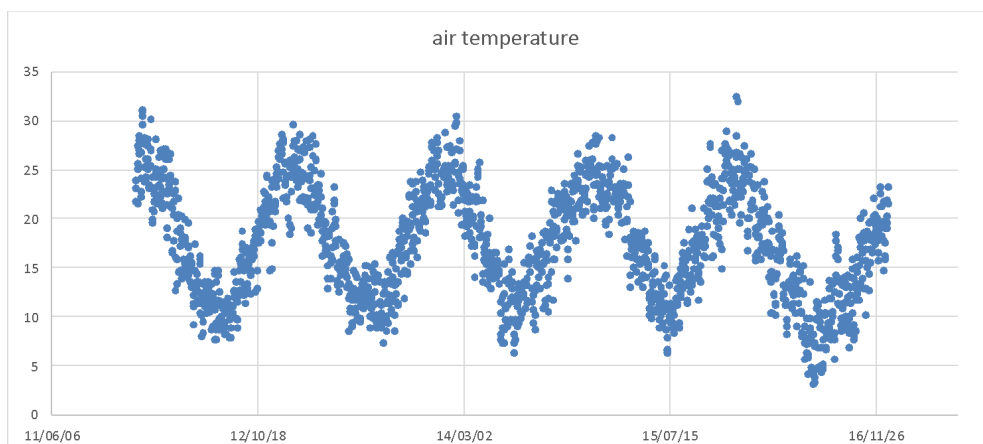


Figure 4.9: Roode Elsberg daily average ambient temperature

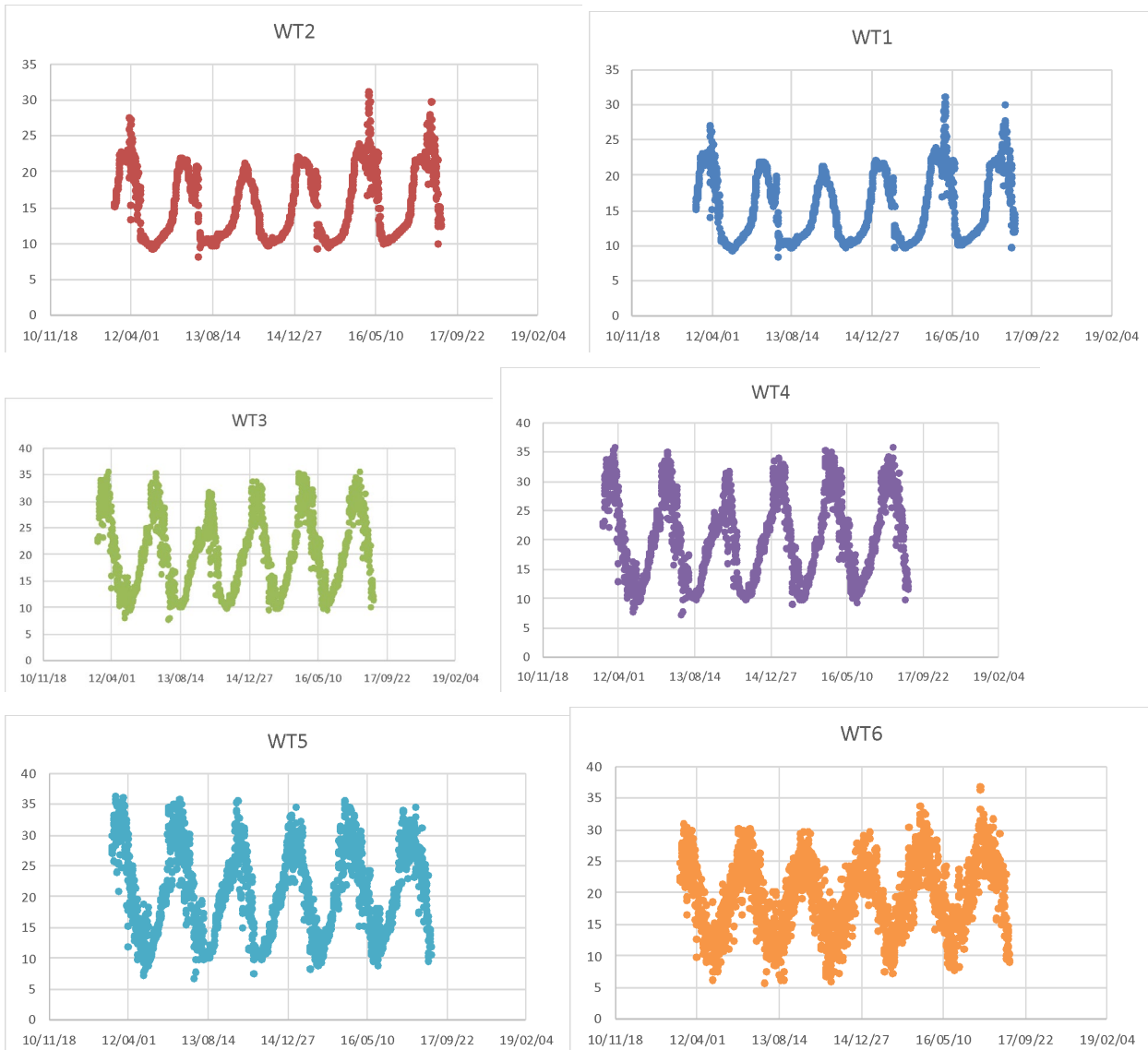


Figure 4.10: Roode Elsberg Water temperature and dam wall surface temperature

4.1.2.3 Geodetic measurements

The relative displacements in the x, y and z directions are shown in Figure 4.11-4.13. The following observations are made:

- i) Downstream trend on vertical displacements of blocks 204 & 205 since 1998 with minimal trends on radial and tangential displacements.
- ii) Trends on the displacement profile of blocks 202 and 207 show that these blocks are moving towards each other in the tangential direction and displacing in the downstream direction.
- iii) Since 1998 the dam has been rotating downstream with the left flank moving more than the right flank.

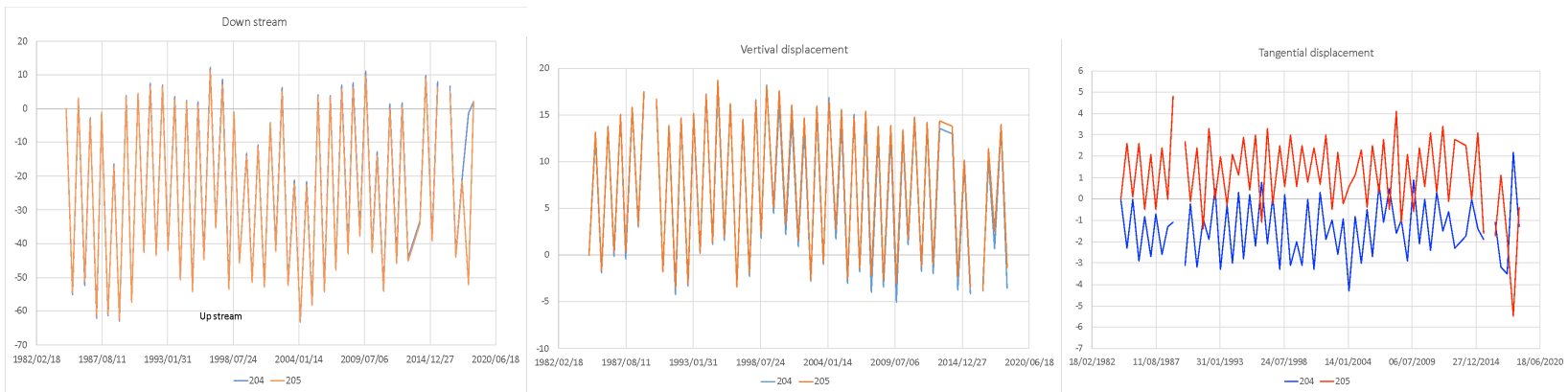


Figure 4.11: Roode Elsberg geodetic measurements at points 204 and 205

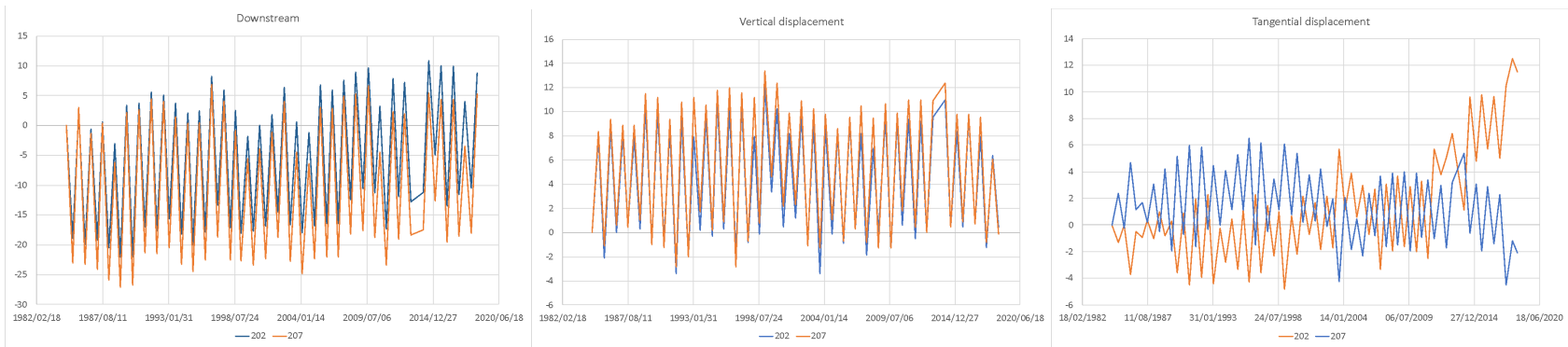


Figure 4.12: Roode Elsberg geodetic measurements at points 202 and 207

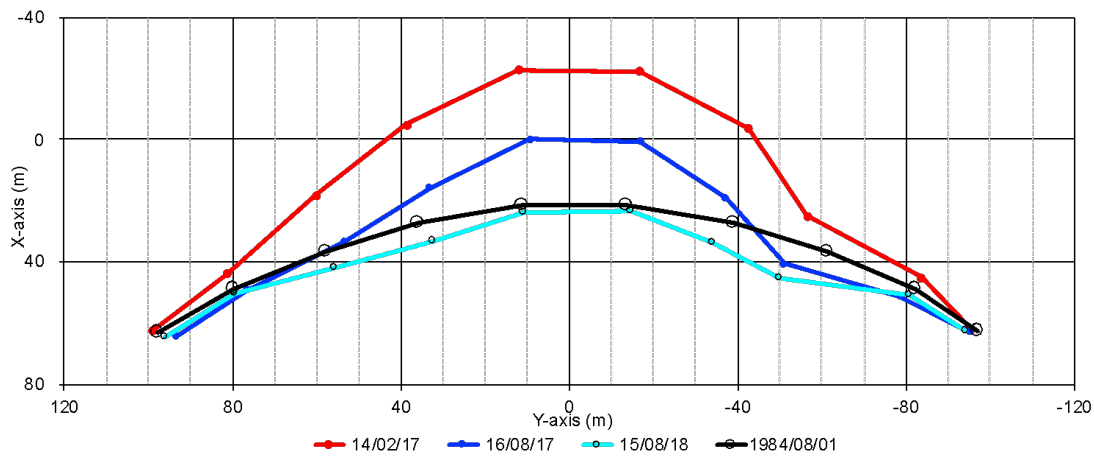


Figure 4.13: Roode Elsberg displacement in the radial tangential direction plane near crest level

4.1.2.4 Ambient vibration monitoring and GNSS

Ambient vibration and monitoring data span a period of only 5 years and hence there are no evident long-term trends in this data. These data however provide some insight into the behaviour of the dam under fluctuating water levels and seasonal temperatures. Figure 4.14 shows that there is a direct correlation between deformation of the dam and seasonal temperature variations. On the other hand, there is a direct correlation between water level and the natural frequencies of the dam. While the observations in Figure 4.14 and Figure 4.15 provide the general global behaviour of the dam under operating conditions, Figure 4.16 shows that the relationship between natural frequency and water level is not strong when water levels are below 30 m, while Figure 4.17 shows that there is a strong correlation between the deformations and the water level when the dam is filling-up. These relationships are exploited in this project in the development and calibration of finite element models of the dam.

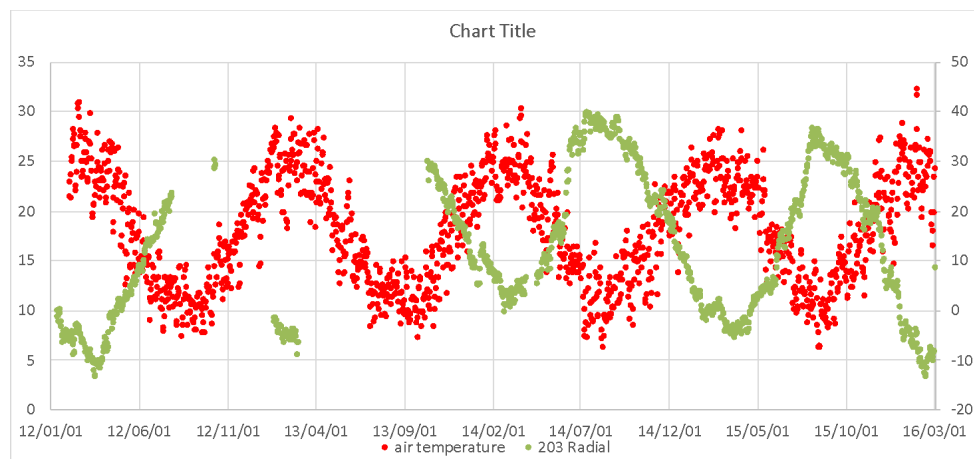


Figure 4.14: Roode Elsberg Air temperature and deformation variation with time

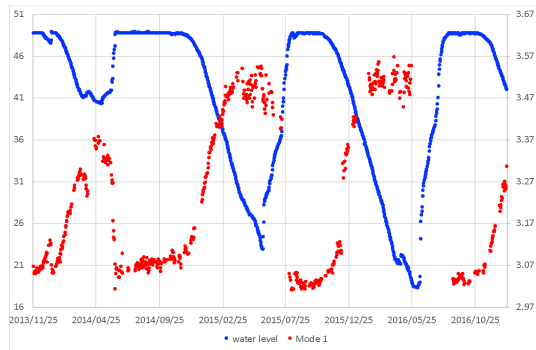


Figure 4.15: Roode Elsberg variation of 1st natural frequency and water level with time

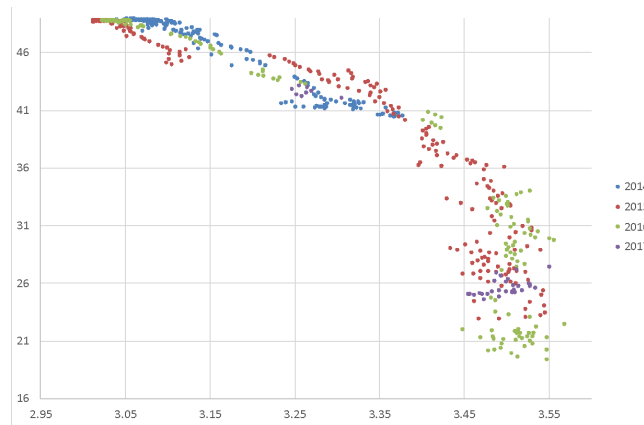


Figure 4.16: Roode Elsberg Water 1st natural frequency vs water level

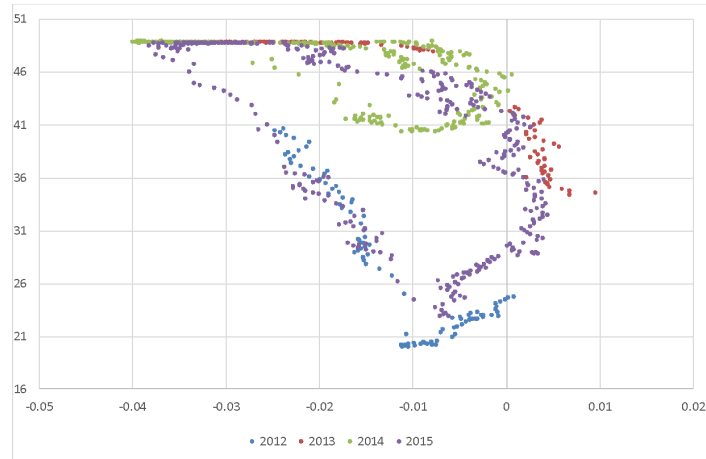


Figure 4.17: Roode Elsberg radial displacement at point 203 vs water level

4.2 Kouga Dam

Kouga Dam (Figure 4.18) is located approximately 27 km West of Patensie, on the Kouga River in the Eastern Cape Province of South Africa. The dam forms part of the Gamtoos River

Government Water Scheme (GRGWS). Kouga Dam primarily supplies water for irrigation to the Gamtoos River Valley and supplements the water supply to the Nelson Mandela Metropolitan. The double curvature concrete arch dam was designed and constructed by the, then Department of Water Affairs. The dam was constructed on a pulvino pad, which is a thicker layer of concrete included to assist in distributing the forces from the dam wall to the foundations. The dam was completed in 1969 (Egles et al., 1995). The initial design of the dam made provision for the possibility of future raising of the wall by up to 12 m, in order to increase the capacity to provide additional water supply to Nelson Mandela Metropolitan (Egles et al., 1995). The dam has a height of 69 m (full supply level to lowest foundation level) and a crest length of 317 m. The spillway system comprises of a centrally located, uncontrolled ogee spillway and a chute spillway on the left flank controlled by two radial gates. The outlet works which releases into a concrete channel is situated on the right flank.



Figure 4.18: Kouga Dam

4.2.1 Dam monitoring

The surveillance program on Kouga Dam started in the early 1970s. The extent of monitoring and range of instrumentation increased following the identification and confirmation that the dam is subject to alkali-aggregate reaction (AAR) (Egles et al., 1995). The main concern arising from AAR in the dam is the potential instability of the right flank resulting from the build-up of compressive forces due to swelling of the dam wall. Currently the following measurements are carried out on the dam.

4.2.1.1 Water Levels

The water level monitoring system consists of a gauge plate and a digital recording system. The gauge plate is read daily, while the digital recording system records data at least twice a day. The digital recording frequency is increased to one reading every fifteen minutes during a flood.

4.2.1.2 Temperature

A total of four thermometers were installed on the upstream face of the dam wall 2011. Two closer to the left flank, and two closer to the right flank. Figure 4.19 shows the approximate locations (red dots) of the thermometers. The exact height of the thermometers could not be verified, however it is speculated to have been installed approximately at the gallery level. Temperature readings are recorded 4 times per day (6-hourly).

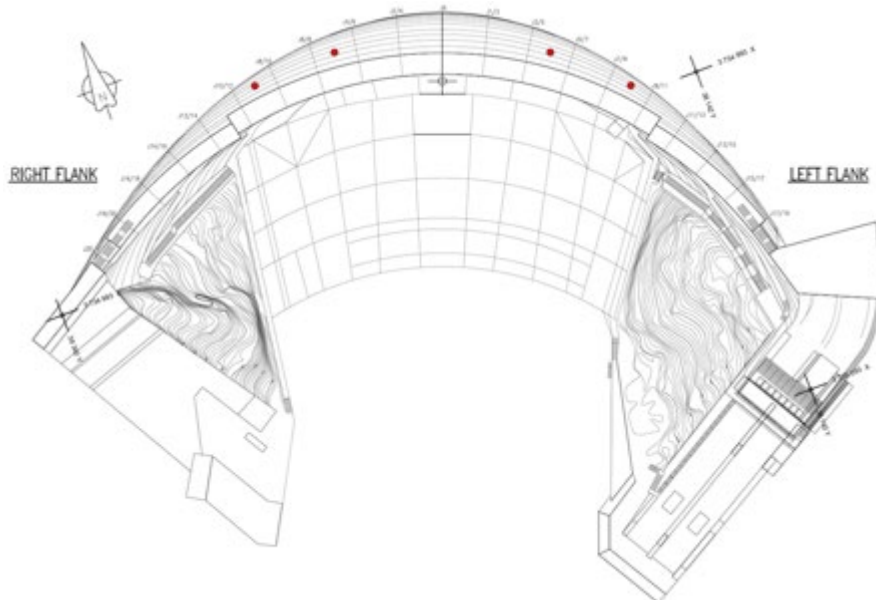


Figure 4.19: Locations of thermometers on upstream face

4.2.1.3 Geodetic Network

Geodetic measurements have been carried out since 1972 to track the deformation behaviour of the dam. The system uses a triangulation network of beacons and targets on the downstream face of the dam wall, complimented by precise traverse measurements within the gallery. The final results are three-dimensional displacements of the monitoring points. The accuracy in the x and y directions are approximately 0.3-0.5 mm, while that of the z (vertical) measurements are 0.1-0.2 mm (Pretorius et al., 2001). Figure 4.20 shows the location of measurement targets for geodetic surveys. The geodetic surveys are carried out twice a year, during summer (February-March) and again during winter (August-September).

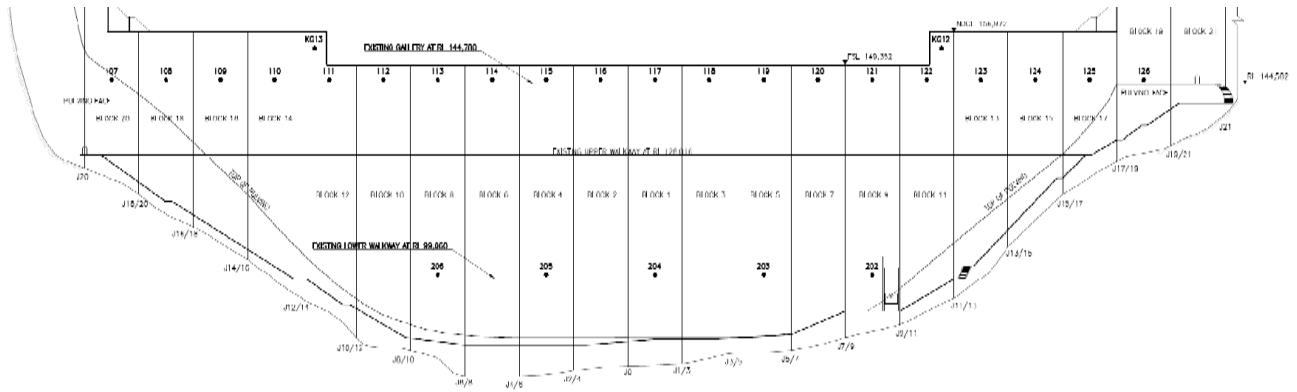


Figure 4.20: Downstream general elevation of monitoring points

4.2.1.4 GNSS/GPS

The GNSS/GPS was installed in 2011 and provides continuous monitoring of deformation in the x, y and z directions. Deformation readings are recorded once every month, allowing the behaviour of the structure to be observed in much more detail compared to the geodetic survey data, which only allows for data points every six months.

The installation layout includes two primary base sensors in the surrounding area of the dam structure, two secondary sensors on the dam structure and a server located in the outlet house. The base stations are used as reference stations for the relative positioning during post-processing. The two secondary sensors are positioned adjacent to the overspill section on the dam wall. The layout is shown graphically in Figure 4.21.



Figure 4.21: Kouga Dam GNSS/GPS Network (Pretorius et al., 2013)

4.2.1.5 Crack width gauges

Three-dimensional crack width gauges measuring crack widths (translations) and relative rotations (tilt) have been in operation since 1991. Figure 4.22 shows the location of crack gauges

at Kouga Dam. Until 2015, the readings were manually recorded on a monthly basis with electronic digital indicator gauges. The accuracy of crack width gauges in the x (across the crack or tangential direction), y (vertical) and z (radial) directions is 0.02 mm for all translations

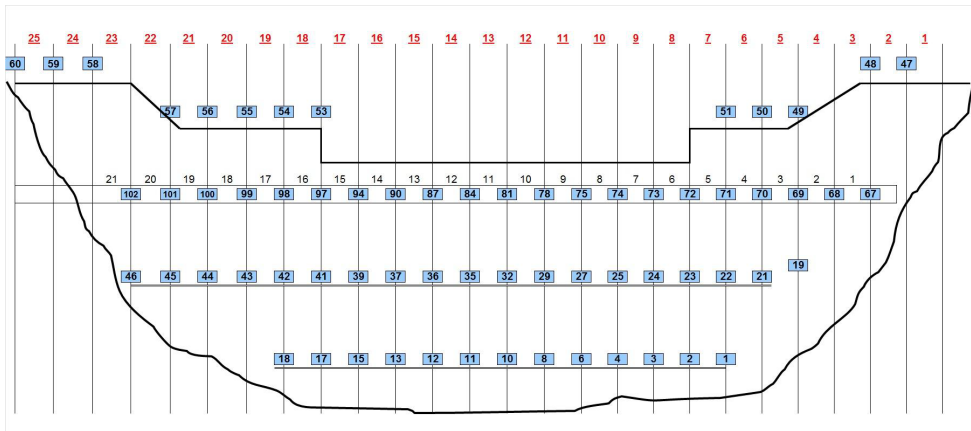


Figure 4.22: Kouga dam: Positions of crack width gauges viewed from downstream direction (DWS, 2019)

4.2.1.6 Trivec

The Trivec system measures the relative displacements in three directions (x, y and z) at 1 m intervals along a vertical borehole. UPVC tubes which are connected with stainless steel measuring couplings are installed within the borehole, and grouted into position. A measuring probe is lowered into the casings and records the displacements in all three directions at the various measuring points. The first set of readings acts as the baseline data set, to which the future readings are compared. The measurements are done bi-annually, once during summer, and another during winter. The equipment used for the system is shown in the Figure 4.23

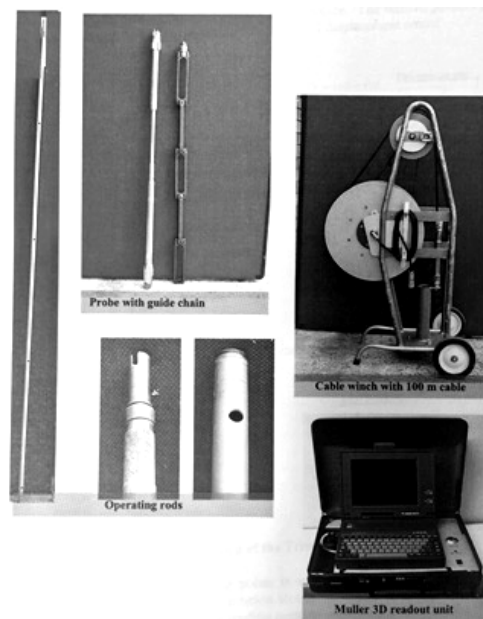


Figure 4.23: Trivec system components (Naude, 2002)

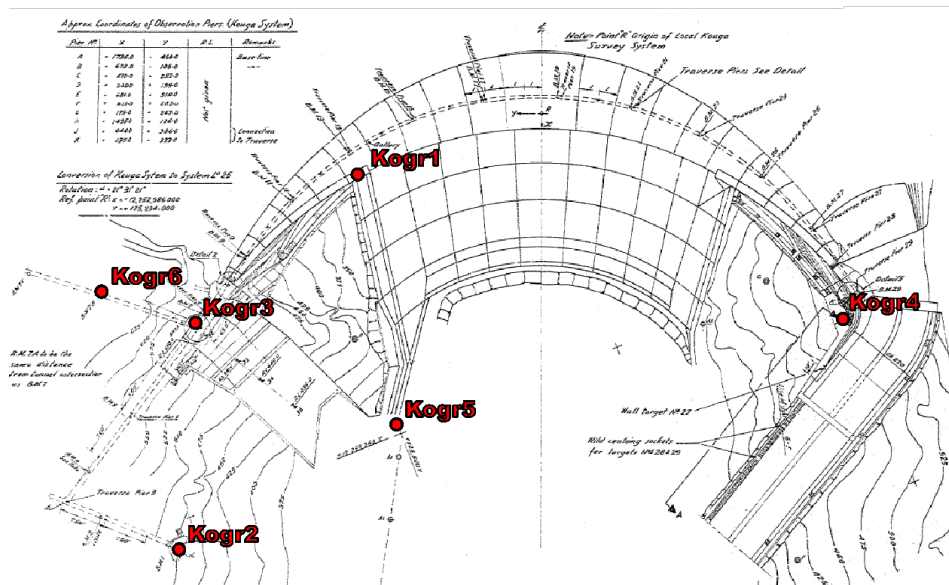


Figure 4.24: Locations of Trivec systems

Figure 4.24 shows the location of Trivec boreholes. Kogr1 is the only probe which has been installed through the dam wall, and extends approximately 25 m into the foundation. Kogr2 and Kogr5 are located on the right flank, and Kogr4 is on the left flank. Kogr3 and Kogr6 were installed in the lowest main inspection tunnel on the right flank. The installation level (highest measuring point on Trivec), and height of the boreholes are given in Table 4.1.

Table 4.1: Levels and height of Trivec systems

Trivec System	RL (m)	Height (m)
Kogr1	156.9	87.2
Kogr2	144.8	47.6
Kogr3	103.6	33.5
Kogr4	140.2	54
Kogr5	99.1	47
Kogr6	103.6	49

4.2.1.7 Ambient Vibration Monitoring

Following three years of exploratory work on the use of ambient vibration monitoring (AVM) in dams, was installed at the gallery level in 2011. The permanent AVM system consists of 24 AC-2x tri-axial accelerometers, a 24bit digitizer and an industrial PC (Figure 4.25).



(a) Accelerometer



(b) digitiser



(c) PC

Figure 4.25: AVM system

4.2.2 Observations from dam monitoring systems at Kouga Dam

Temperature data, water level, geodetic measurements and GPS measurements will be discussed for the purposes of this report.

4.2.2.1 Temperature

The dam spans approximately East to West between a narrow valley, along the Kouga River. Therefore, the upstream side of the dam wall is North-facing, resulting in the un-wetted portion of the upstream wall being constantly exposed to direct sunlight during the day. Conversely, the downstream side of the wall is in constant shade. Figure 4.26 shows the position of the dam wall within the valley and the trajectory of the Sun.



Figure 4.26: Trajectory of the Sun across the dam wall

4.2.2.2 Water level

The dam has experienced, periods of flooding and periods of drought since it started impounding water in 1969 as shown in Figure 4.27. The most prominent flooding occurred in the period April 1981 to July 1982 and the dam was near full throughout this period (Figure 4.28). The lowest water level was recorded in May-December 2018 (Figure 4.29).

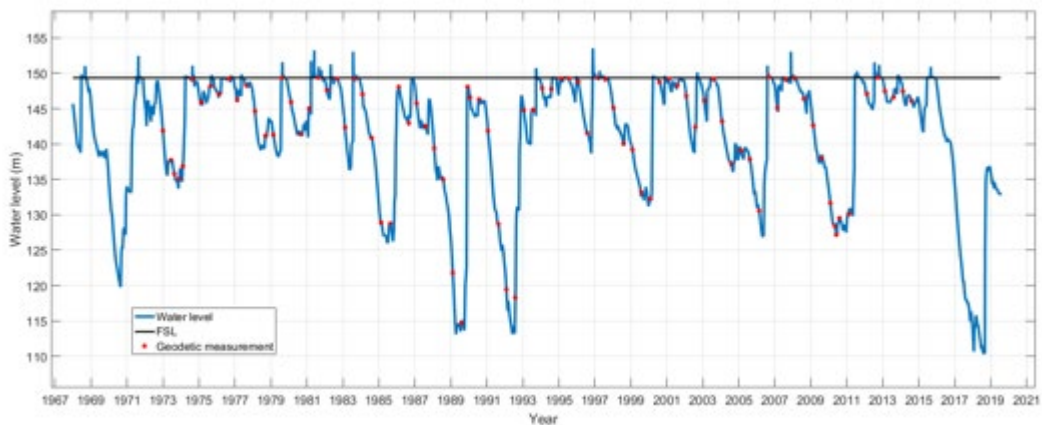


Figure 4.27: Kouga Water level

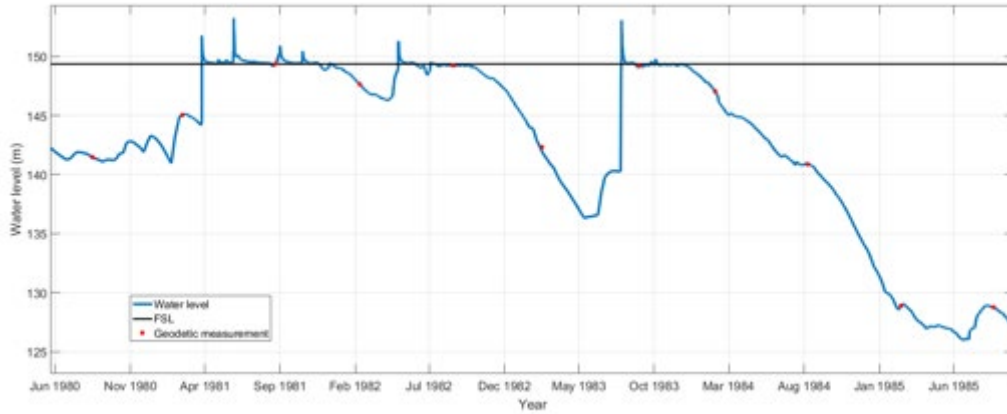


Figure 4.28: Kouga flood condition

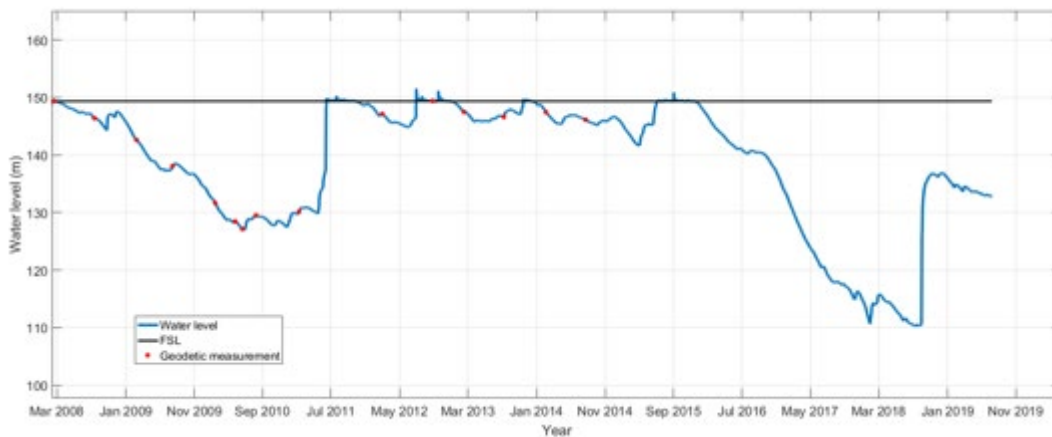


Figure 4.29: Lowest water level

4.2.2.3 Geodetic Data

The relative displacements in the x, y and z directions are shown in Figure 4.30. The following observations are made:

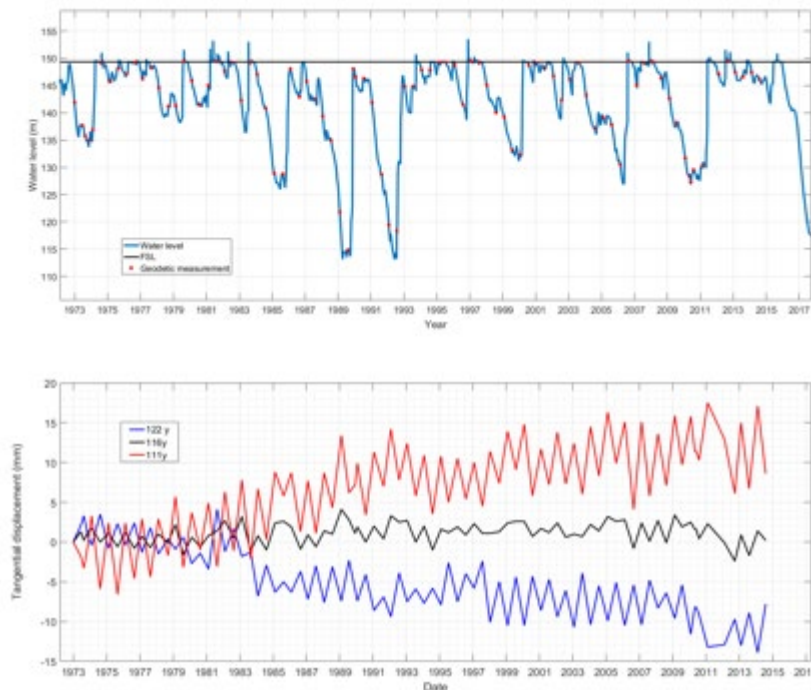
As expected, the radial (upstream/downstream) displacements are dependent on temperature and the water level. The severe droughts can easily be identified in the displacement graphs as the low extremities, indicating upstream displacement (negative direction). The radial displacement for both quarter and centre points follow a similar signature. However, the right flank generally exhibits 10 mm larger displacement seasonal fluctuations compared to the left flank since 1985.

Between 1972 and 1976, vertical displacements were mainly seasonal variations, largely driven by temperature. Permanent vertical displacements have been increasing since 1977.

There was a shift in the behaviour of the dam in 1982 as reflected in the permanent displacements clearly observable in the tangential direction. This permanent deformation follows a period of two years of flooding (Figure 4.30) and it is postulated that these events contributed to the permanent deformation.

The structure continues to deform in all directions, contrary to the postulation that the swelling effect will be minimal by 2000 (Egles et al., 1995).

Since 1972 the whole structure has moved upstream (Figure 4.31), with the right flank undergoing significantly larger relative displacement compared to the rest of the structure. It appears that due to the increased axial load associated with the swelling, the structure may be buckling to relieve the swelling stresses. Based on engineering drawings, the dam wall is not completely symmetrical, and the buckling is occurring at the slightly longer section on the right portion of the wall.



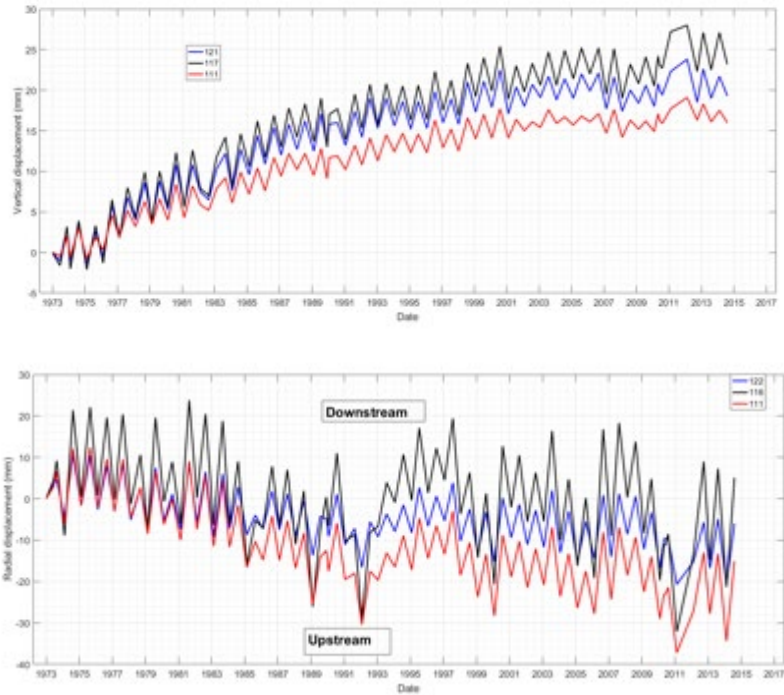


Figure 4.30: Geodetic measurements

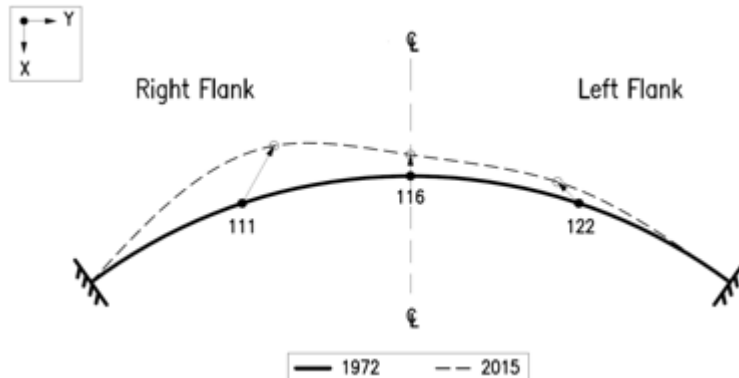


Figure 4.31: Schematic of permanent x-y displacement of dam wall

4.2.2.4 GNSS/GPS Data

The GNSS/GPS provides continuous measurements, enabling the behaviour of the structure to be observed throughout the year as opposed to geodetic measurements taken only twice a year. The available data from the GPS system is for the period August 2011 to March 2015 with displacements taken once every month. Figures 4.32 & 4.33 show radial displacements for the left and right flank respectively. The seasonal displacements of the flanks are about 22 mm.

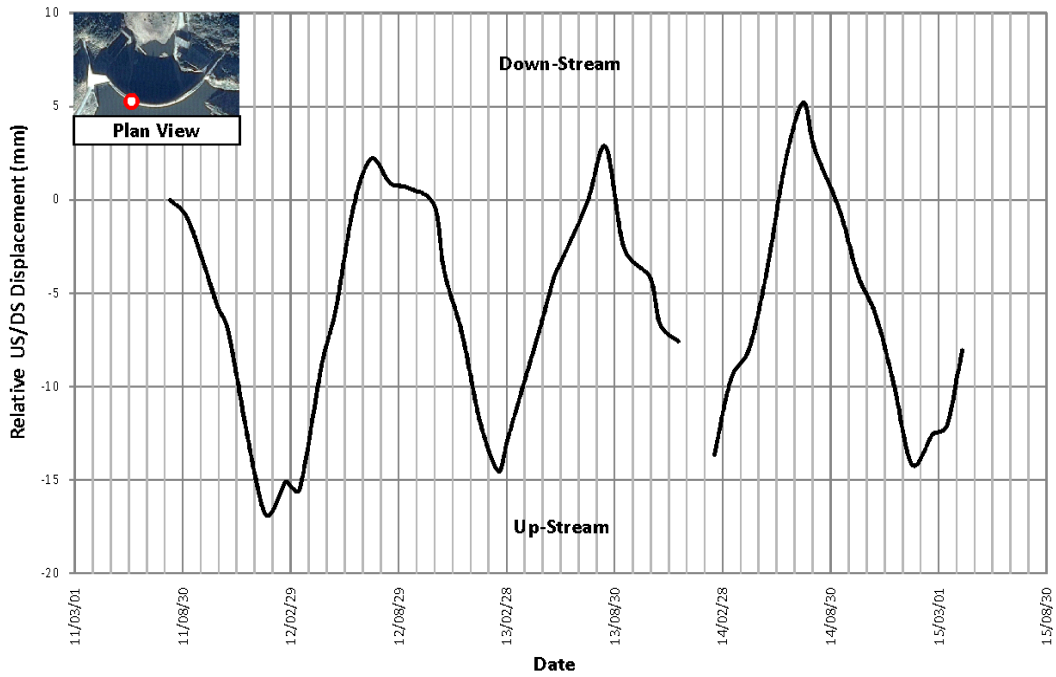


Figure 4.32: Displacement data for left flank (KG12)

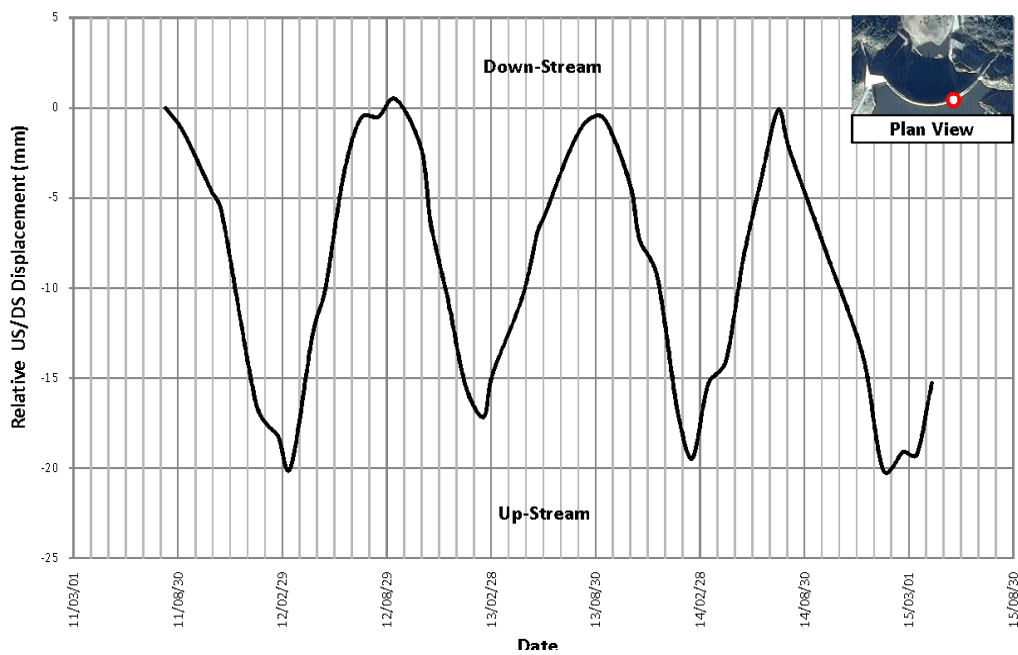


Figure 4.33: Displacement data for right flank (KG13)

Figures 4.34 & 4.35 shows time variation of water level and radial displacement. While both the water level and radial displacement exhibit some seasonal variation, there is no strong relationship between the two (Figure 4.21). On the other hand, there is a strong relationship between temperature and radial deformations as shown in Figures 4.23-4.26

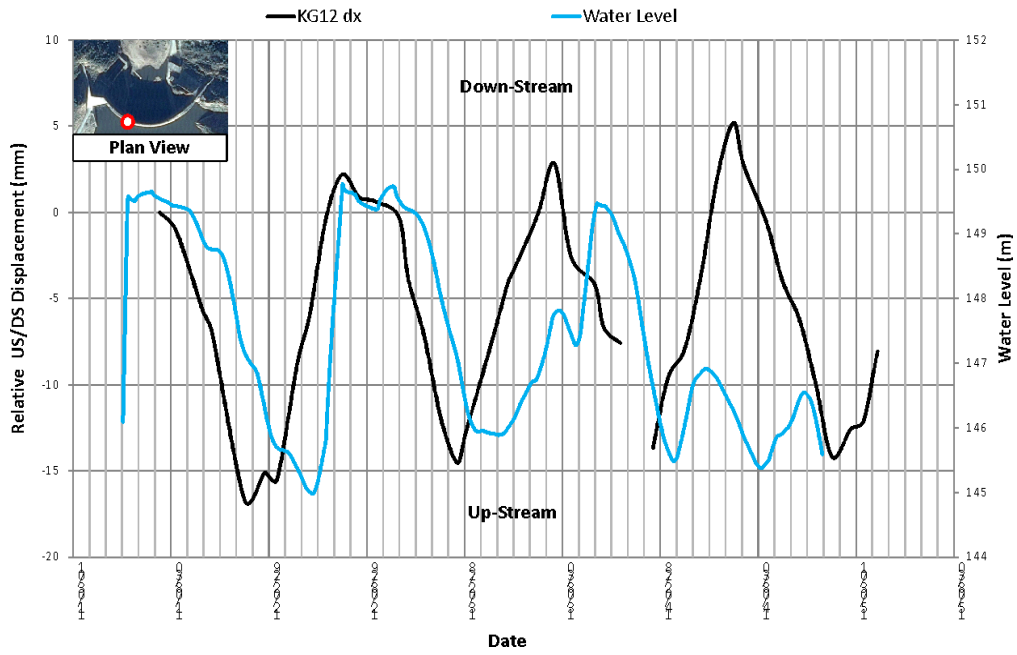


Figure 4.34: Displacement and WL data for left flank

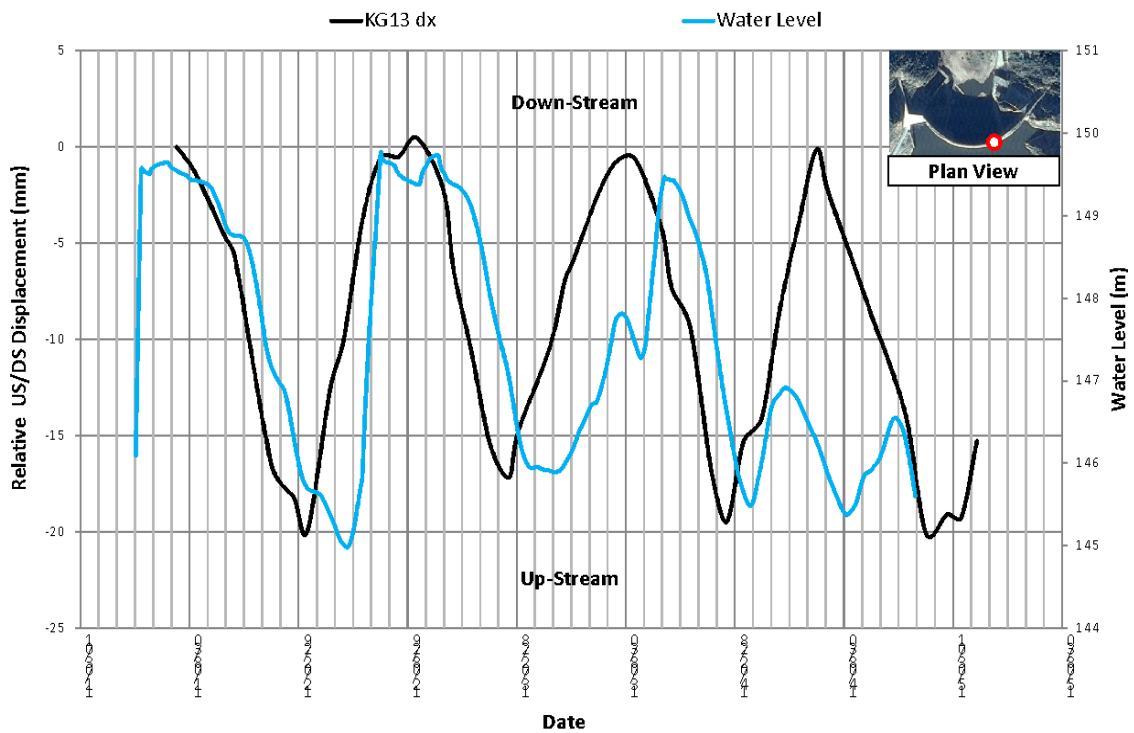


Figure 4.35: Displacement and WL data for right flank

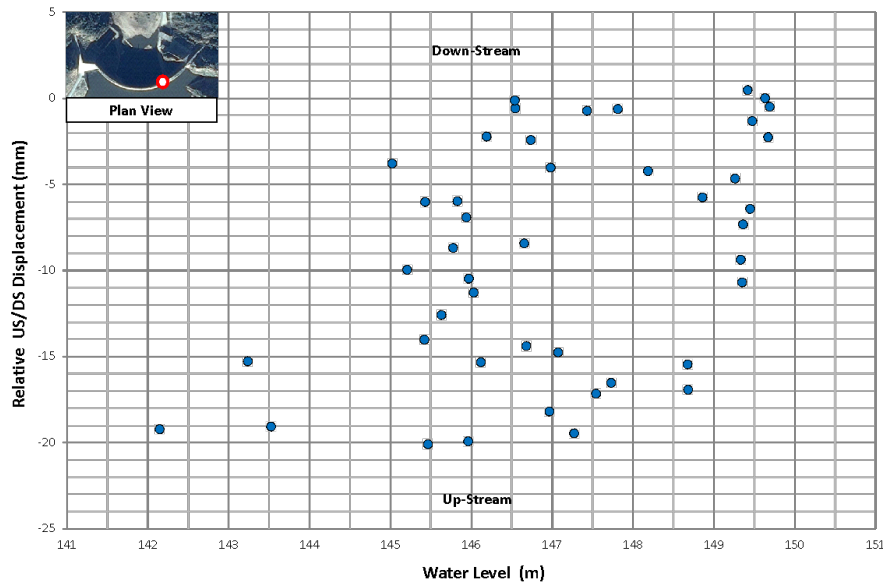


Figure 4.36: Displacement vs Water Level

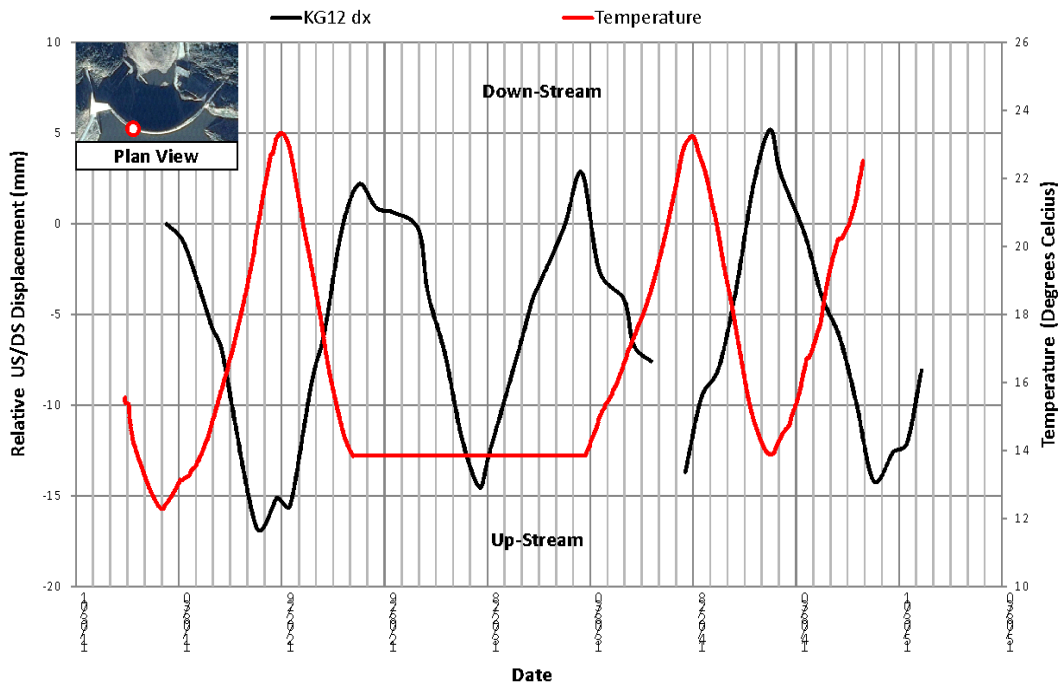


Figure 4.37: Displacement and Temperature data for left flank

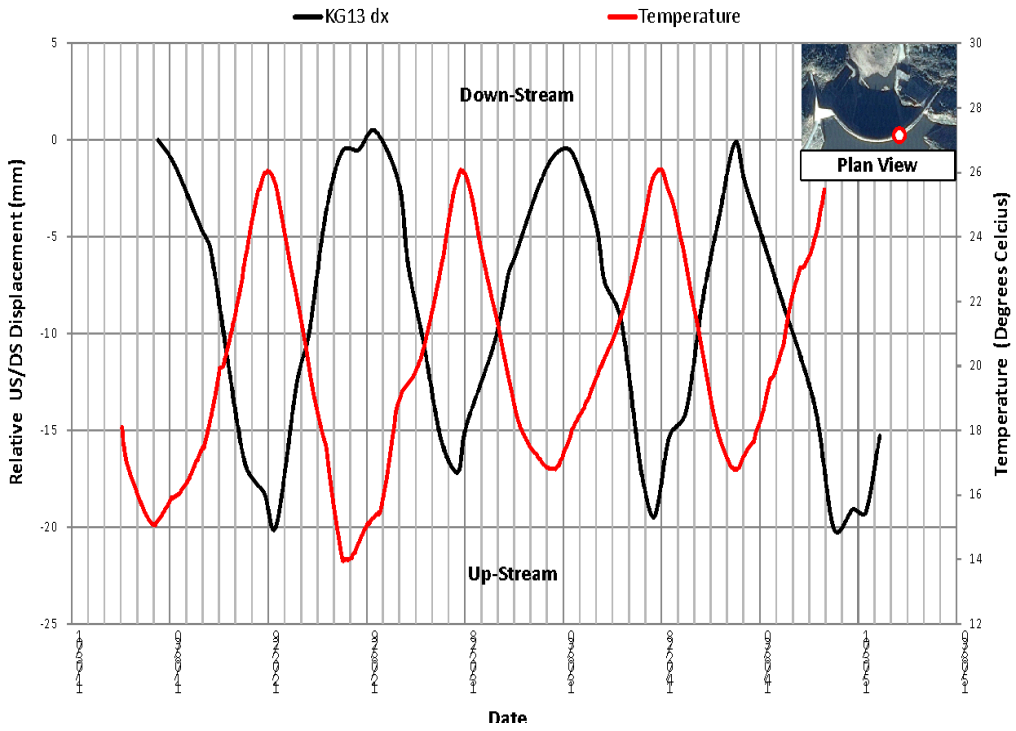


Figure 4.38: Displacement and Temperature data for right flank

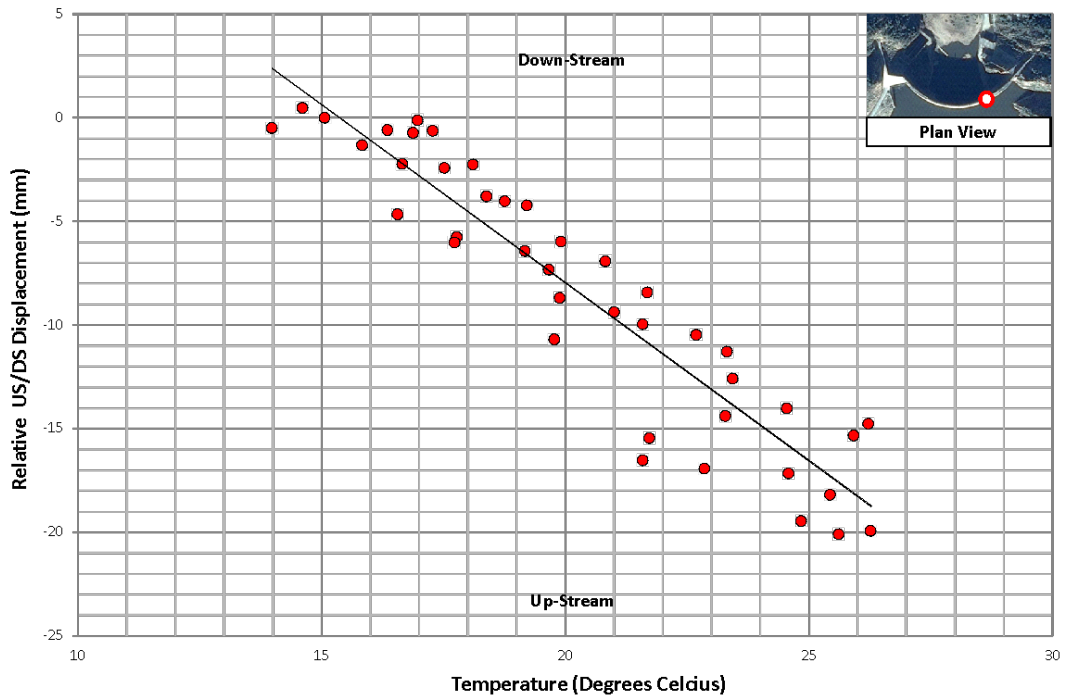


Figure 4.39: Displacement VS Temperature

Monitoring data provides information essential for the calibration and validation of numerical models which can be used to predict the structural behaviour of the dam under various loading conditions. The sections which follow present the development, calibration and validation of a finite element of Kouga Dam. The model is then used to predict the behaviour of the dam under future climatic conditions.

5 Finite element modelling, validation and validation

The future behaviour of Roode Elsberg Dam and Kouga Dam under the three adaptation scenarios described in section 2.4 was evaluated using finite element models. The finite element models of the dams were calibrated and validated to ensure that they represent the behaviour of the as built dams as far as possible. This was achieved through a three-step process: 1) matching theoretical dynamic properties of the dam to measured dynamic properties, 2) matching theoretical deformations of the dam with measured deformations and 3) validating the behaviour of the dam using measured deformations. An additional calibration step was introduced for Kouga Dam to model the swelling process due to AAR. A precise match between theoretical and measured parameters is often difficult to achieve and an error margin of less than 5% was considered acceptable.

5.1 Roode Elsberg Dam model calibration and validation

5.1.1 Model Geometry

Figure 5.1 shows the FEM geometry of Roode Elsberg Dam. The model geometry of the model was based on drawings provided by the Department of Water Affairs. Long-term deformations show that the left flank foundation is stiffer than the right flank. Thus the foundation was split into three regions of varying stiffnesses (Figure 5.2). The dam wall is modelled as isotropic and monolithic on the assumption that the interlock mechanism between blocks permits this monolithic behaviour. The water on the upstream side is modelled as a fluid. The material properties used are given in Table 5.1.



Figure 5.1: Roode Elsberg FEM geometry

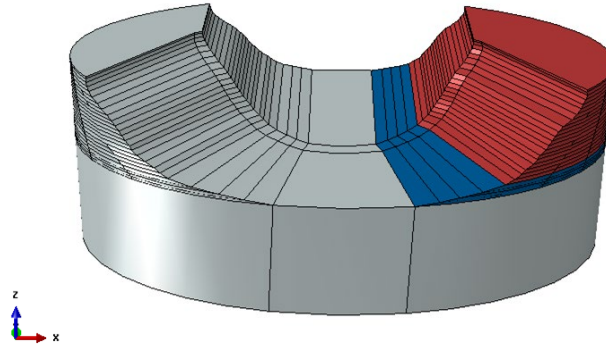


Figure 5.2: Roode Elsberg foundation partitioning

Table 5.1: Elastic material properties of Roode Elsberg Dam wall and foundation

Property and Symbol	SI Units	Concrete Wall	Rock Foundation		
			Left flank	Bedrock	Right flank
Modulus of elasticity (E_d)	GPa	25	25	20	23
Density (ρ)	$\frac{kg}{m^3}$	2400	-	-	-
Poisson's ratio (ν)	-	0.25	0.22	0.22	0.22

5.1.2 Thermal load modelling

The temperature model is assumed to be governed by the laws of heat transmission through radiation, irradiation and convection. The models defining these processes require information about the prevailing climate. This includes air temperature, wind speeds, orientation of the dam, water temperature and foundation temperature. Solar radiation loads depend on dam location (latitude, longitude), month of the year, time of the day, amount of cloud cover, and dam orientation. Figure 5.3 shows the trajectory of the sun and the position of the shadow at Roode Elsberg Dam. The downstream side of the dam is in the shadow most of the day while the upstream site is exposed to direct sun rays most of the day. A summary of the key parameters used for the thermal modelling are summarised in Table 5.2.

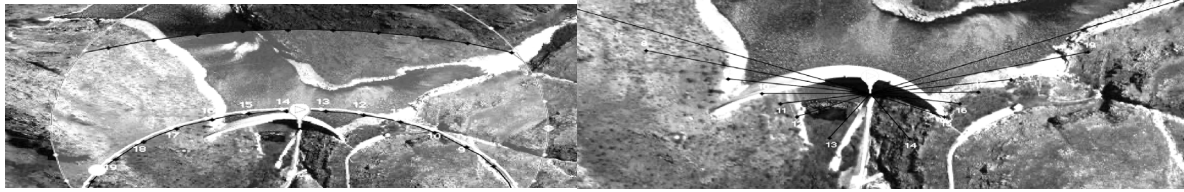


Figure 5.3: Sun's trajectory at Roode Elsberg Dam

Table 5.2: Thermal material properties used for the concrete wall

Property and Symbol	SI Units	Concrete Wall
Specific heat, c	J/(kg.K)	900
Thermal conductivity, k	W/(m K)	2.2
Convection coefficient, h		23.2
Emissivity		0.88
Solar absorptivity		0.65

5.1.3 Hydrostatic load modelling

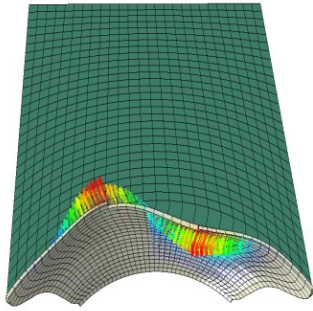
The hydrostatic load was modelled using the usual linearly varying function for static analysis for each considered load cases.

5.1.4 Calibration of the dynamic properties

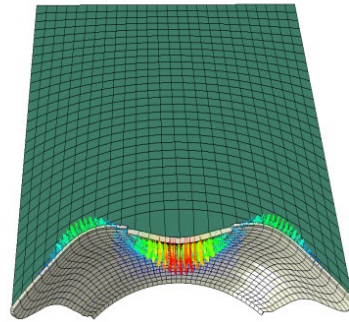
Ambient vibration testing of Roode Elsberg Dam has been on-going since 2008 (Moyo & Oosthuizen, 2009; Moyo & Oosthuizen, 2010; Bukenya et al., 2012; Moyo & Oosthuizen, 2013; Moyo et al., 2016). The finite element model of the dam was calibrated using measured natural frequencies of the reservoir at full supply level in winter. Table 5.3 shows the measured and theoretical natural frequencies and Figure 5.4 shows the corresponding theoretical mode shapes. There is good agreement between measured and theoretical natural frequencies, with the first six natural frequencies within 3% error.

Table 5.3: Comparison of theoretical and measured natural frequencies for Roode-Elsberg Dam

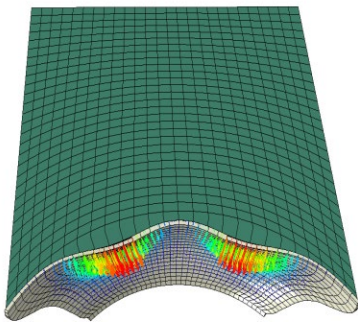
Mode Number	Measured natural frequency (Hz)	Theoretical natural frequency (Hz)	FSI % Error
1	3.05	2.96	2.81
2	3.23	3.23	0.05
3	4.43	4.49	1.44
4	5.62	5.54	1.41
5	6.50	6.67	2.61
6	7.23	7.20	0.43



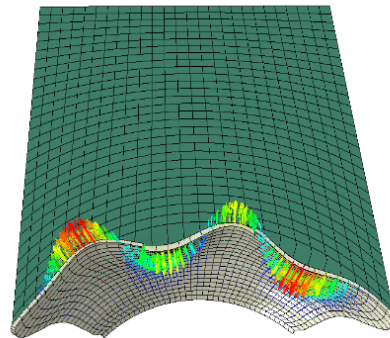
Mode 1 – 2.96 Asymmetric



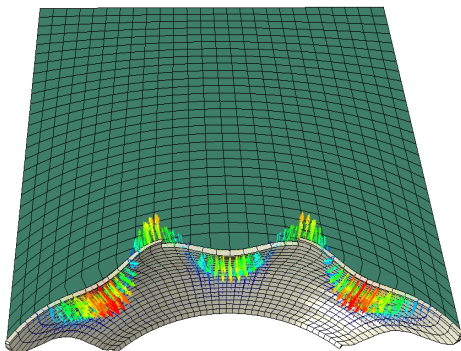
Mode 2 – 3.23 Hz Symmetric



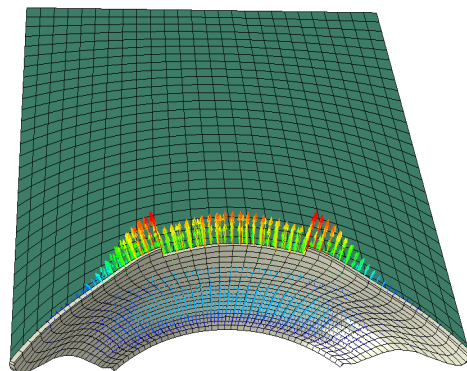
Mode 3 – 4.49 Hz Symmetric



Mode 4 – 5.54 Hz Asymmetric



Mode 5 – 6.67 Hz Symmetric



Mode 6 – 7.20 Hz Symmetric

Figure 5.4: Roode Elsberg Dam theoretical mode shapes

5.1.5 Deformation calibration

The deformation behaviour of the dam was calibrated using geodetic measurements taken: 1) 15 February 1985 with water level at 558.00 m and 2) 21 August 2002 with water level at 573.040 m. These scenarios represent summer and winter conditions. Deformation calibration ensures that that foundation-wall interaction is representative of the as built behaviour of the dam.

Figure 5.5 shows the downstream – upstream displacement of the central block of the dam for the two load scenarios, after adjusting the foundation stiffness. While there is a close match between the model and the measurements, the behaviour of the dam near foundation level, indicates that the rotational stiffness of the dam is lower than that of the model near foundation level. Figure 5.6 shows the downstream-upstream displacement of the dam near the crest level. The difference between measured and theoretical displacements is less than 5% indicating good agreement between the model and the as built behaviour.

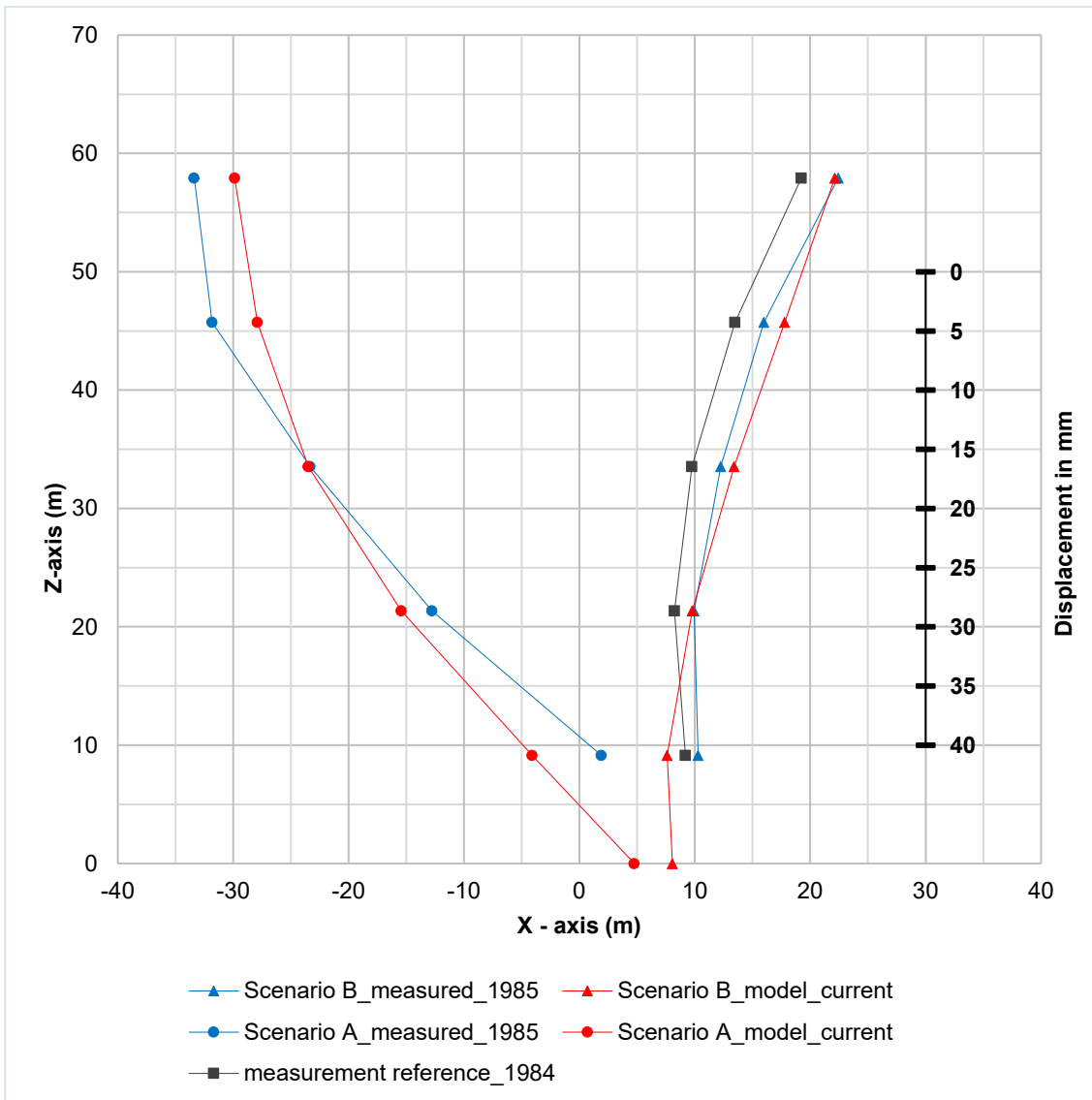


Figure 5.5: Roode Elsberg displacement

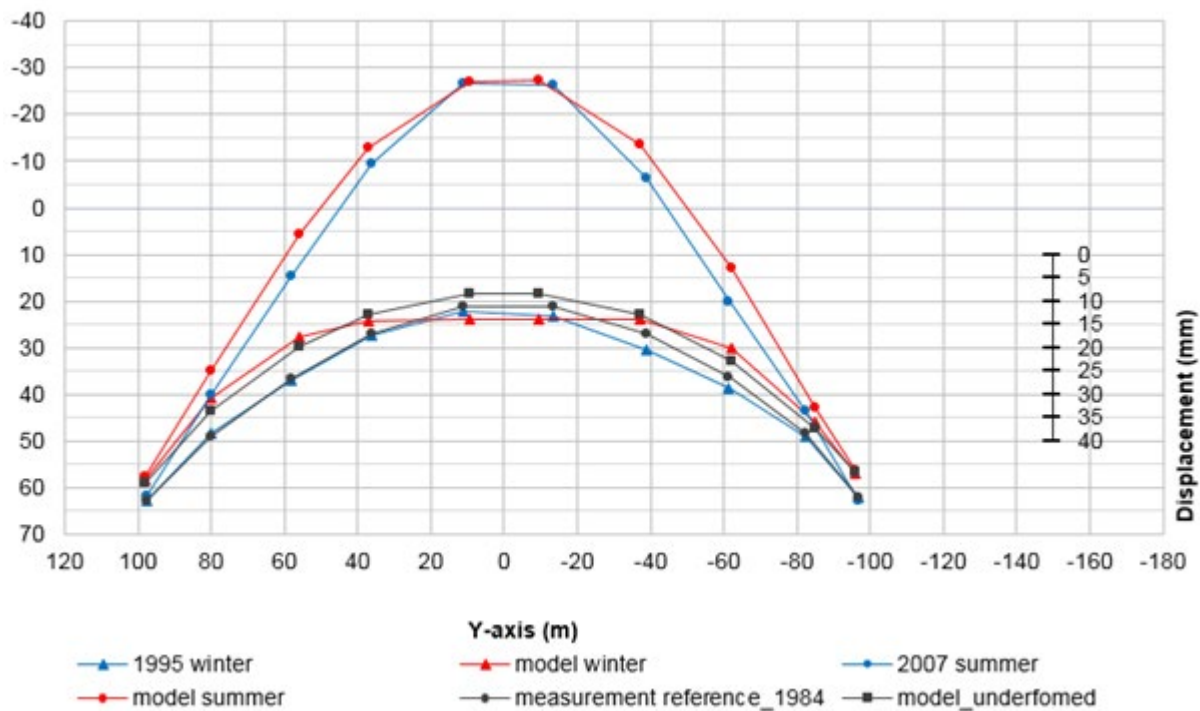


Figure 5.6: Roode Elsberg displacement in the radial tangential direction plane near crest level

5.2 Kouga Dam model calibration and validation

5.2.1 Model Geometry

A 3-dimensional model (3D) using continuum elements was used in the analysis of the dam. The model geometry was based on drawings provided by the Department of Water Affairs. The assembled geometry of the model consisted of the fluid part and the dam wall as shown in Figure 5.7. The dam wall is modelled as isotropic and monolithic on the assumption that the interlock mechanism between blocks permits this monolithic behaviour. The water on the upstream side is modelled as a fluid, using acoustic elements. Based on the available information on the geology of the site and long-term measurements, the foundation was modelled in two parts to enable adjustment of stiffness during the calibration process. Table 5.4 gives a summary of the material properties used for Kouga Dam model.



Figure 5.7: Kouga Dam Finite element model geometry

Table 5.4: Linear elastic material properties of dam wall and foundation part

Property and Symbol	SI Units	Concrete Wall	Varying foundation stiffness		
			Left flank	Bedrock	Right flank
Modulus of elasticity (E_d)	GPa	35	25	20	23
Density (ρ)	$\frac{kg}{m^3}$	2300	-	-	-
Poisson's ratio (ν)	-	0.2	0.22	0.22	0.22

5.2.2 Thermal load modelling

The same principles adopted for modelling temperature load for Roode Elsberg Dam were used to model the temperature load for Kouga Dam. The trajectory of the sun and the position of the shadow at Kouga Dam is shown in Figure 5.8. The downstream side of the dam is in the shadow from sunrise to sunset. A summary of the key parameters used for the thermal modelling are summarised in Table 5.5.



Figure 5.8: Sun's trajectory at Kouga Dam

Table 5.5: Thermal material properties used for the concrete wall

Property and Symbol	SI Units	Concrete Wall
Specific heat, c	J/(kg.K)	900
Thermal conductivity, k	W/(m K)	2.00
Convection coefficient, h		19
Emissivity		0.88
Solar absorptivity		0.65

5.2.3 Hydrostatic load modelling

The hydrostatic load was modelled using the usual linearly varying function for static analysis for each considered load cases.

5.2.4 Aggregate Alkali Reaction

The loading induced by swelling due to aggregate alkali reaction was considered for Kouga dam. A number of constitutive models have been proposed to simulate the swelling process and its effects on structural behaviour Charlwood (1994), Léger et al. (1996), Ulm et al. (2000), Farage et al. (2004) Saouma and Perotti (2006). The constitutive model used in this study is that proposed by Saouma and Perotti (2006). This thermo-chemo-mechanical is an extension of the model proposed by Ulm et al. (2000). The model (Equation 5.1) combines the kinetics of the chemical reaction and diffusion processes to estimate volumetric expansion of concrete.

$$\dot{\epsilon}_V^{AAR}(t, T) = \underbrace{\Gamma_t(f'_t | w_c, \sigma_I | COD_{max}) \Gamma_c(\bar{\sigma}, f'_c)}_{\text{Retardation}} \underbrace{g(h)}_{\text{Humidity kinetics}} \underbrace{\dot{\xi}(t, T)}_{\text{AAR}} \underbrace{\epsilon(\infty)}_{\text{Strain}} \quad \text{Equation 5.1}$$

The kinetics of the chemical reaction and diffusion process in the proposed model were largely inspired by the research conducted by Larive (1998). The basic assumption is that volumetric expansion is dependent on the reaction extent and follows the reaction kinetics shown in Figure 5.9. The critical parameters for this curve are the latency time (τ_l) and the characteristic time (τ_c) and the AAR ultimate strain. These parameters should be determined for each structure via accelerated tests.

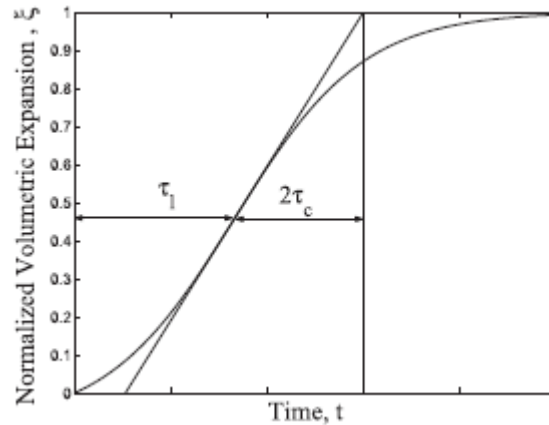


Figure 5.9: Normalised Expansion curve (Saouma, 2014)

The retardation term accounts for hydrostatic compressive stress (triaxial compressive stress) and the presence of cracks. This is because AAR related expansion and stress distribution are sensitive to confining stresses. It is generally accepted that at a compressive stress of about 8 Mpa, expansion in the corresponding direction is entirely prevented or limited (US Department of Transport, 2012). On the other hand, the presence of cracks in concrete suffering from AAR is somewhat beneficial, as these can relieve the gel-induced stresses by providing space that is fillable by the expanding gel. Ultimately, this may result in the reduction of the final volumetric expansion.

Another major proposition of the constitutive model in relation to fracture mechanics which affects volume of expansion is that the volumetric AAR strain must be redistributed to the three principal directions according to their propensity to expand on the basis of weights which are a function of the respective stresses along the principal direction (i.e. stress state). Consequently, the constitutive model will result in anisotropic AAR expansion even when not expressed in tensor form because the anisotropy stems from the various weights assigned to each of the three principal directions.

The deterioration of the elastic modulus and tensile strength is accounted for in the model using time-dependent nonlinear models shown in Figure 5 and mathematically described using equation 5.2 and 5.3.

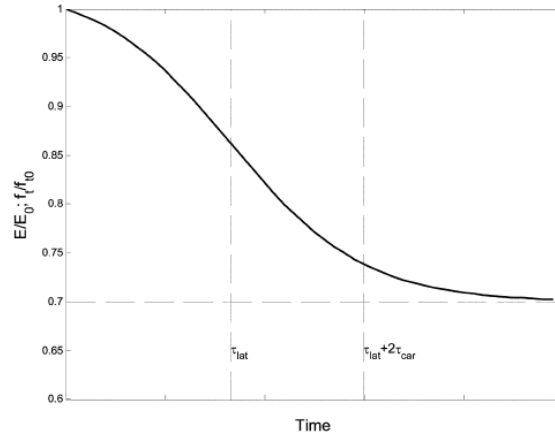


Figure 5.10: Degradation of E and f'_t (Saouma & Perotti, 2006)

$$E(t, E) = E_0[1 - (1 - \beta_E)\xi(t, T)] \quad \text{Equation 5.2}$$

$$f'_t(t, T) = f'_{t,0}[1 - (1 - \beta_f)\xi(t, T)] \quad \text{Equation 5.3}$$

Moisture availability, one of the requirements for deleterious AAR to occur, affects the progression of the reaction. Humidity related effects on the reaction are accounted for using a reduction function (equation 5.4).

$$0 \leq g(h) \leq \frac{\epsilon(t = \infty, RH = h)}{\epsilon(t = \infty, RH = 1)} \quad \text{Equation 5.4}$$

where, $g(h)$ (equation 5.5) is a function in terms of the relative humidity (h) which results in a reduction of the maximum expansion as at lower RH values.

$$g(h) = ae^{b \cdot h} \quad \text{Equation 5.5}$$

with a and b as constants have values of 0:0002917 and 8.156 respectively (Saouma, 2014). Generally, it is accepted that an RH of at least 0.8 is required for ASR to occur (Saouma, 2014). Moreover, a separate analysis should ideally be conducted in order to determine the spatial and temporal distribution of RH inside a structure (i.e. $RH(t, x, y, z)$). For dams however, the RH can be reasonably assumed to lie between 90-95% throughout the dam structure. Consequently, for dam structures, $g(h)$ can be assumed to be 1 inside a dam for all temperatures (Saouma & Perotti, 2006).

5.2.5 AAR Calibration

Swelling of the Kouga Dam due to AAR affects both dynamic and static behaviour of the dam. Thus dynamic and deformation calibration should account for the presence of AAR in the dam. The most informed calibration approach for AAR is to conduct accelerated AAR tests on samples extracted from the dam to obtain reaction rates. These experiments require a minimum of 1 year to obtain meaningful results. For Kouga Dam, AAR calibration was based on the deformation observations measured since 1972. The critical parameters of the reaction kinetics curve are the latency time, the characteristic and the ultimate strain. The best fit parameters for Kouga dam are:

$$\tau_c = 8000 ; \quad \tau_l = 1000$$

Figure 5.11 shows the updated reaction curve. While the curve is a best estimate of the observations, the reliability of this to predict behaviour over a long period remains uncertain due to the fundamental assumption that the reaction will cease after a period of time. Observations from real structures indicate that the reaction continues beyond the expected cessation time (Sellier et al., 2017). It is thus advisable to review the calibration at regular time intervals.

Figure 5.12 shows the vertical displacement due to ARR and the geodetic measurement for point 117 on the dam wall. The displacement trend obtained from the AAR model produces a good approximation of the measured displacement trend.

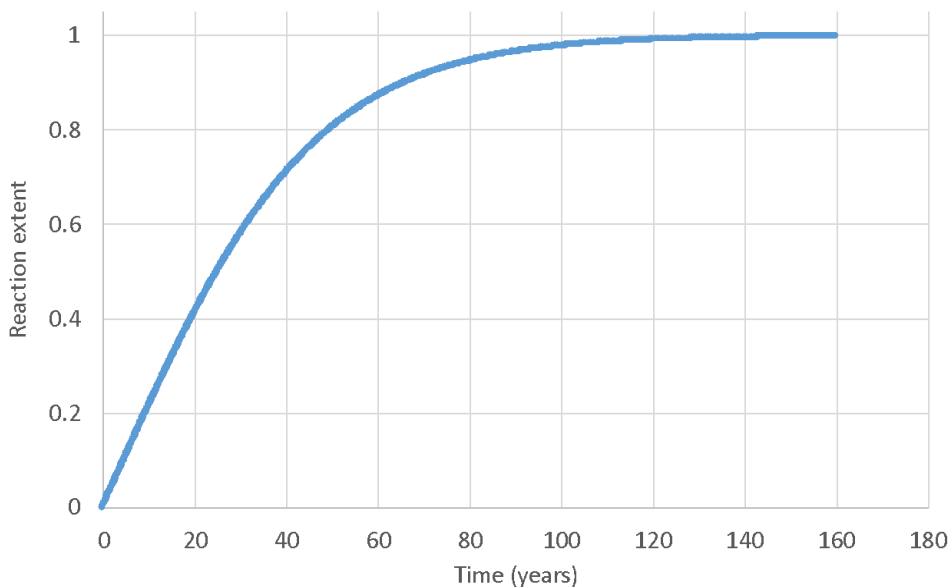


Figure 5.11: Calibrated expansion curve

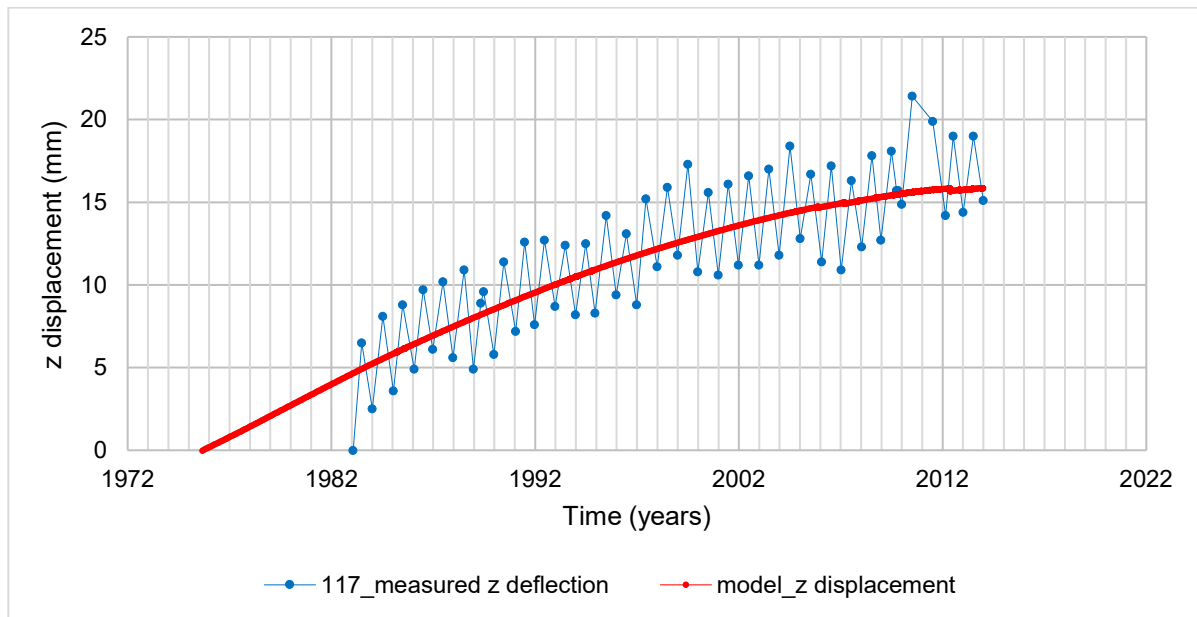


Figure 5.12: AAR Calibration

5.2.6 Calibration of the dynamic properties

Swelling of the dam wall due to AAR introduces internal stress which results in load induced increase in stiffness of the wall, often referred to as the geometric stiffness. Therefore, for dams subject to AAR, the effect of internal compression on the dynamic properties of the dam should be carefully considered. The approach followed for Kouga Dam is to first determine the dynamic properties of the empty dam for two situations namely, dam with AAR and dam with no AAR in order to quantify the effect of AAR on dynamic, followed by fluid structure interaction model with no AAR. The assumption here is linear behaviour of the dam.

Table 5.6 shows the dynamic properties of the empty dam with and without AAR. AAR increases the natural frequencies of the dam by up to 14%. Table 5.7 shows the measured natural frequencies of the dam at full supply level, the natural frequencies estimated from fluid-structure interaction model as well as the estimated natural frequencies of the full dam including AAR. Figure 5.13 shows the first four mode shapes obtained from the finite element model and the measured mode shapes. There is good agreement between the measured mode shapes and the

Table 5.6: Kouga Dam AVT and FEM Natural Frequencies when Dam is full

Mode	Dam empty with No AAR	Dam empty with AAR	% Difference		
1	3.31	2.84	-14.2		
2	3.63	3.24	-10.7		
3	4.63	4.34	-6.3		
4	5.11	5.01	-2.0		
5	6.08	5.83	-4.1		

Table 5.7: Kouga Dam measured and theoretical natural frequencies (Dam full)

Mode	Measured natural frequency (Hz)	Theoretical natural frequency with no AAR (Hz)	% Estimated Difference	Theoretical natural frequency with AAR (Hz)	% difference
1	3.31	2.84	-14.2	3.23	-2.4
2	3.63	3.24	-10.7	3.63	0.0
3	4.63	4.34	-6.3	4.73	2.2
4	5.11	5.01	-2.0	5.40	5.7
5	6.08	5.83	-4.1	6.22	2.3

Mode FEM Mode Shape

Measured Mode Shape

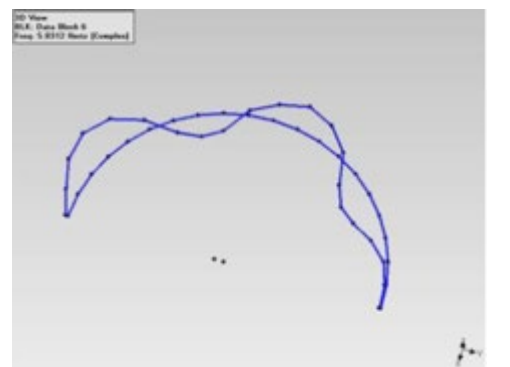
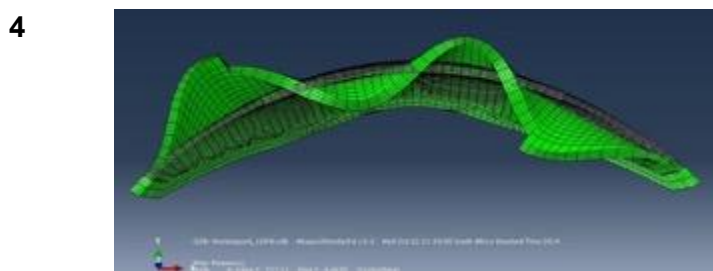
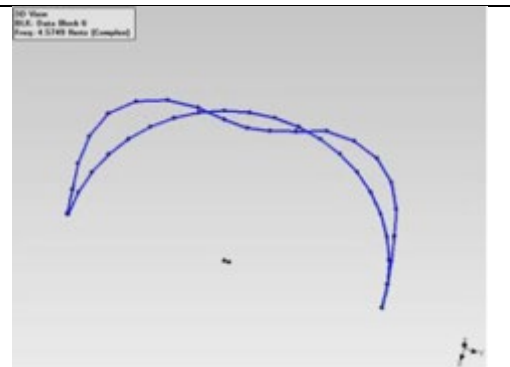
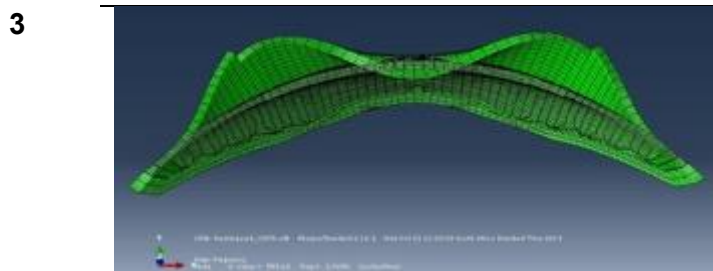
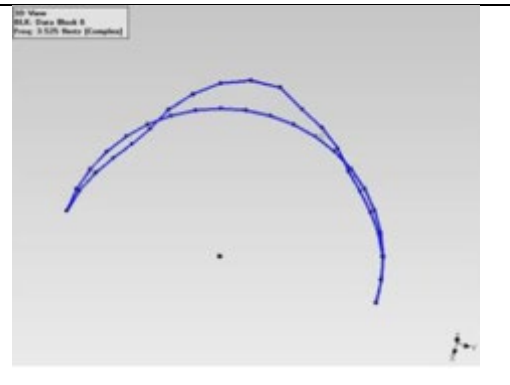
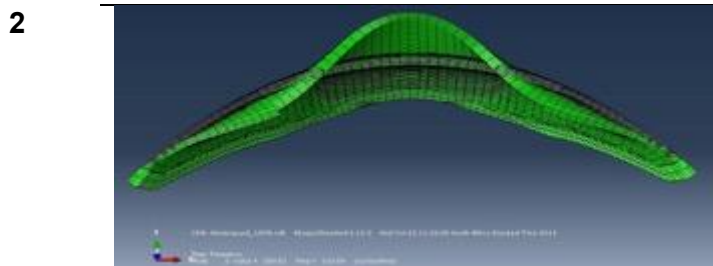
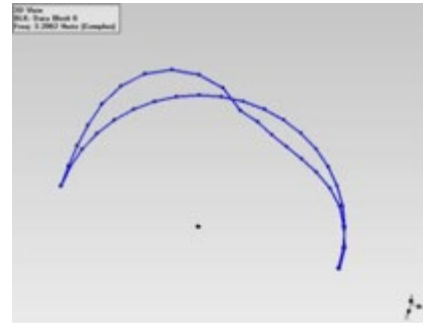
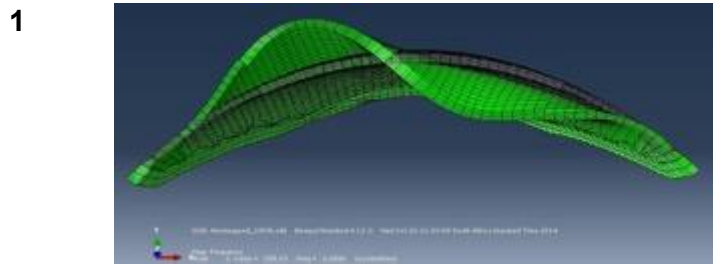


Figure 5.13: Comparison of the first four modes extracted from the model and ambient vibrations tests

5.2.7 Deformation calibration

The deformation analysis for Kouga dam in validating the model was carried out and compared with the observed measurements for the period 2011-2014. This period was selected because there exists geodetic and GNSS GPS upstream-downstream (radial) displacements of the left flank and right flank of the dam structure. Continuous measurement of displacement using GPS ensures that near true maximum displacements are measured. Table 5.5 shows seasonal (maximum winter minus minimum summer displacement) in the period 2013-2014 season. All the seasonal displacements above were calculated at approximately the crest height level. There is close agreement between theoretical and measured displacements confirming that the theoretical model is a good representation of the as built structure.

Table 5.8: Seasonal radial displacement values

Seasonal displacements observed from	Left flank (mm)	Centre (mm)	Right Flank (mm)
GNSS GPS	20		19
FEM	21	28	21

6 Structural performance under future climate

Concrete arch dams generally fail by at foundation level or dam wall by sliding, shearing, cracking and erosion caused by several loading and deterioration mechanisms including, thermal stresses, differential settlements between dam and foundation, high hydraulic gradients, internal erosion and chemical attack of the dam wall and foundation improvements. A combination of monitoring and surveillance provides early warning systems to enable mitigation against failure. Finite element models provide a sound basis for evaluating the possible failure mechanisms as well as predicting future behaviour. In the context of the current study, the future behaviour of Roode Elsberg Dam and Kouga Dam under the three adaptation scenarios described in section 2.4 was evaluated using the calibrated finite element models.

6.1 Future climate scenarios

In order to evaluate the effects of future climates on the structural behaviour of the dams, the calibrated finite element models were used with loading based on climate change adaptation scenarios. As shown in Chapter 2 of this report, all climate change scenarios indicate increasing temperature into the future. Behaviour analysis of the dams was thus done assuming increasing temperature due to climate change. The following climate change load scenarios were considered:

- i) Summer (high temperature) with the water level low – Scenario A;
- ii) Winter (low temperature) with high water level – Scenario B; and
- iii) Summer (high temperature) with high water level – Scenario C.

Note: Low water level for Roode Elsberg Dam was taken as 506.882 m, and high-water level as 573.024 m which is the full supply level of the dam. Low water level for Kouga Dam was taken as 115.824 m and the high-water level as 149.352 m which is the full supply level for the dam.

In each scenario the following the dams were evaluated for the following temperature increases: 1) Roode Elsberg Dam 1.5°C and 3°C, 2) Kouga, 1°C, 2°C and 3°C.

6.2 Roode Elsberg dam

6.2.1 Deformations

Figure 6.1 shows current displacement profiles of the central block with both situations described above and three possible climates. The upstream deflection of the dam increased by about 7 mm with a 3°C rise in temperature while the downstream deflection decreased by about 5 mm for a 3°C rise in temperature.

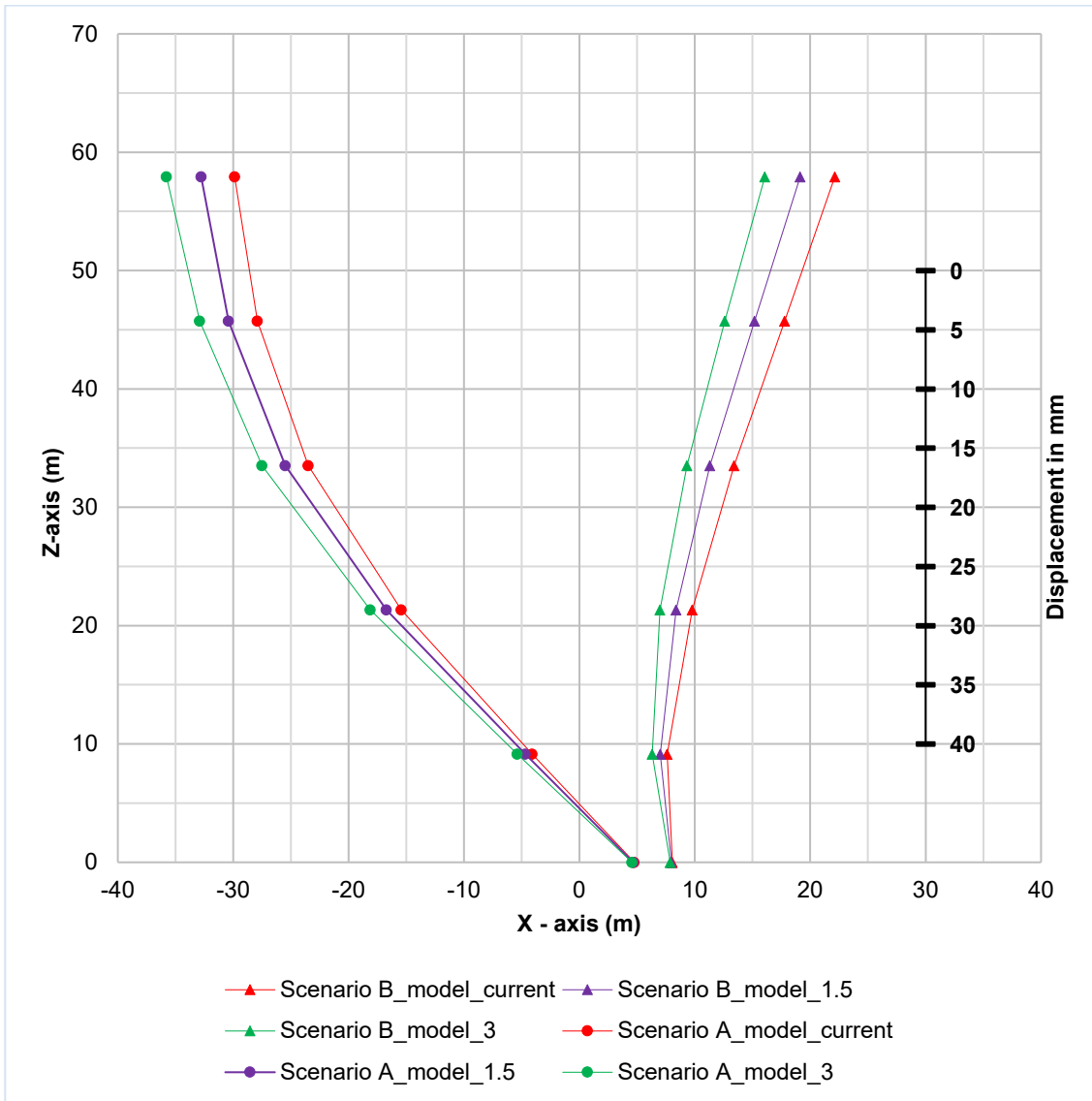


Figure 6.1: Roode Elsberg: Displacements of centre block for 1.5°C and 3°C temperature increases

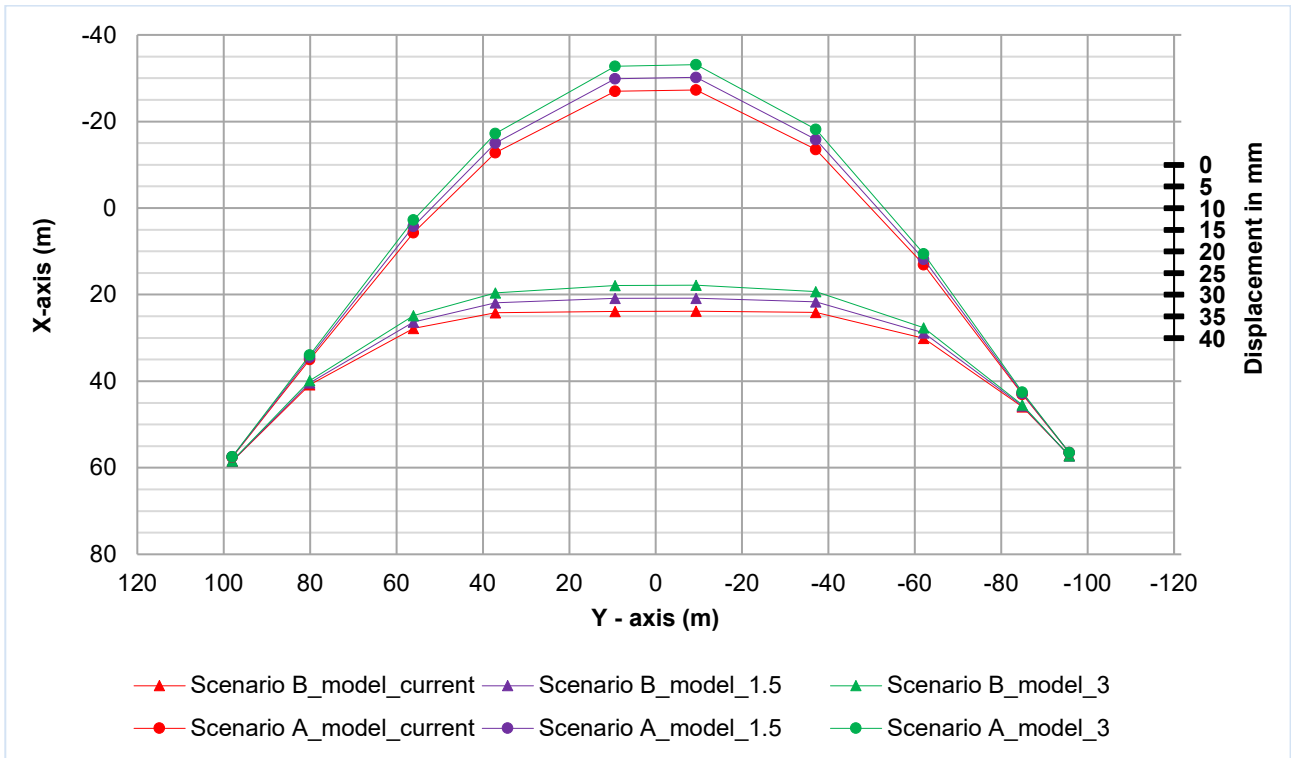


Figure 6.2: Roode Elsberg: Radial displacements near crest level for 1.5°C and 3°C temperature increases

6.2.2 Stress distribution

Figures 6.3 and 6.4 show the stress distributions on Roode Elsberg Dam, viewed from the upstream side of the dam for scenario A and scenario B. Based on these figures it is clear that the critical elements with respect to tensile stress are the abutments, central part of the wall, wall crest, and the wall foundation interface. Compression is dominant along wall-foundation interface and central part of the wall.

Table 6.1 shows the direction of direct tensile stresses at the critical locations. The critical stresses at foundation level are the vertical and radial stresses. Scenario B is critical with respect to vertical tensile stress on the upstream side of the wall which increases by about 30% with a 3°C rise in temperature (Table 6.3).

The wall and the abutments on the other hand is largely subjected to vertical tension in both summer and winter both on the upstream and downstream side. Scenario A is critical for the upstream side of the wall with vertical tensile stresses increasing by about 30%. Scenario B is critical for the downstream side of the wall with vertical tension increasing by about 30% for a 3°C temperature increase (Table 6.4). Scenario A is critical for the downstream side of the abutments and scenario B is critical for the upstream side of the abutments with vertical tensile stresses

increasing by 30% (Table 6.5) The crest of the dam is subject to tangential stresses and the critical scenario is scenario A. Compressive stresses on both the wall and the abutments are mainly in the tangential direction locations in the concrete wall for the three climates. There is a reduction in compressive stress near the foundation level in summer as well as the reduction in tensile on the upstream side of the dam wall. During winter there is an increase in the tensile upstream of the dam wall, as well as near the foundation level.

Considering the stress conditions on Rood Elsberg Dam, the likely modes of failure are (Figure 6.5):

- i) Structural failure
- ii) Shear failure
- iii) Sliding failure

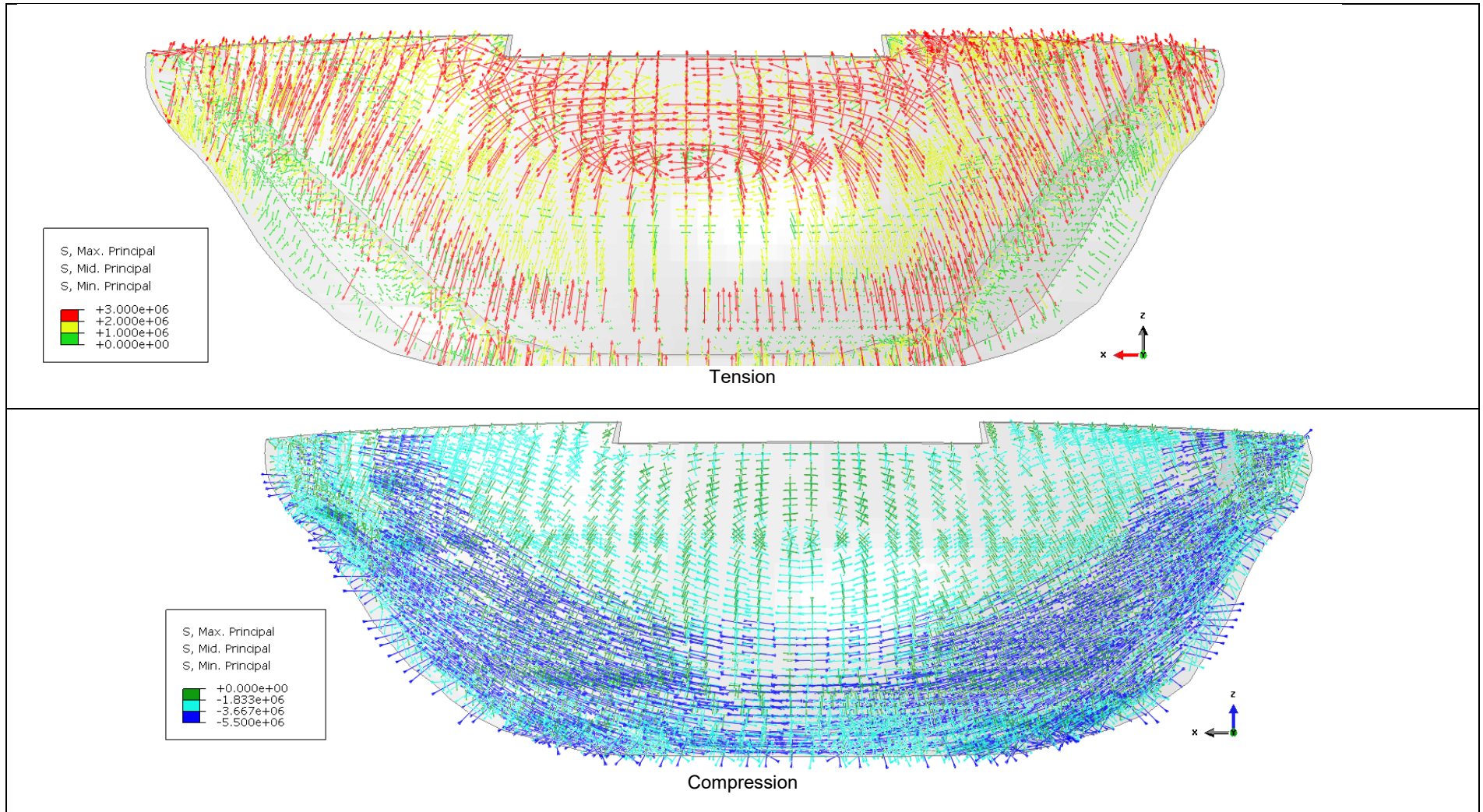


Figure 6.3: Roode Elsberg: Scenario A (summer with dam full), current climate stresses

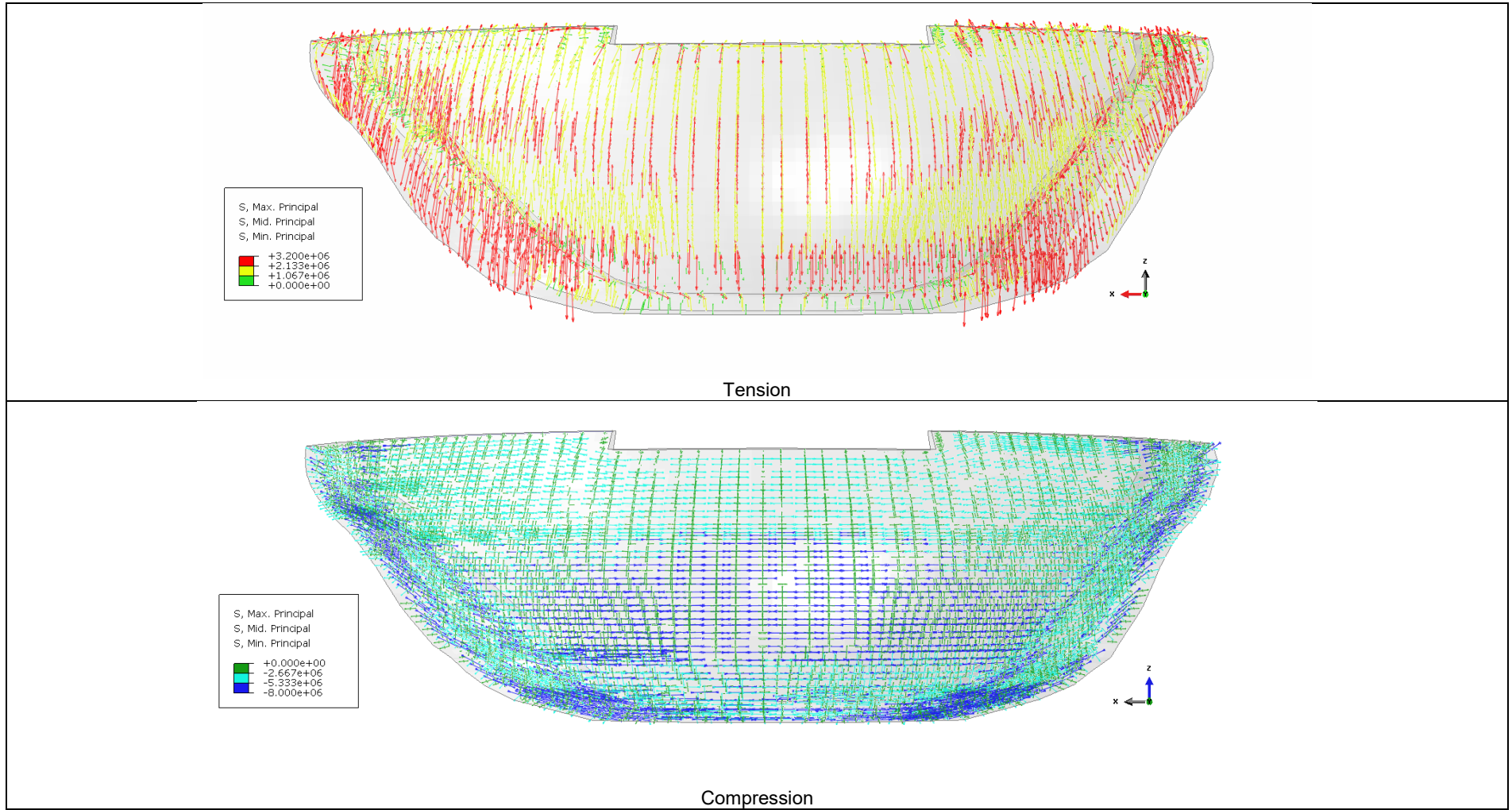


Figure 6.4: Roode Elsberg: Scenario B (winter with dam full), current climate stresses

Table 6.1: Dominant tensile stresses

Tensile stresses								
Position on dam	Foundation (ds)	Foundation (us)	Wall (ds)	Wall (us)	Abutment (ds)	Abutment (us)	Crest (ds)	Crest (us)
Scenario A	V	N	V	V/T	V	N	V/T	T
Scenario B	V	V	V	V	V	V	V/T	V/T

Table 6.2: Dominant compression stresses

Compressive stresses								
	Foundation (ds)	Foundation (us)	Wall (ds)	Wall (us)	Abutment (ds)	Abutment (us)	Crest (ds)	Crest (us)
Scenario A	T	V/T	N	N	V/T	T	N	V/T
Scenario B	V/T	T	V/T	T	V/T	V/T	V/T	N

Table 6.3: Foundation tensile stresses

Foundation tensile stresses						
Climate condition	Current		1.5		3	
	ds	us	ds	us	ds	us
Scenario A	3.2	0	2.7	0	2.5	0
Scenario B	1.9	1.8	2.0	2.3	2.1	2.5

Table 6.4: Wall tensile stresses

Wall tensile stresses						
Climate condition	Current		1.5		3	
	ds	us	ds	us	ds	us
Scenario A	0.7	1.9	0.8	2.1	0.9	2.3
Scenario B	2.2	1.15	2.3	1.3	2.4	1.5

Table 6.5: Abutment tensile stresses

Abutment tensile stresses						
Climate condition	Current		1.5		3	
	ds	us	ds	us	ds	us
Scenario A	2.7	0	3	0	3.3	0
Scenario B	2	1.65	2.2	1.8	2.35	2.1

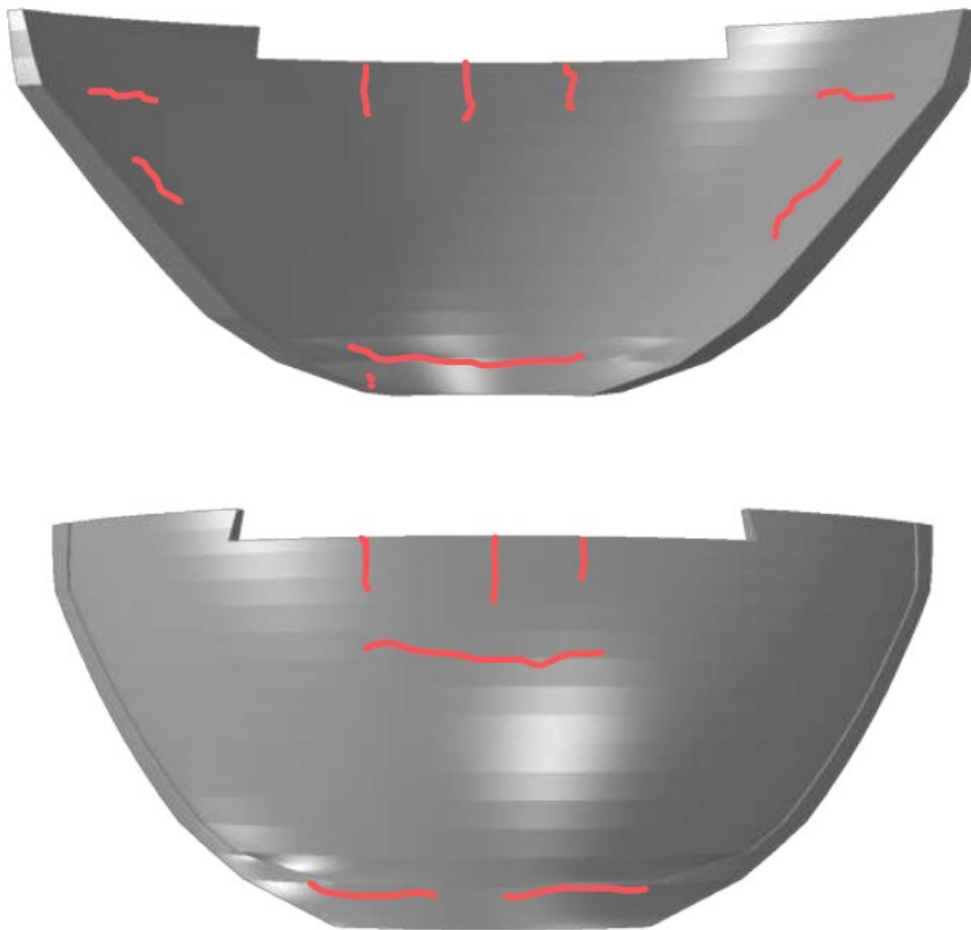


Figure 6.4: Roode Elsberg: possible crack locations

6.3 Kouga dam

The long-term behaviour of Kouga dam is influenced by swelling of the dam wall due to AAR. The dam generally fills up either in the period May to August or December to February depending on the time of start of the rainfall season. Therefore, the dam regularly experiences high hydrostatic load both in winter and summer. Temperature measurements on the upstream side of the dam show that the left flank is warmer than the right flank by about 2°C. Considering this unusual combination of loading on the dam, it is helpful to analyse the behaviour of the dam for each load (i.e. temperature, hydrostatic and AAR loading) in order to gain a better understanding of the individual contributions of the loads.

6.3.1 Deformation behaviour

Figure 6.6 shows thermal displacements for the three scenarios considered. A 1°C temperature rise results in approximately 3 mm of permanent displacement towards the upstream direction of the dam.

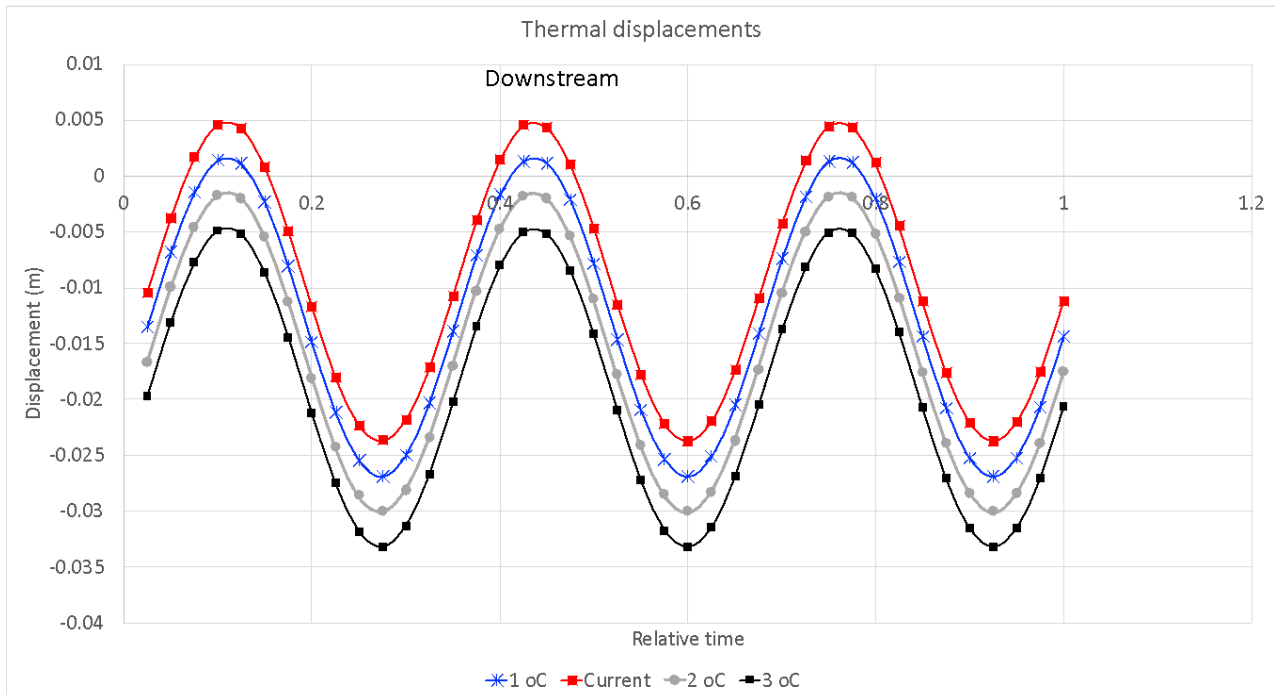


Figure 6.5: Kouga dam: Thermal displacements

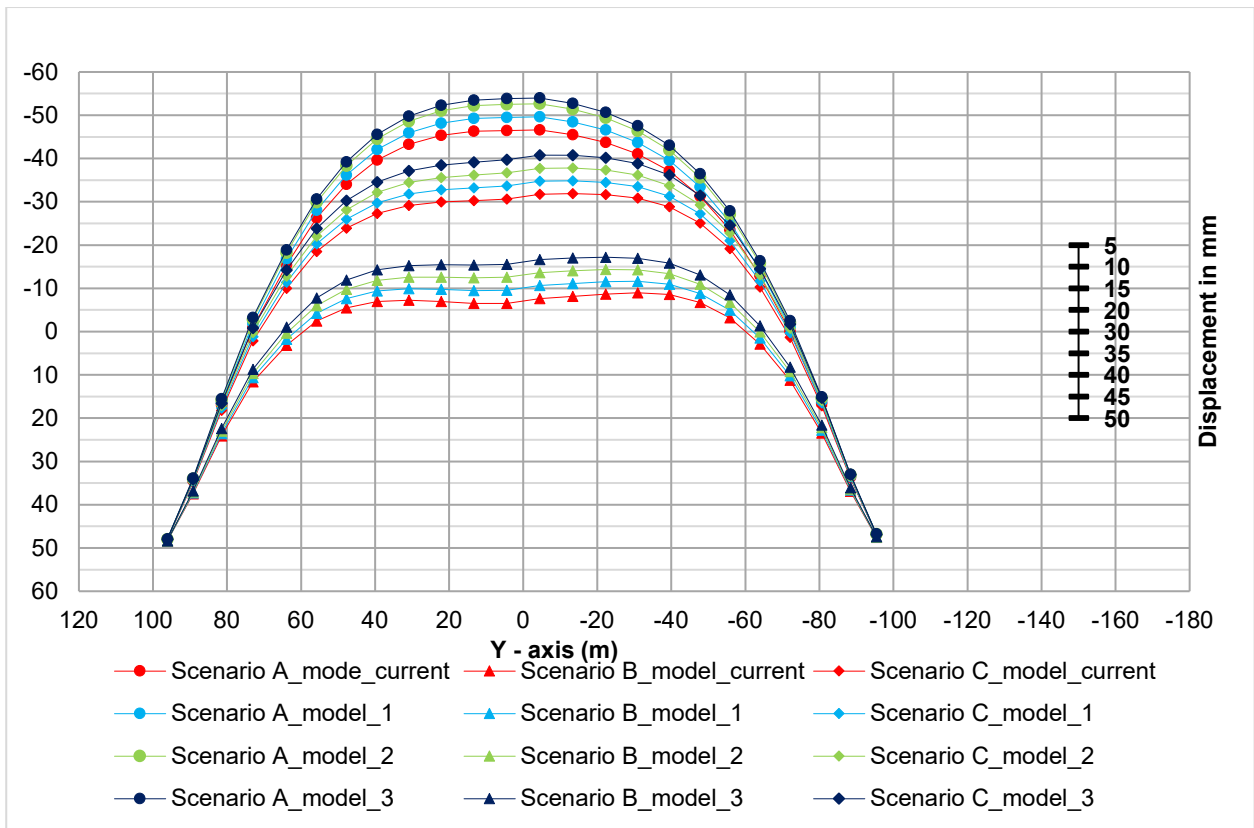


Figure 6.6: Winter stress distributions

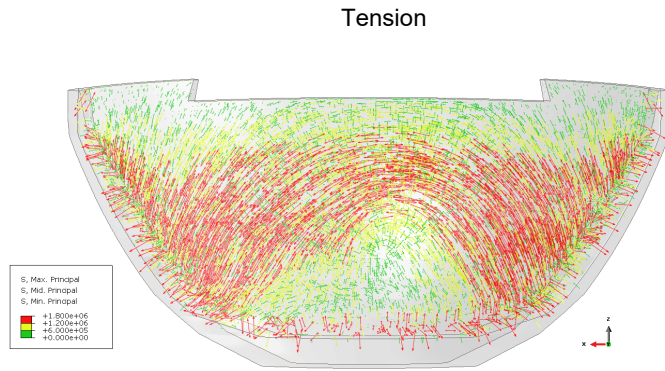
6.3.2 Stress distribution

Figures 6.8 and 6.9 show the tensile stress and compressive stress distribution viewed from the upstream side of the dam for the current loading conditions. The following observations can be made:

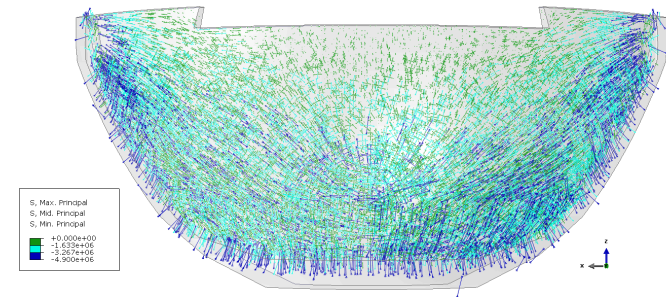
- i) Both tensile and compressive stresses due to AAR are higher than thermal stresses with AAR compressive stress 50% higher and tensile stress about 25% higher.
- ii) The critical areas for high tensile stress are the crest of the wall, the central part of the wall, foundation level of central block, right flank.
- iii) Compressive stresses due to both AAR and temperature are highest at abutments.

The evaluation of the future behaviour of the dam will focus on the critical areas identified above. The potential structural problems at these locations would be cracking at crest level, cracking on the dam wall, cracking at the foundation-wall interface as well as sliding or shear failure at the abutments due to increased thrust force.

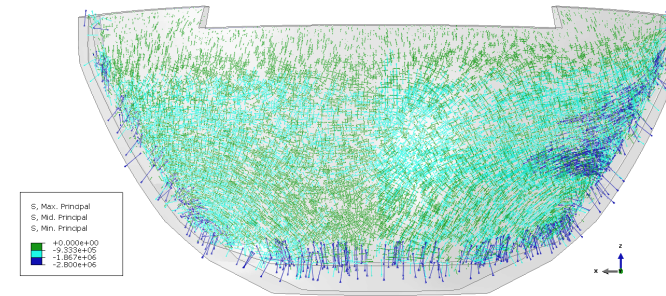
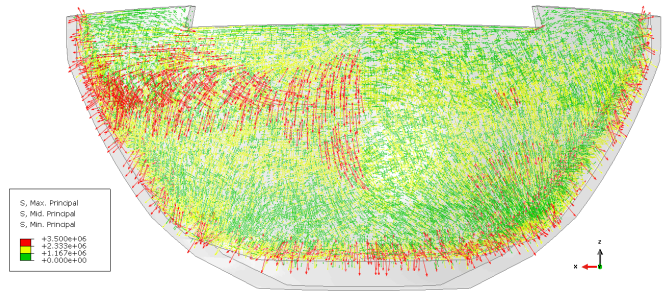
Scenario A
(Thermal load)



Compression



Scenario B
(Thermal load)



Scenario C
(Thermal load)

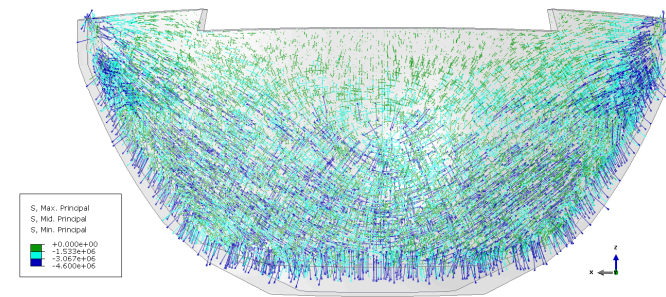
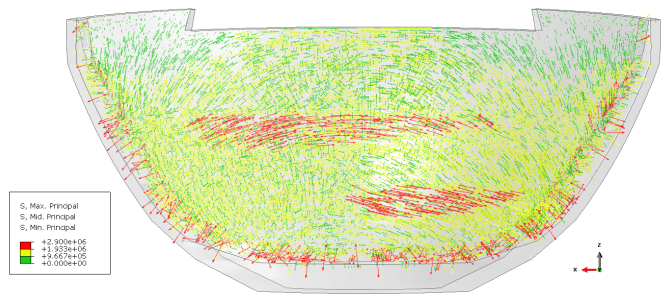


Figure 6.7: Thermal stress distributions

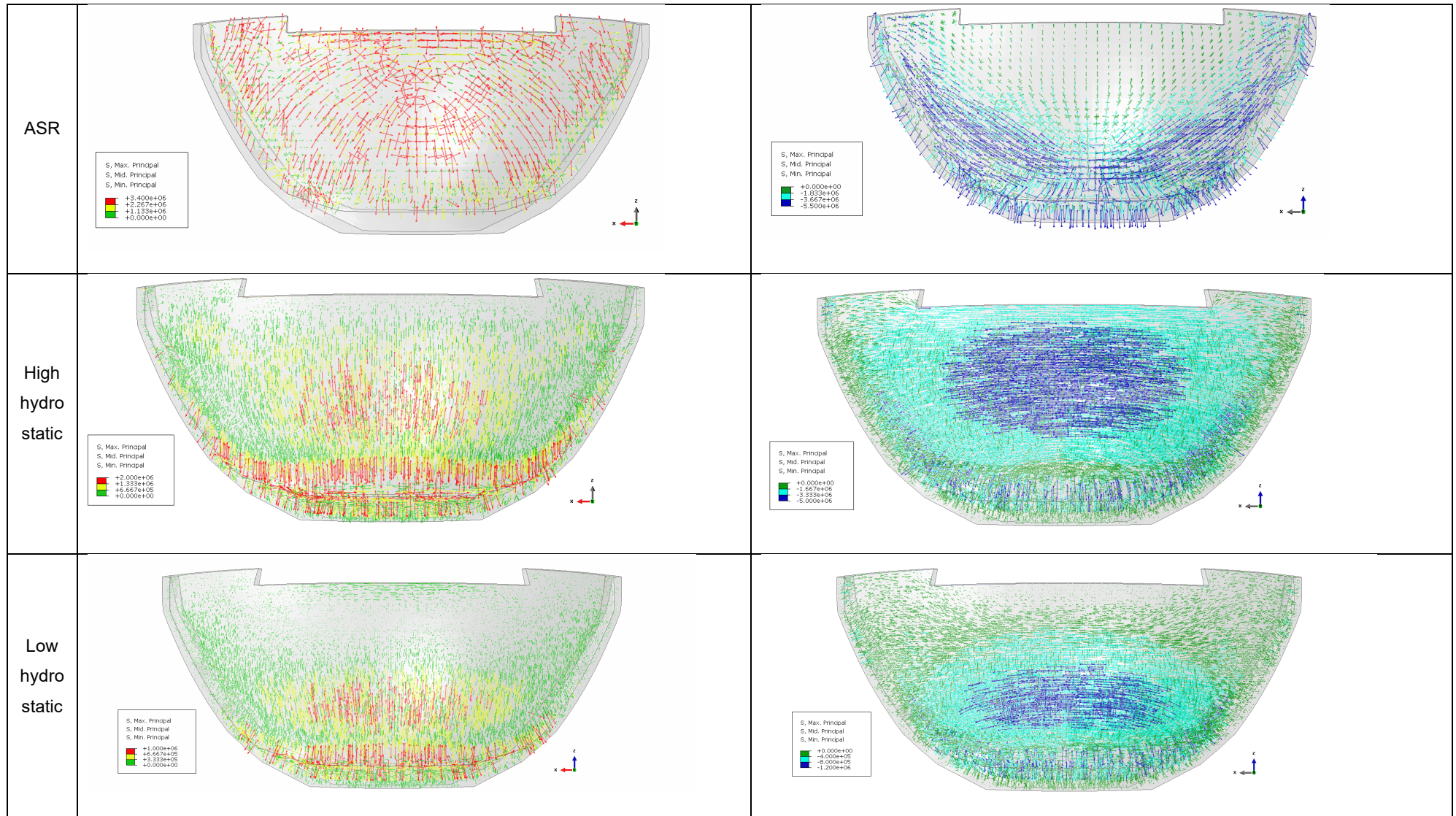


Figure 6.8: AAR and hydrostatic stress distribution

Table 6.6: Tensile stress at critical locations

Scenario A tensile stresses								
Position on dam	Foundation (ds)	Foundation (us)	Wall(ds)	Wall (us)	Abutment (ds)	Abutment (us)	Crest (ds)	Crest (us)
AAR	V	V	N	V	V	N	T	T
Hydrostatic	V	V	V	N	N	V	N	N
Thermal	V	H	T	T	V/T	N	T	T
Scenario B tensile stresses								
Position on dam	Foundation (ds)	Foundation (us)	Wall(ds)	Wall (us)	Abutment (ds)	Abutment (us)	Crest (ds)	Crest (us)
AAR	V	V	N	V	V	N	T	T
Hydrostatic	V	V	V	N	N	V	N	N
Thermal	V	V	V	T	V/T	N	T	T
Scenario C tensile stresses								
Position on dam	Foundation (ds)	Foundation (us)	Wall(ds)	Wall (us)	Abutment (ds)	Abutment (us)	Crest (ds)	Crest (us)
AAR	V	V	N	V	V	N	T	T
Hydrostatic	V	V	V	N	N	V	N	N
Thermal	V	V	N	T	V	N	T	T

Table 6.7: Compressive stress at critical locations

Scenario A compressive stresses								
	Foundation (ds)	Foundation (us)	Wall(ds)	Wall (us)	Abutment (ds)	Abutment (us)	Crest (ds)	Crest (us)
AAR	V/T	V/T	T	N	T/V	T/V	N	N
Hydrostatic	V/H	N	N	T	T	N	N	N
Thermal	V/T	V	V	V	N	V/T	N	N
Scenario B compressive stresses								
	Foundation (ds)	Foundation (us)	Wall(ds)	Wall (us)	Abutment (ds)	Abutment (us)	Crest (ds)	Crest (us)
AAR	V/T	V/T	T	N	T/V	T/V	N	N
Hydrostatic	V/H	N	N	T	T	N	N	N
Thermal	V	V	N	N	V/T	V/T	N	N
Scenario C compressive stresses								
	Foundation (ds)	Foundation (us)	Wall(ds)	Wall (us)	Abutment (ds)	Abutment (us)	Crest (ds)	Crest (us)
AAR	V/T	V/T	T	N	T/V	T/V	N	N
Hydrostatic	V/H	N	N	T	T	N	N	N
Thermal	T/V	N	T/V	N	T/V	N	N	N

Tables 6.6 and 6.7 shows the dominant direct stresses at the critical locations, on the downstream and upstream side of the dam. At the foundation level of the central block, cracking on the

upstream side of the could occur in summer with the dam full as a result of high vertical tensile stresses due to the hydrostatic load and the thermal load. The AAR tensile stress is largely along the central part of the block and would not contribute to upstream tensile cracking. However, the AAR tensile stress in combination with the horizontal thermal tensile stress would develop shear stresses at this level. Table 6.8 shows the tensile stresses for the three temperature increments at the foundation level. There is no significant change of AAR tensile stresses at this level, with increasing temperature. However there is a clear decrease of the tensile stress due to thermal load with increasing temperature. This has the effect of relieving the tensile stress due to the hydrostatic pressure and thus reducing the potential for cracking of the dam-foundation interface.

Table 6.8: Foundation tensile stresses

Foundation tensile stresses								
Climate condition	Current		1		2		3	
	ds	us	ds	us	ds	us	ds	us
Scenario A (Thermal load)	1.7	1.65	1.8	1.7	1.9	1.75	1.95	1.8
Scenario B (Thermal load)	3.4	3.4	3.6	3.5	3.8	3.6	4	3.7
Scenario C (Thermal load)	2.6	1.97	2.6	2	2.7	2.21	2.9	2.5
AAR	2 (C)	2 (C)	1.9 (C)	1.9 (C)	1.8 (C)	1.8 (C)		

The critical scenario for the wall happens in summer on the upstream side of the dam with the dam full. In this scenario cracking can occur due to high vertical tensile stresses induced by AAR and temperature effects. Table 6.9 show the tensile stresses for the three temperature scenarios. Both vertical AAR and thermal stresses increase with temperature. Thus the dam is likely to continue to crack at this level on the upstream side near central part of the wall and towards the right flank. The wall will also continue to crack on the downstream side of the dam near to the abutments (Table 6.10) at the same tensile stress combination occurs at these locations.

Table 6.9: Wall tensile stresses

Wall tensile stresses								
Climate condition	Current		1		2		3	
	ds	us	ds	us	ds	us	ds	us
Scenario A (Thermal load)	0	0	0	0	0	0	0	0
Scenario B (Thermal load)	1.3	2.6	1.23	2.7	1.17	2.8	0.8	2.9
Scenario C (Thermal load)	0	2.2	0	2.3	0	2.4	0	2.5
AAR	0	2.4	0	2.5	0	2.65		

Table 6.10: Abutment tensile stresses

Abutment tensile stresses								
Climate condition	Current		1		2		3	
	ds	us	ds	us	ds	us	ds	us
Scenario A (Thermal load)	1.5	0	1.5	0	1.5	0	1.5	0
Scenario B (Thermal load)	3	2.9	3.2	2.2	3.4	1.5	3.6	0.9
Scenario C (Thermal load)	1.7	0	1.9	0	2.1	0	2.3	0
AAR	2.5	0	2.9	0	3.3	0	-	

The crest experiences high tangential AAR and thermal tensile stresses in summer both on the upstream and downstream sides. While the current tensile stresses at the crest level are borderline compared to the expected tensile strength of concrete, the dam is likely to crack at this level with increasing temperature.

The combination of cracking of the wall and cracking at crest level can trigger structural failure mode (Figure 6.10) as blocks separate due to tangential tensile stress as well as crack horizontally due to vertical tensile stresses.

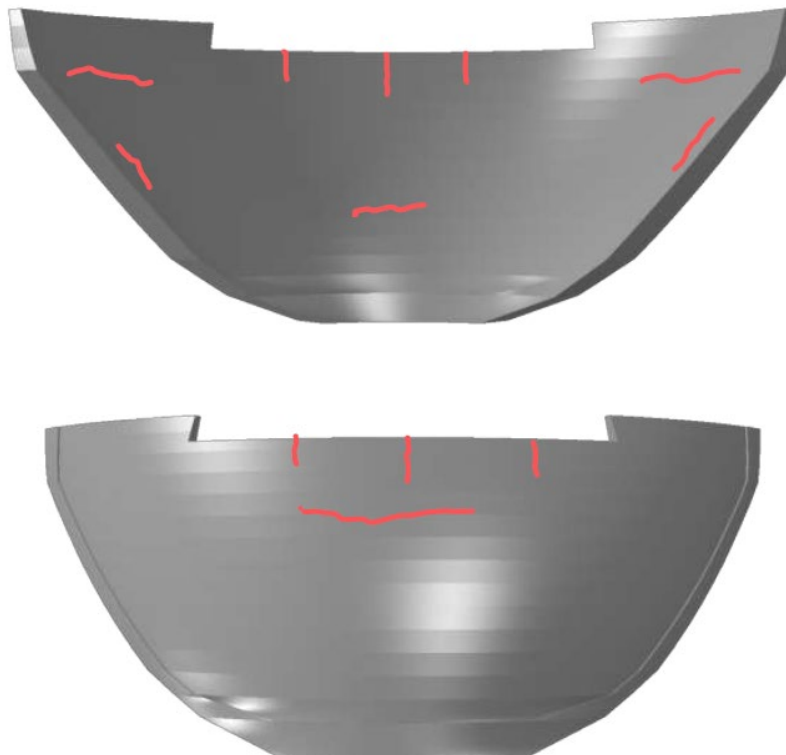


Figure 6.9: Kouga Dam possible crack locations

7 Conclusions

This project investigated the impact of climate change on the structural integrity of concrete arch dams. Specifically, the effect of gradual temperature increase on seasonal internal stresses and stresses due to AAR was considered. The approach adopted in this investigation was application of finite element modelling for predicting the long-term structural behaviour of dams. The novelty in the finite element modelling was the combination of ambient vibration testing and geodetic measurements to calibrate and validate the models. Another unique feature of the project was the inclusion of AAR in model calibration. Finite element models of two dams with different weather systems were successfully calibrated and validated.

Based on the results of this study the following conclusions are drawn:

- i) Gradual temperature increase will lead to:
 - a. Increased thermal tensile stresses on the downstream side of the foundation-wall interface which could lead to cracking. However for dams subjected to AAR, this increase is negated by increased compression at this level.
 - b. Increased tensile stresses on the abutments, central part the wall and the crest level of the wall which could lead to cracking.
 - c. Increased thrust forces at foundation level and this can lead to foundation failure where the bedrock is heavily jointed.
 - d. Permanent displacements in the upstream direction causing increases in tensile stresses on the dam wall, downstream side of foundation-wall interface abutments and crest of level of the dam wall. This is exacerbated by the effect of swelling due to chemical reaction.
- ii) Global warming will lead to gradual deterioration of the structural integrity of concrete arch dams.
- iii) The evaluation of the effects of global warming on the structural integrity of concrete dams should consider the most prevalent failure modes which include: 1) shear failure of the foundation-wall interface, 2) shear failure of the wall, 3) sliding failure along abutments, 3) structural failure of wall..
- iv) Proper monitoring of concrete arch dams is essential for the behavioural analysis of the structure without which no opinion of the safety of the structure is possible.
- v) The availability of local climate data is essential for reliable climate change projections. Such data was lacking for this project.

8 Recommendations

It is recommended that a 'no regrets'-approach is adopted to mitigate against the impacts of climate change on dam safety of concrete arch dams as well as other types of concrete dams. To this end the following recommendations are made:

- i) Extend the study to investigate the effects of extreme events (flooding, heat waves, siltation) on the safety arch dams.
- ii) Extend the study to investigate other dam types.
- iii) Consideration should be given to include the effects of climate change in the safety evaluation of concrete arch dams.
- iv) Improve dam surveillance and monitoring program. Continuous monitoring of dams provides the necessary information to detect the onset of possible failure early. In addition to enabling early detection of adverse events, such information provides the basis for tracking the effects of climate change on dam safety. It is thus critical to ensure that data collection is done diligently and that all instrumentation is in working order all the time.
- v) Install weather stations and instrumentation to measure climate related data at each major dam site in South Africa. This is essential to provide site specific data for prediction of future climate, which was a major limitation for this project.

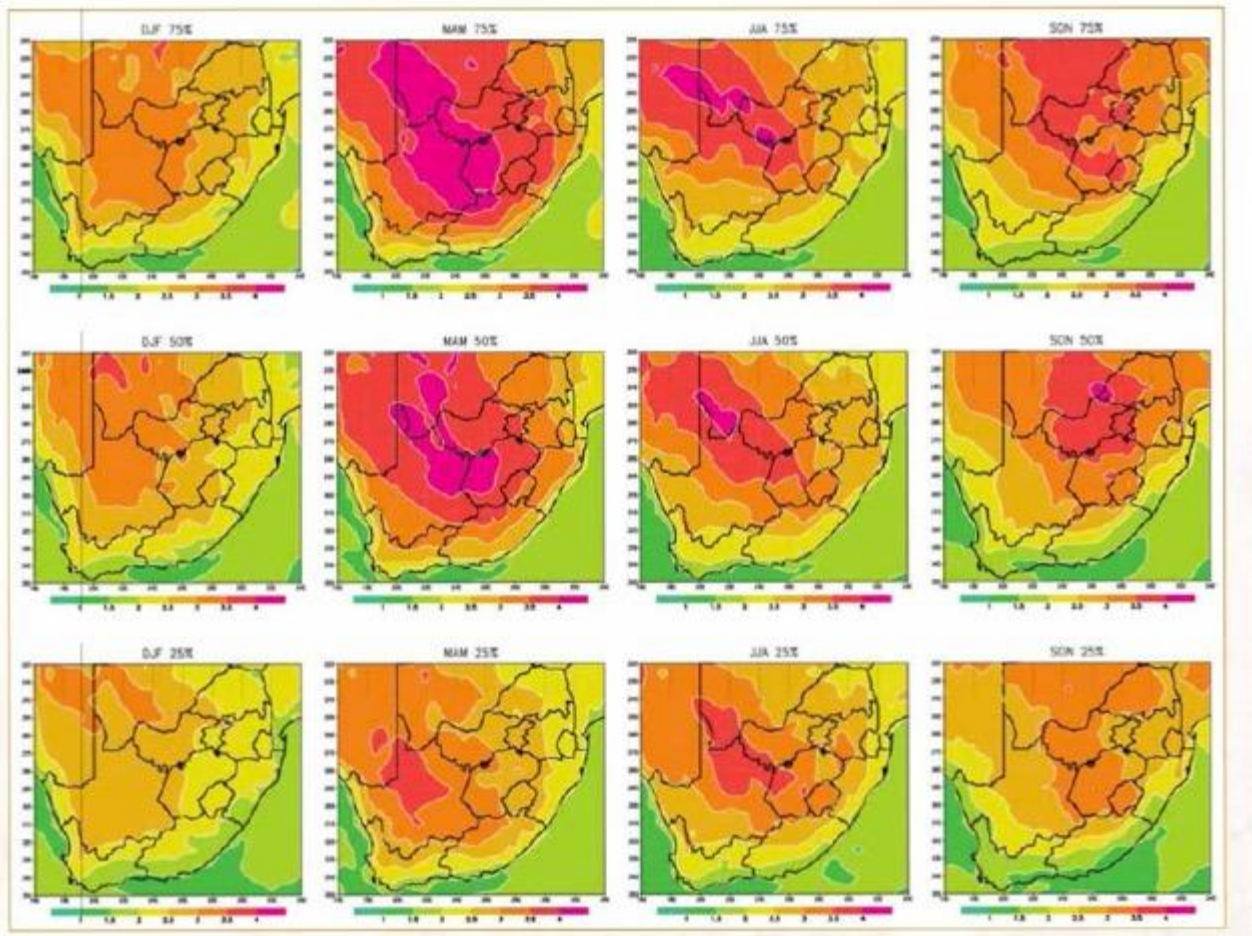
9 References

1. DEA (Department of Environmental Affairs). (2016a). Climate Change Adaptation Perspectives for Disaster Risk Reduction and Management in South Africa – Provisional modelling of drought, flood and sea level rise impacts and a description of adaptation responses. (ed. Munzhedzi, SM, Khavhagali, VP., Midgley, GM., de Abreu, P., Scorgie, S., Braun, M., Abdul, Z., Cullis, J., Channing Arndt, C., De Jager, G. and Strzepek, K.). Long-Term Adaptation Scenarios Flagship Research Programme. Pretoria.
2. DEA (Department of Environmental Affairs).(2016b). The Economics of Adaptation to Future Climates in South Africa – An integrated biophysical and economic analysis (ed. Munzhedzi,S.M., Khavhagali,V.P., Midgley, G.M., de Abreu, P., Scorgie, S., Braun, M., Abdul, Z., Cullis, J.,Channing Arndt, C., De Jager, G. and Strzepek, K). Long-Term Adaptation Scenarios Flagship Research Programme. Pretoria.
3. DEA (Department of Environmental Affairs). (2016c). Climate Information and Early Warning Systems for supporting the Risk Reduction and Management Sector in South Africa under future climates. (ed. Munzhedzi,S.M., Khavhagali,V.P., Midgley, G.M.,de Abreu, P., Scorgie, S., Braun, M., Abdul,Z., Cullis, J., Channing Arndt, C., De Jager, G. and Strzepek, K.). Long-Term Adaptation Scenarios Flagship Research Programme. Pretoria.
4. DEA (Department of Environmental Affairs). (2016d). Long Term Adaptation Scenarios for South Africa. (ed. Munzhedzi,S.M., Khavhagali,V.P., Midgley, G.M.,de Abreu, P., Scorgie, S., Braun, M., Abdul,Z., Cullis, J., Channing Arndt, C., De Jager, G. and Strzepek, KM.). Long-Term Adaptation Scenarios Flagship Research Programme. Pretoria.
5. DEA (Department of Environmental Affairs). (2011). Scoping of the Approximate Climate Change Adaptation Costs in Several Key Sectors for South Africa up to 2050, South Africa, Pretoria
6. DST (Department of Science and Technology) (2010). The South African Risk and Vulnerability atlas, Pretoria, South Africa.
7. Government of South Africa (2011). National Climate Change Response White Paper, Republic of South Africa, Pretoria.
8. Seidel, D.J., Fu, Q., Randel, W.J. and Reichler T.J. (2008). Widening of the tropical belt in a changing climate. *Nature Geoscience* 1, 21-24

9. Sellier, A., Grim, al É., Multon, S. and Bourdarot, É. (2017). Swelling Concrete in Dams and Hydraulic Structures, ISTE Ltd and John Wiley & Sons, Inc., London & Hobekon, p 251
10. SANS 204-2 Energy efficiency in buildings Part 2: The application of the energy efficiency requirements for buildings with natural environmental control
11. WRC and SAWS (2017), A climate change reference atlas, Pretoria, South Africa.
12. Allsop, W. (2007). Failure mechanisms for flood defence assets, FLOODsite report T04-06-01, Edition 1, www.floodsite.net.
13. Babbie (2002). "Climate change impacts on the safety of British Reservoirs", Babbie Group, Glasgow, UK, pp 129
14. DEA (Department of Environmental Affairs). (2016). The Economics of Adaptation to Future Climates in South Africa – An integrated biophysical and economic analysis (ed. Munzhedzi, S.M, Khavhagali, V.P., Midgley, G.M., de Abreu, P., Scorgie, S., Braun, M., Abdul, Z., Cullis, J., Channing Arndt, C., De Jager, G. and Strzepek, K.). Long-Term Adaptation Scenarios Flagship Research Programme. Pretoria.
15. DEA (Department of Environmental Affairs). (2011). Scoping of the Approximate Climate Change Adaptation Costs in Several Key Sectors for South Africa up to 2050, South Africa, Pretoria
16. Environment Agency (2011). Modes of dam failure and monitoring and measuring techniques, Environment Agency, Bristol
17. Federal Energy Regulatory Commission (1999). Engineering guidelines for the evaluation of hydropower projects, Arch Dams, Washington DC.
18. Federal Energy Regulatory Commission (2017). Engineering guidelines for the evaluation of hydropower projects, Arch Dams, Washington DC.
19. Government of South Africa (2011). National Climate Change Response White Paper, Republic of South Africa, Pretoria.
20. ICOLD (1999). Seismic observation of dams – guidelines and case studies, Bulletin 113", ICOLD, Paris. ICOLD-CIGB, Paris, France,
21. ICOLD (2004). Automated dam monitoring systems: Guidelines and case histories: Gulletin 118, ICOLD – CIGB, Paris, France, p 252
22. ICOLD (2005) .Risk assessment in dam safety management: Bulletin 130", ICOLD – CIGB, Paris, France, p 275.
23. ICOLD (2016). Global climate change, dams, reservoirs and related water resources :Bulletin 169, ICOLD – CIGB, Paris, France, p 89

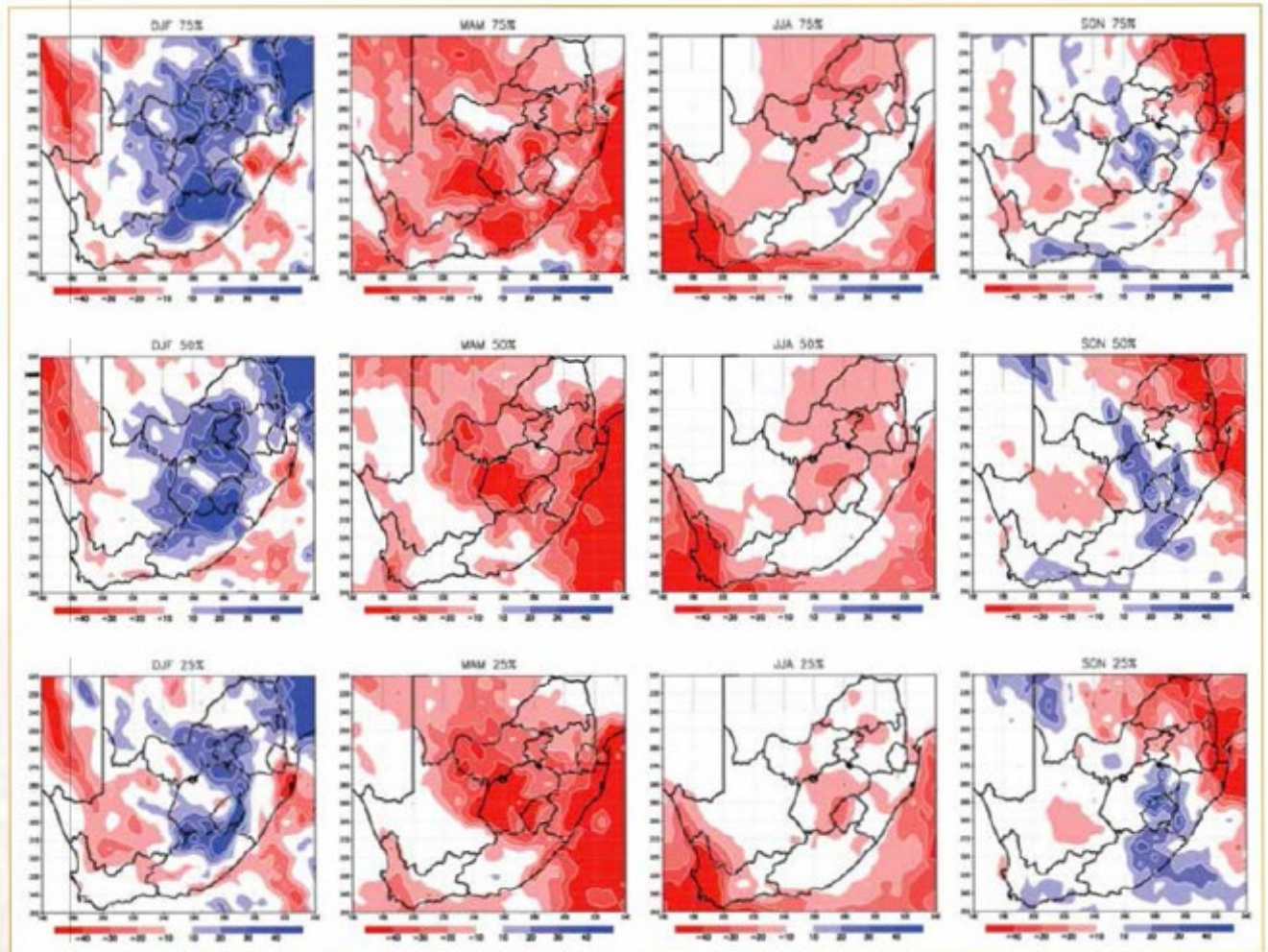
24. Pilate Moyo, Louis Hattingh, Chris Oosthuizen (2013). Ambient vibration measurements at Kouga dam – getting much more information than expected, Proceedings of ICOLD 2013 International Symposium, 14 August 2013, Seattle, Washington USA, pp 2507-2514, ISBN 978-1-884575-63-1
25. ICOLD B167 (2017). Regulation of Dam Safety: An overview of current practice world wide
26. Sellier, A., Grim, al É., Multon, S. and Bourdarot, É. (2017). Swelling Concrete in Dams and Hydraulic Structures, ISTE Ltd and John Wiley & Sons, Inc., London & Hobekon, p 251
27. US Bureau of Reclamation & US Army Corps of Engineers (2015). Best practices in dam and levee safety risk analysis, USA.
28. Farage, M., Alves, J. & Fairbairn, E. (2004). Macroscopic model of concrete subjected to alkali-aggregate reaction. Cement and Concrete Research, 34, 495-505.
29. Charlwood, R. (1994). A review of alkali aggregate in hydro-electric plants and dams. Hydropower Dams, 5, 31-62.
30. Léger, P., Côté, P. & Tinawi, R. (1996). Finite element analysis of concrete swelling due to alkali-aggregate reactions in dams. Computers & Structures, 60, 601-611.
31. Saouma, V. & Perotti, L. (2006). Constitutive model for alkali-aggregate reactions. ACI Materials Journal, 103, 194-202.
32. Ulm, F.-J., Coussy, O., Li, K. & Larive, C. (2000). Thermo-chemo-mechanics of ASR expansion in concrete structures. ASCE Journal of Engineering Mechanics, 126, 233-242.
33. Engelbrecht, F., Adegoke, J., Bopape, M.J., Naidoo, M., Garland, R., Thatcher, M., McGregor, J., Katzfey, J., Werner, M., Ichoku, C. and Gatebe, C. (2015). Projections of rapidly rising surface temperatures over Africa under low mitigation. Environmental Research Letters, 10(8), p.085004.
34. Dosio, A. and Panitz, H.J. (2016). Climate change projections for CORDEX-Africa with COSMO-CLM regional climate model and differences with the driving global climate models. Climate Dynamics, 46(5-6), pp.1599-1625.
35. Dosio, A. (2017). Projection of temperature and heat waves for Africa with an ensemble of CORDEX Regional Climate Models. Climate Dynamics, 49(1-2), pp.493-519.

Appendix A



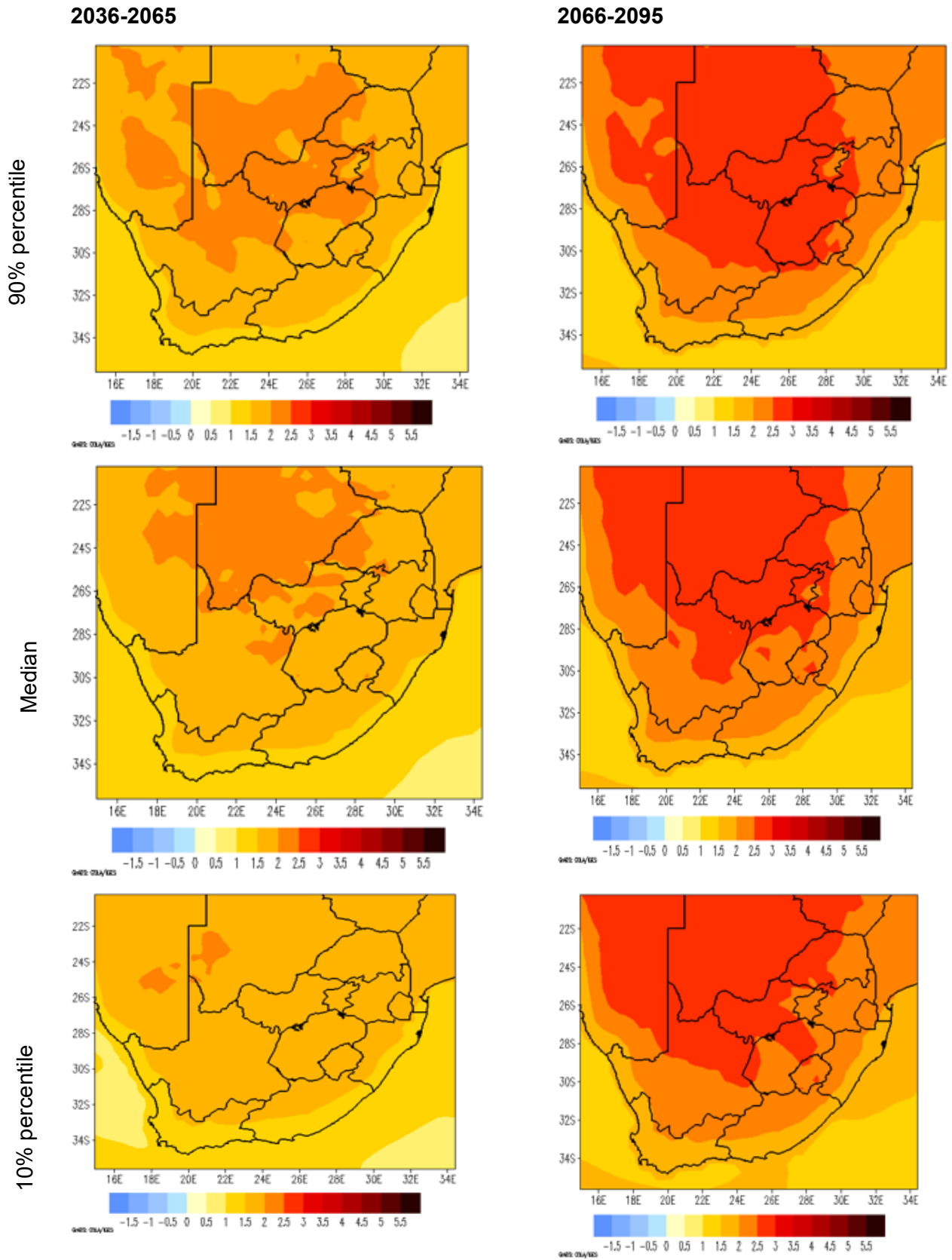
Map1: Projected temperature for period 2070-2100 based on 1991-2005 data: Source: DST (2010)

Appendix A



Map 2: Projected rainfall for period 2070-2100 based on 1991-2005 data: Source: DST (2010)

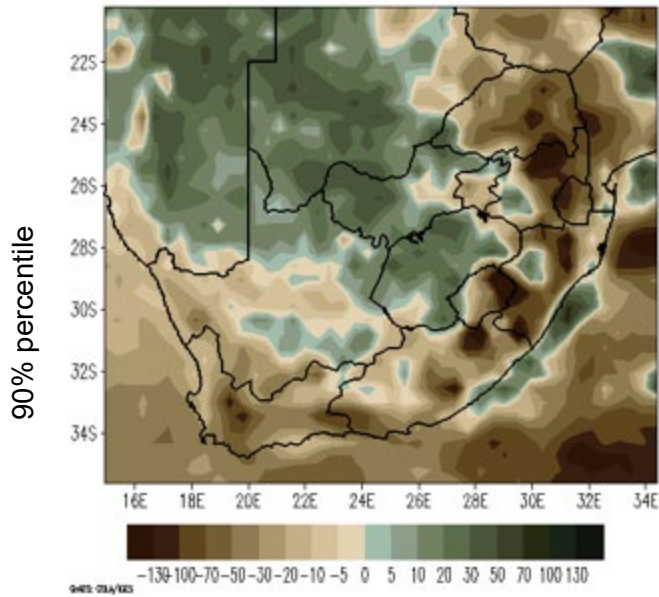
Appendix B



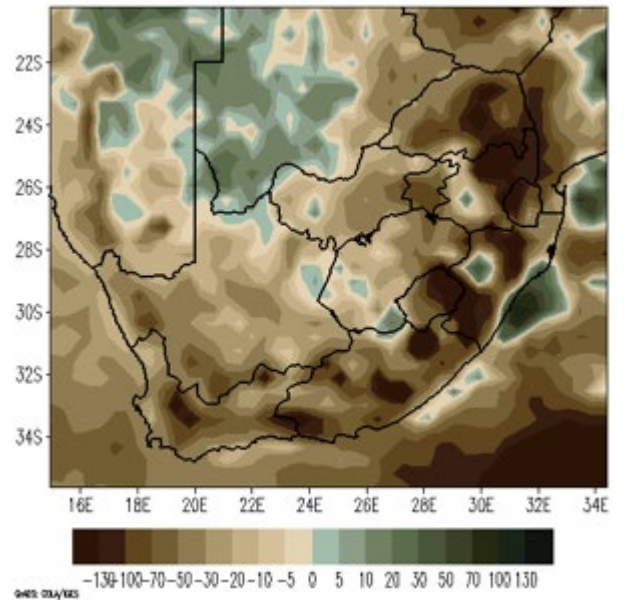
Map 3: Annual temperature for 2036-2065 & 2066-2095: Scenario RCP4.5: Source: WRC & SAWS (2017)

Appendix B

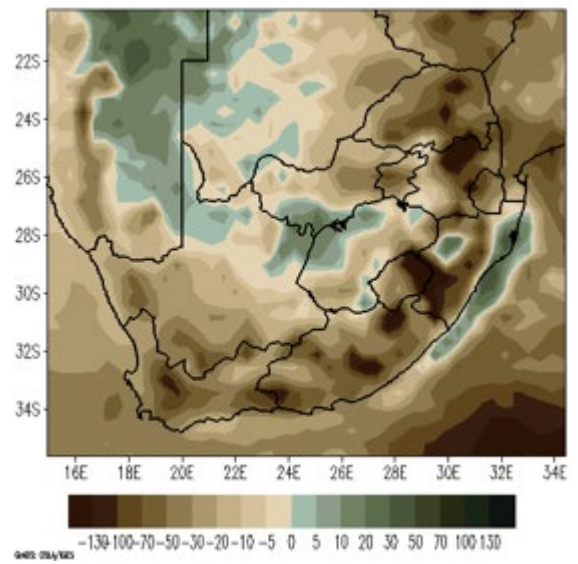
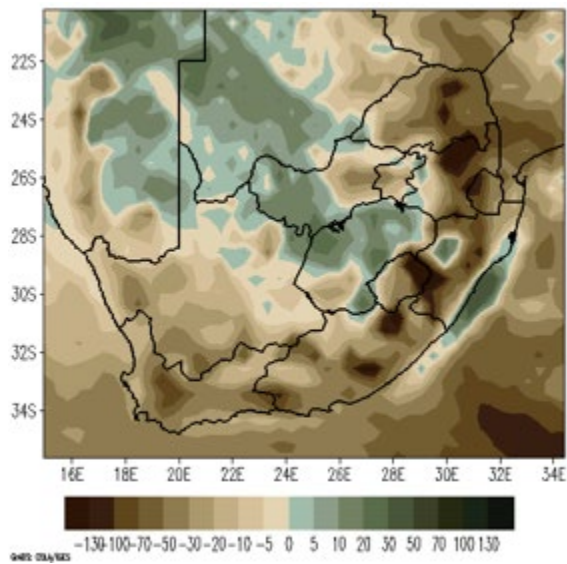
2036-2065



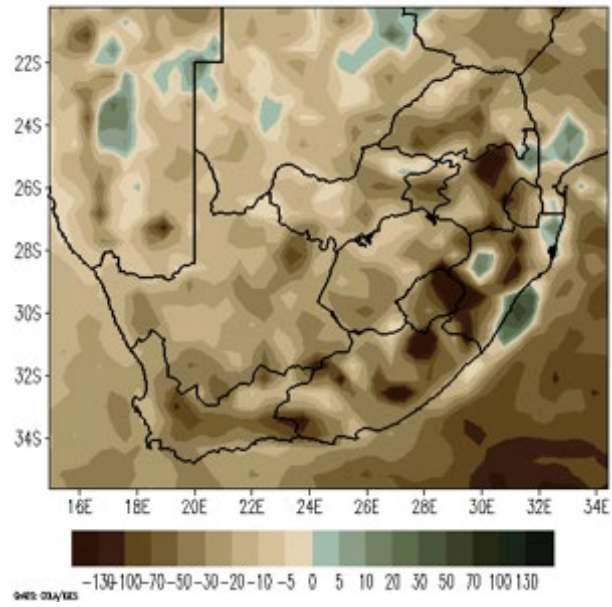
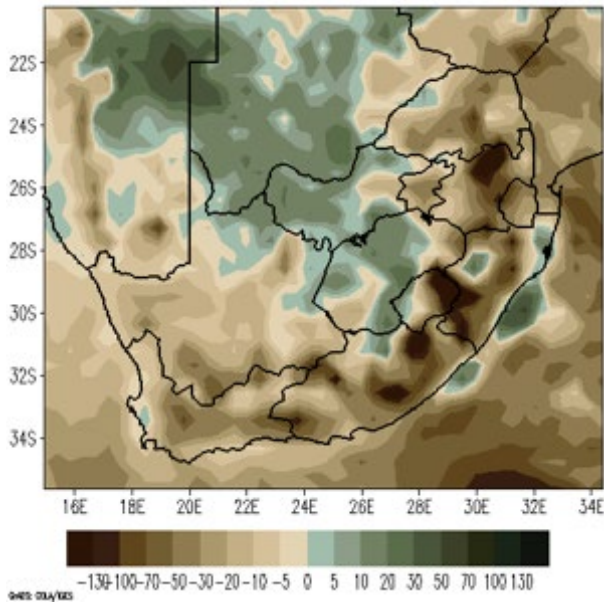
2066-2095



Median



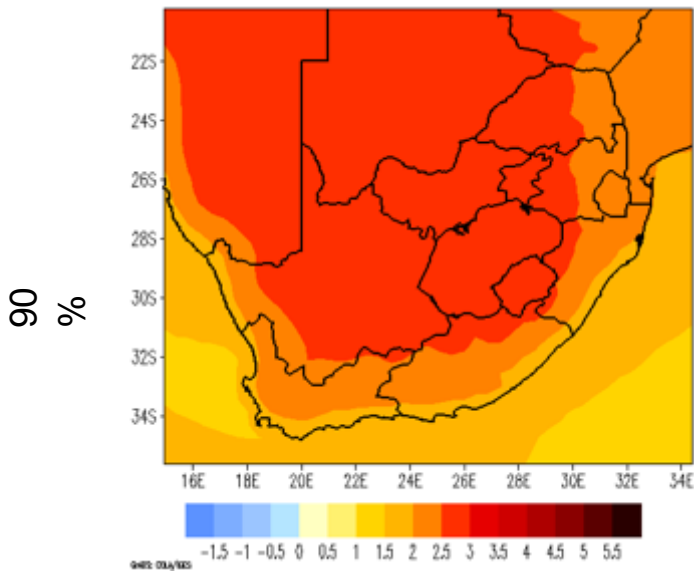
10% percentile



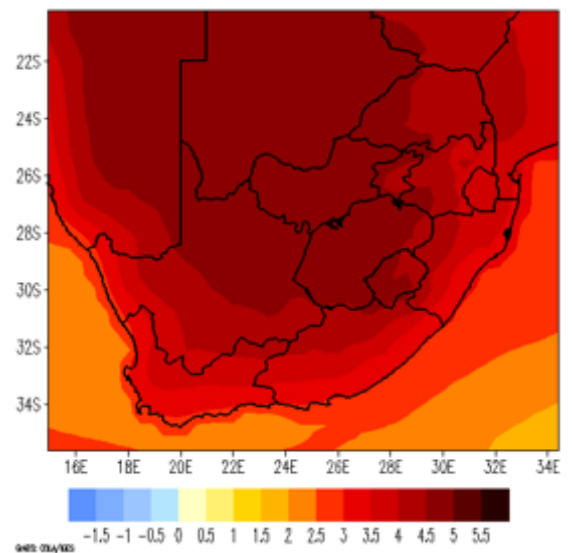
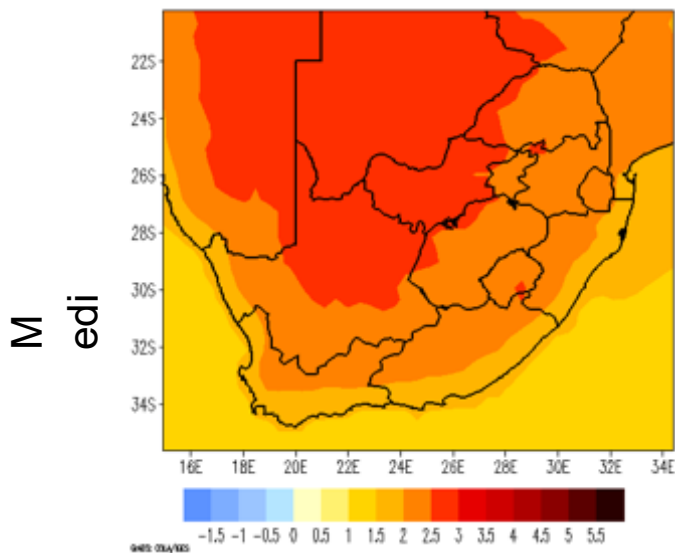
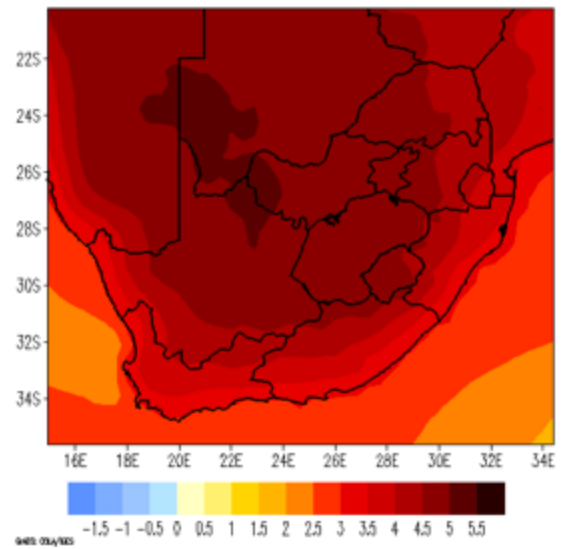
Map 4: Annual rainfall for 2036-2065 & 2066-2095: Scenario RCP4.5: Source: WRC & SAWS (2017)

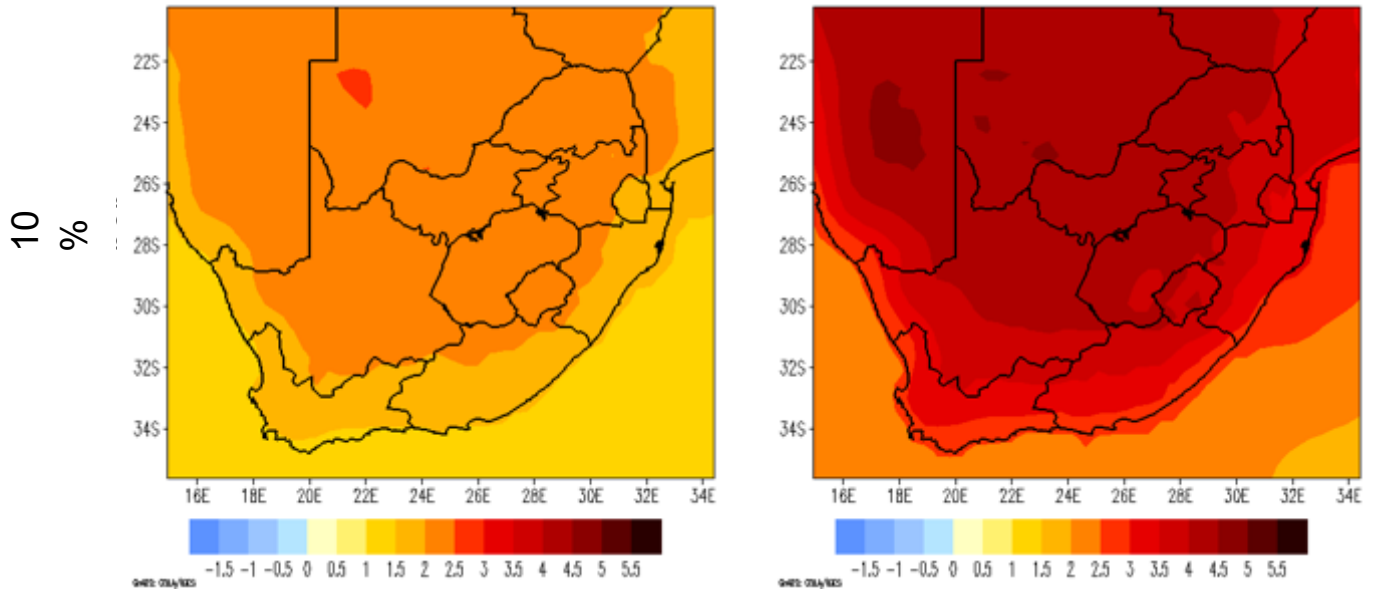
Appendix B

2036-2065



2066-2095

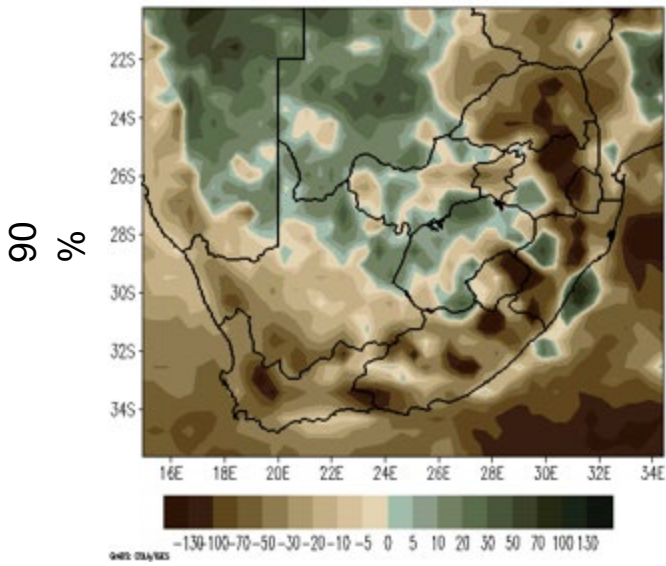




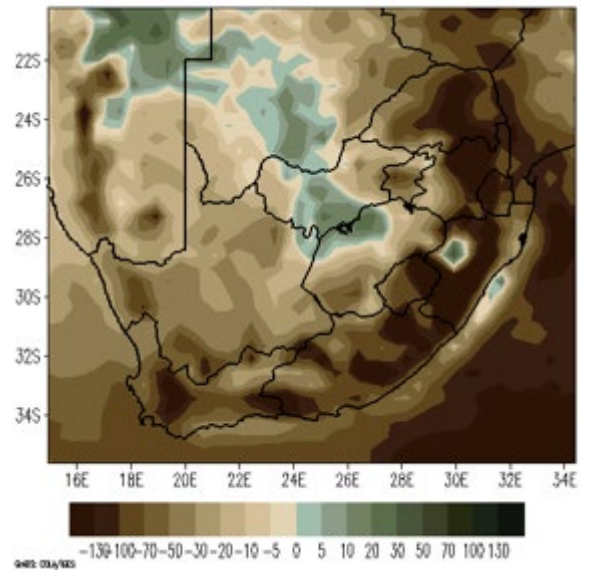
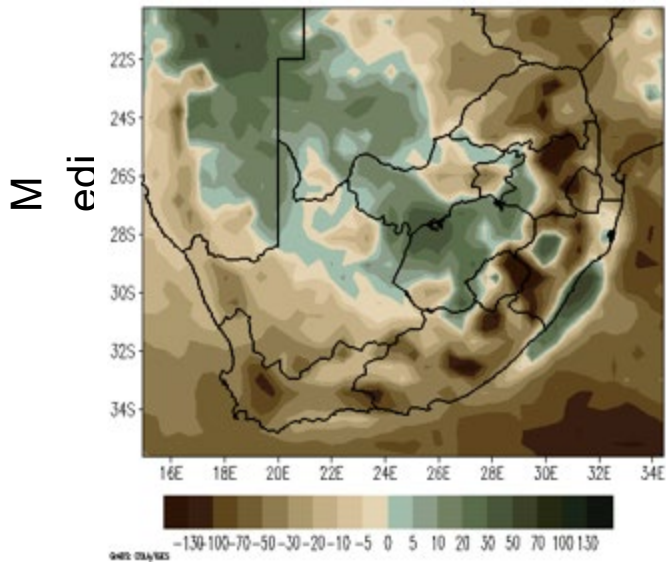
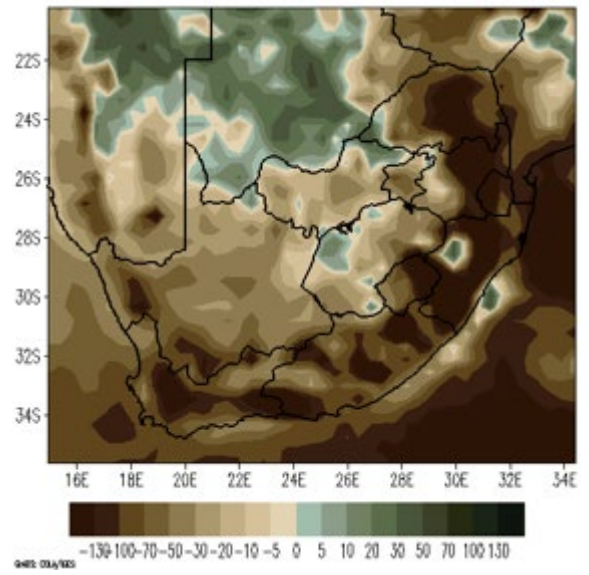
Map 5: Annual temperature for 2036-2065 & 2066-2095: Scenario RCP8.5: Source: WRC & SAWS (2017)

Appendix B

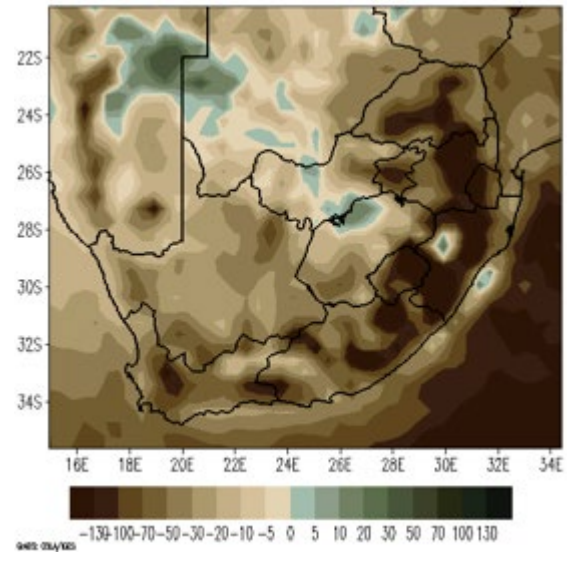
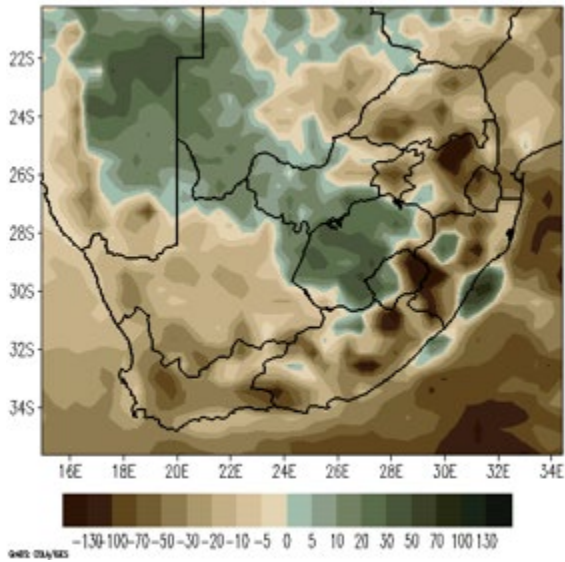
2036-2065



2066-2095

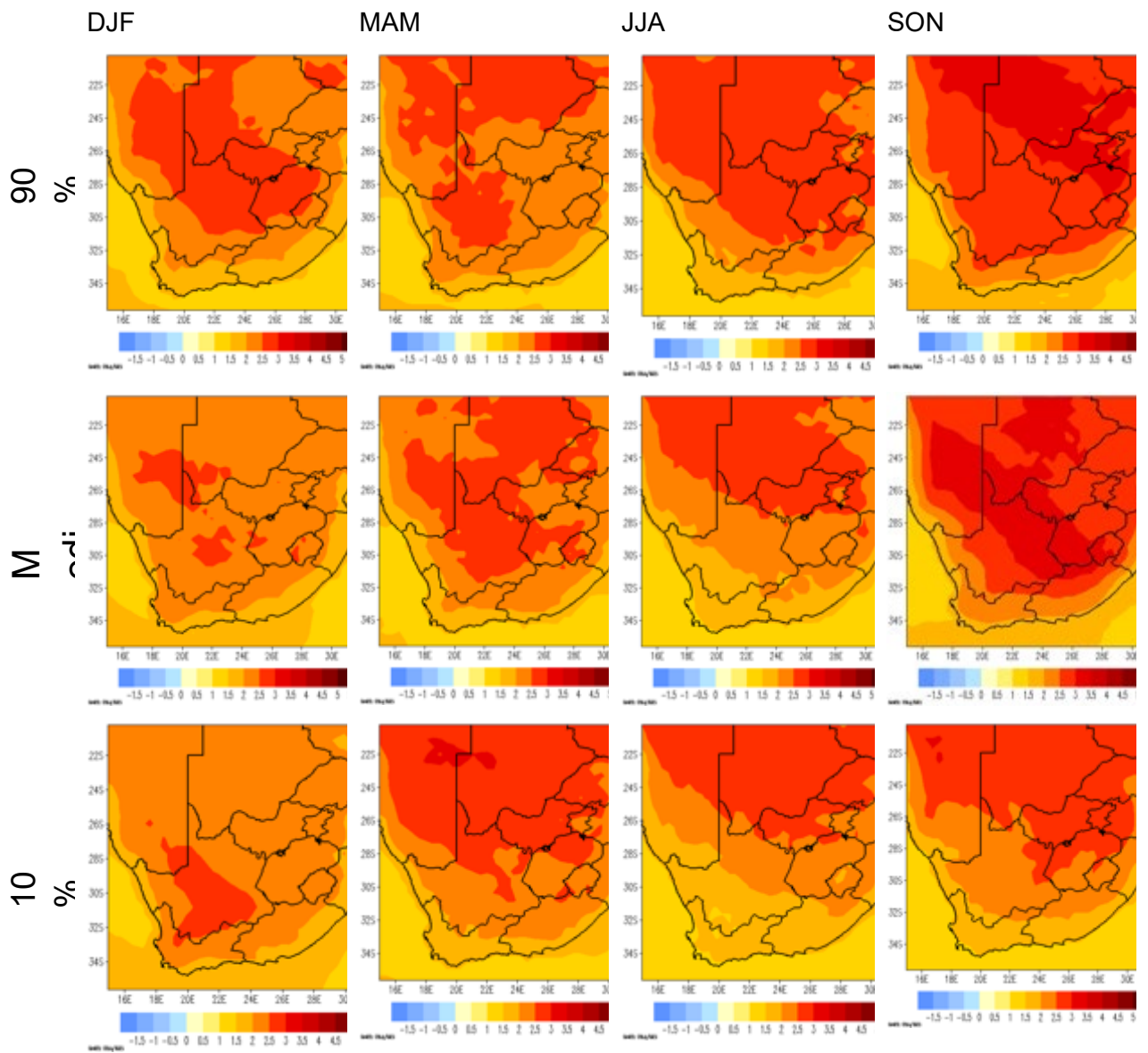


10
%



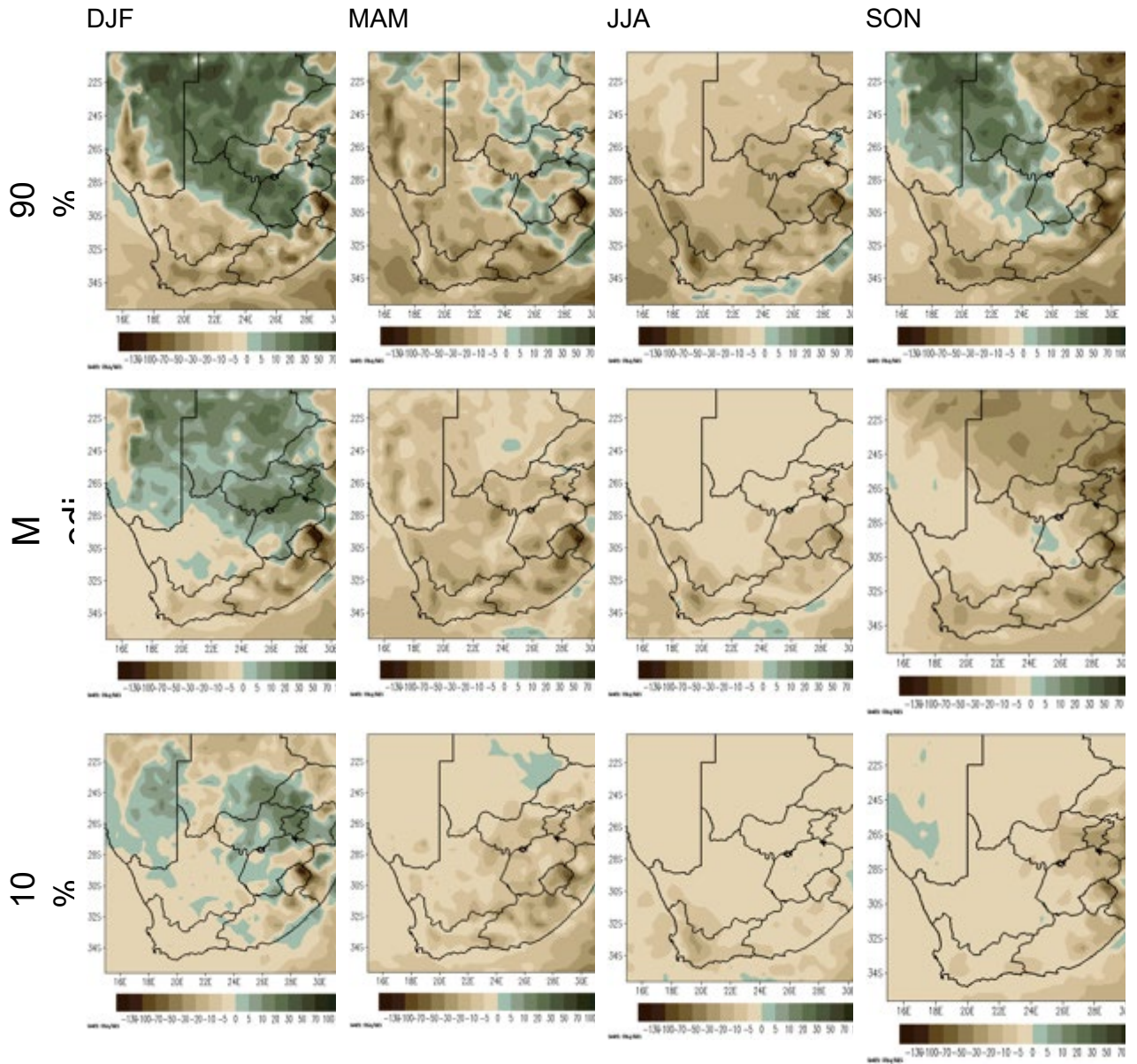
Map 6: Annual rainfall for 2036-2065 & 2066-2095: Scenario RCP8.5: Source: WRC & SAWS (2017)

Appendix B



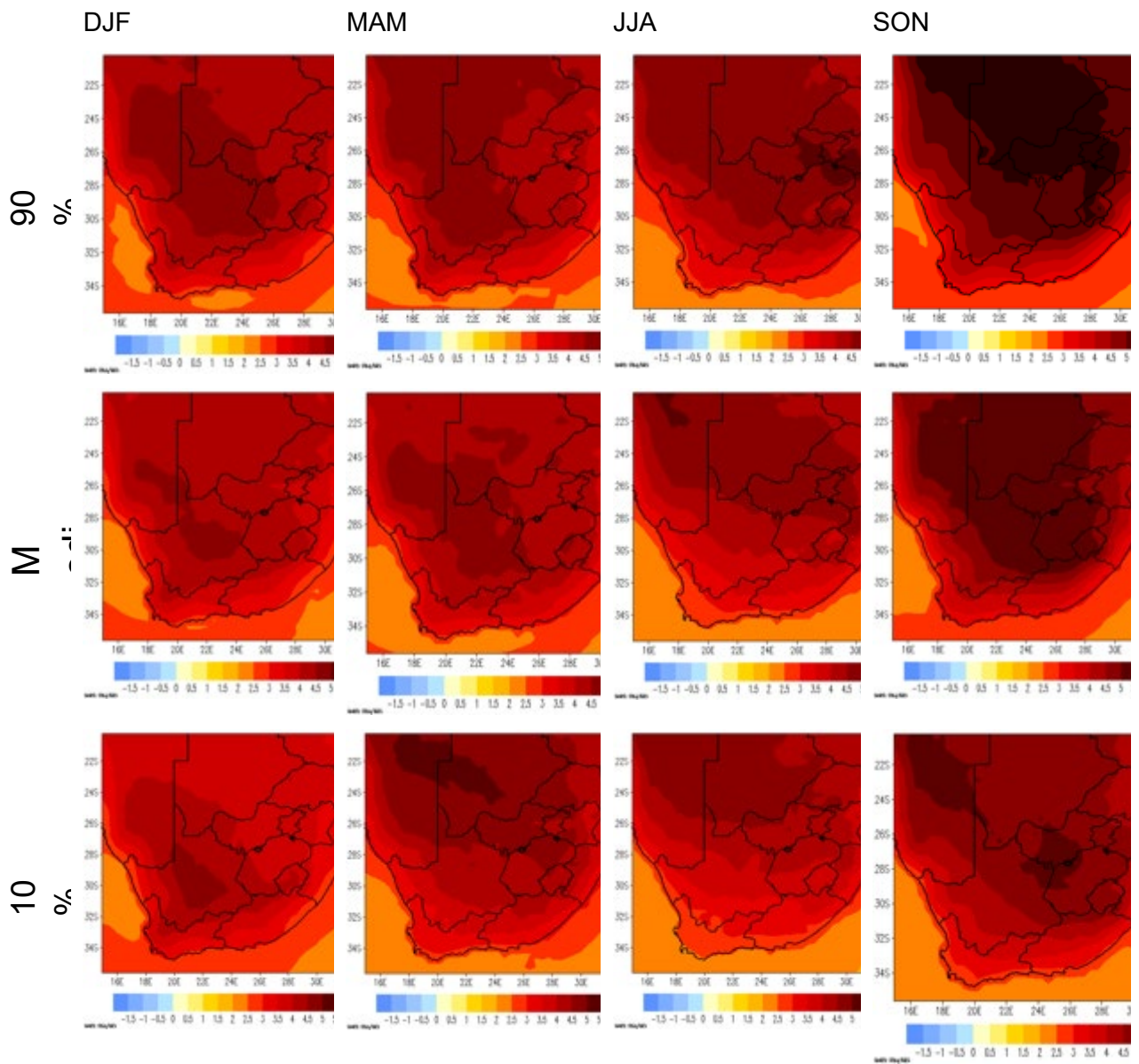
Map 7: Seasonal temperature for 2066-2095: Scenario RCP4.5: Source: WRC & SAWS (2017)

Appendix B



Map 8: Seasonal rainfall for 2066-2095: Scenario RCP4.5: Source: WRC & SAWS (2017)

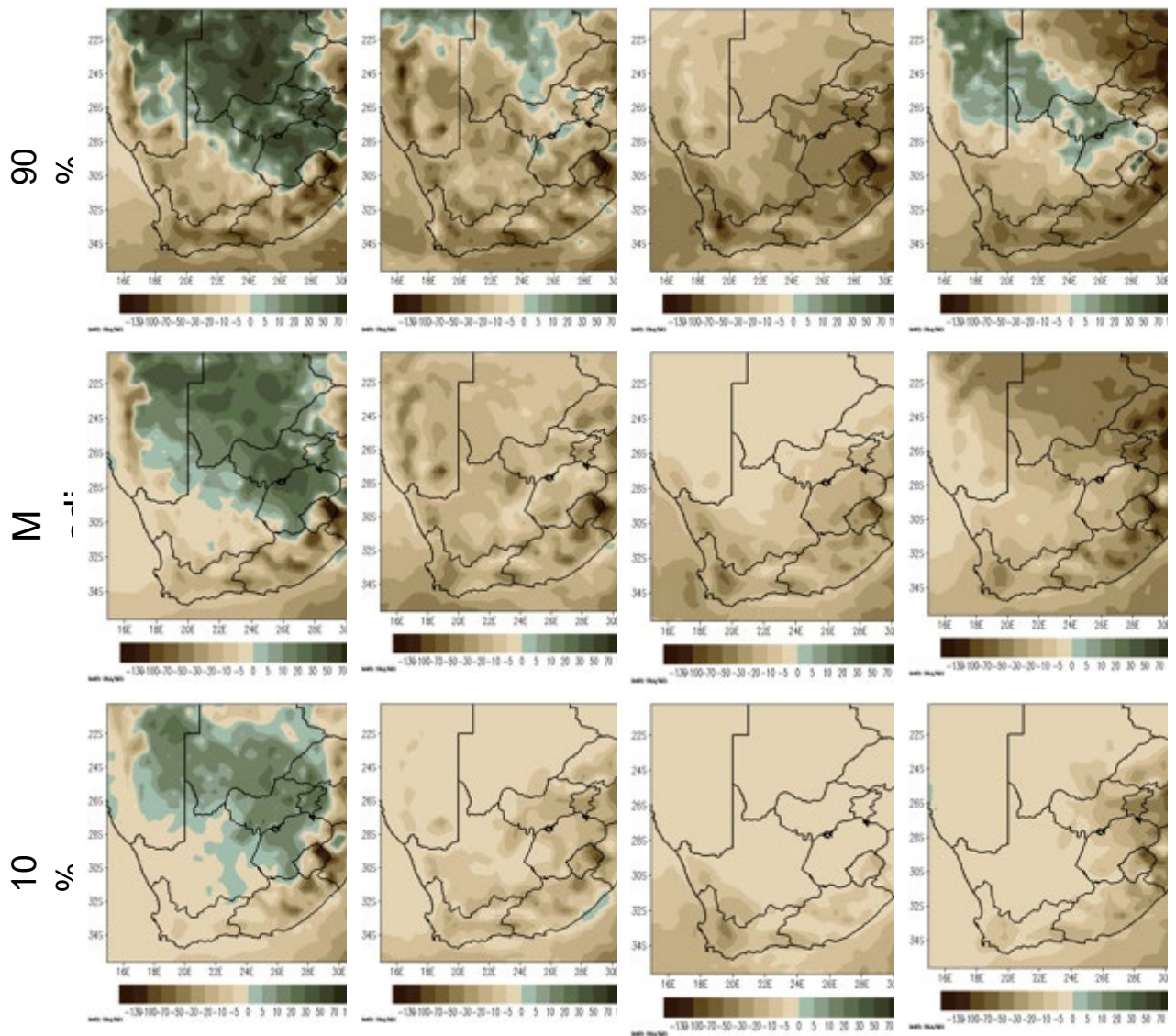
Appendix B



Map 9: Seasonal temperature for 2066-2095: Scenario RCP8.5: Source: WRC & SAWS (2017)

Appendix B

DJF MAM JJA SON



Map 10: Seasonal rainfall for 2066-2095: Scenario RCP8.5: Source: WRC & SAWS (2017)

Appendix C: Threats

- ageing
- aircraft strike
- changes in groundwater flow/chemistry
- earthquake
- extreme rainfall/flood
- failure of nearby infrastructure
- failure of reservoir in cascade
- human activity
- layout, design or construction inadequate or inappropriate
- mal-operation
- mining/ mineral extraction
- terrorism/sabotage/accident
- water loading

Appendix D: Hazards

- Differential settlement or deformation
- Rapid drawdown
- Reduced freeboard
- Settlement of foundation
- Seepage
- Concentrated erosion
- Backward erosion (piping)
- Contact erosion
- Internal erosion along an appurtenant structure
- Features on the downstream face
- High pore-water pressures
- High uplift pressures on foundation
- High uplift pressures on lift joints
- Hydraulic fracture
- Blockage of spillway
- Inadequate energy dissipation
- Overflow capacity exceeded
- Concrete cut-off deterioration
- Concrete deterioration by chemical or other attack
- Deterioration in foundation soil strength
- Deterioration of concrete or rock foundation
- Blocked drains and relief wells
- Blocked screens
- Other damage to ancillary structures
- Failure of controls, valves or gates
- Hydrodynamic forces that result in structural damage or failure
- Surge in pipework
- Corrosion
- Wave attack on upstream face
- Wave caused by external threat
- Controlled holding of water at a lower level
- Exceeding intended design loads in use of dam or ancillary structures
- Earthquake loading